2023

Transgenic Tools in Ants and the Representation of Alarm Pheromones in the Ant Antennial Lobe

Taylor Eco Hart

TRANSGENIC TOOLS IN ANTS AND THE REPRESENTATION OF ALARM PHEROMONES IN THE ANT ANTENNAL LOBE

A Thesis Presented to the Faculty of

The Rockefeller University

in Partial Fulfillment of the Requirements for

the degree of Doctor of Philosophy

by

Taylor Eco Hart

December 2022

TRANSGENIC TOOLS IN ANTS AND THE REPRESENTATION OF ALARM PHEROMONES IN THE ANT ANTENNAL LOBE

Taylor Eco Hart, Ph.D.
The Rockefeller University 2022

For decades, ants have served as major study species for ethologists, theorists, geneticists, and chemical ecologists, who have been drawn to understand how their unique features contribute to the evolution and maintenance of insect societies. These features, especially their extreme morphological plasticity, collective behavior, and complex chemical communication, together with their small sizes and relatively simple brains, make ants intriguing model systems for many topics in neurobiology. While many ant species possess brains no larger than the well-characterized vinegar fly, the primary olfactory processing centers (antennal lobes) contain an order of magnitude more functional units compared to the vinegar fly, presumably to facilitate detecting and discriminating between vast numbers of pheromones. The discovery of additional developmental differences between ants and flies led to a proposed but untested model where ant olfactory sensory neurons target the appropriate antennal lobe compartment via receptor dependent activity, as occurs in mammals.

However, while transgenic tools have allowed dissection of the olfactory system's development and functional organization in some solitary insect species, these tools have so far been impossible to implement in ants. Taking advantage of the unusual experimental tractability of the clonal raider ant *Ooceraea biroi*, we implemented piggyBac transgenesis for the first time in ants, and generated a toolkit of transgenic lines. These protocols and transgenic tools greatly expand the space of feasible experiments in ants, and make clonal raider ants the most experimentally tractable model system among eusocial insects. We then used these transgenic lines to study outstanding questions in social insect olfaction. The major set of experiments in

this thesis focus on understanding how the expanded ant olfactory system encodes alarm pheromones, the chemical signals for danger.

To study the representation of alarm pheromones in the ant antennal lobe, we developed a system for recording odor-evoked calcium responses throughout the lobe, using a transgenic line expressing the genetically encoded calcium indicator GCaMP in olfactory sensory neurons, combined with volumetric calcium imaging. We found that alarm pheromones and general odorants activate highly robust and spatially stereotyped activity patterns across different individuals, suggesting that ant antennal lobes do not develop through receptor activity-dependent processes. While ants have greatly expanded olfactory systems, only a small number of glomeruli robustly responded to alarm pheromones. This finding is contrary to expectations from prior studies of alarm pheromone representation. By comparing response patterns generated by alarm pheromone types that induce panic alarm vs. those that lack this activity, we identified a single glomerulus that potentially plays a core role in mediating panic-alarm behavior. Our initial investigation of general odorant encoding suggests that most odorants might also be encoded by few glomeruli, in opposition to the combinatorial odor coding schemes described in the vinegar fly.

The tools reported here open new experimental avenues for mechanistic studies of the adaptations to eusociality. The results of these studies extend the understanding of how odor coding and alarm pheromone perception function within the expanded olfactory systems of ants.

ACKNOWLEDGMENTS

This thesis has been the better part of an odyssey, with so many obstacles, apparent dead ends, side challenges, and surprises along the way. Completing this thesis changed me, and required me to change myself, and now I am a vastly different person than when I began. Making it to the finish line seemed impossible at so many points, and I want to express my deepest gratitude to the people who helped me make it to the end.

When I joined the lab, my advisor Daniel Kronauer had the vision of what I could achieve if I set myself to it, and provided the knife-sharp analysis, the long view of perspective, and the understanding, grace, and space that together allowed me to work through each challenge as it arose. My faculty advisory committee members, Leslie Vosshall and Vanessa Ruta, reciprocated my tales of struggle and sometimes, success, with a balance of rigor and encouragement. My external thesis committee member, Patrizia d'Ettorre, provided many useful critiques and suggestions for this thesis. A big thanks to all of them!

Completing the studies in this thesis was only possible thanks to many collaborators, all of the following who collected or played a key role in generating data described here. From the start, Waring “Buck” Trible and Leonora Olivos-Cisneros provided extensive guidance and expertise on genome editing in the clonal raider ant. Maintaining ant colonies and collecting and preparing eggs for microinjection was highly labor intensive, requiring coordination among a team that included Leonora, Stephany Valdés-Rodríguez, and Amelia Ritger alongside myself at various times. Stephany also maintained many of the experimental colonies. Kip D. Lacy performed genome re-sequencing on the transgenic lines and analyzed the genomic data. Dominic Frank performed brain dissections, immunohistochemistry, and confocal microscopy to reveal the fluorescent phenotypes. His helpful advice also helped me overcome major challenges

in developing in vivo calcium imaging for the clonal raider ant. Dominic also built the olfactometer and maintained the two-photon microscope used in the calcium imaging experiments. Lindsey E. Lopes performed the behavior experiments, allowing us to link behavioral and neural encoding correlates of alarm pheromone stimulus.

Thanks also to the many others whose efforts contributed to this thesis. Meg Younger taught me to use a two-photon microscope and helped me get started with my functional neuroscience ventures using her equipment. Ben Matthews shared helpful advice on developing transgenic methods in a new model system. Daniel Pastor developed and graciously shared his method for performing immunohistochemistry on the whole-mounted antennal club of the clonal raider ant. Many other members of the Kronauer, Ruta, and Vosshall labs also provided advice and useful discussions on developing transgenics and calcium imaging methods. Thanks also to Christina Pyrgaki, Alison North, the Rockefeller University Bio-Imaging Resource Center, and the Rockefeller University Genomics Resource Center. Ben Matthews provided samples of the hyPBase^{apis}, pBAC-ECFP-15xQUAS_TATA-SV40, and pBac-DsRed-ORCO_9kbProm-QF2 plasmids. Thanks to Martin Beye for permission to use the hyPBase^{apis} plasmid, and Chris Potter for permission to use the pBAC-ECFP-15xQUAS_TATA-SV40 and pBac-DsRed-ORCO_9kbProm-QF2 plasmids prior to their appearance in publications. Thanks to Rob Harrell for sending an alternate [ie1-DsRed] plasmid which was used in test injection experiments.

Credit to Vikram Chandra, Sean McKenzie, and Buck Trible for convincing me that studying ants was a good idea. Their intelligence, enthusiasm, and friendship drew me in to the intricacies and explanatory power of understanding ants, social behavior, and social evolution, beginning at my first student retreat and for so many discussions afterward. Thanks to Ingrid

Fetter Pruneda for taking me under her wing as a rotation student, where she introduced me both to the study of ants and neurobiology.

Many thanks to Jeanne Garbarino and the rest of RockEdu for their infectious excitement about science communication, and for the opportunities and preparation to teach science. Thanks to Teffen, Fei, Jay, Sarafina, Catty, Henry, Hila, Beck, Kaylin, Daria, Irina, Vincent, and Moli and many others for friendship, comradery, and good times.

Thanks so much to my parents for raising me with care, love, and openness, and for fostering my curiosity and love of exploration. Thanks to my grandparents, siblings, aunts, uncles, and many cousins for your love and care.

To all the many people who have stuck with me and supported me over the years, thank you for that and for taking me at my word when I told you who I am.

TABLE OF CONTENTS

LIST OF FIGURES

LIST OF TABLES

CHAPTER 1: INTRODUCTION

1.1: Eusocial insects are primary systems for the study of social behavior

Eusocial insects including ants, termites, some wasps, and some bees, have fascinated both scholars and enthusiasts for centuries. Their miniature cities and organized behavior mirror the familiar, while at the same time exhibiting incredible variety and their own distinctions. Eusocial organisms live in highly-integrated colonies which share the following features: division of labor between reproducers and non-reproducers, overlapping generations, and cooperative brood care (Batra, 1966; Batra, 1968; Michener, 1969; Crespi and Yanega, 1995). Adopting this type of social organization has set many insect lineages down evolutionary paths leading to extreme phenotypic plasticity, complex division of tasks, and communication using vast arrays of chemical signals. These phenomena have been intensely studied across a variety of disciplines, building a wealth of literature on the biology of eusocial species and adaptations to social living.

1.2: The origins of chemical communication

The conditions of eusocial insect colonies favor the evolution of complex chemical communication systems. In these societies, relatedness is very high and the inclusive fitness interests of colony members are typically aligned. As a result, within-group genetic conflict is low, and cooperation between colony members simply makes sense from an inclusive fitness point of view (Hamilton, 1963; Hamilton, 1964a-b). With dense populations living together inside underground burrows or beehives, survival depends on ensuring that essential tasks like caring for brood, securing a sustainable food supply, and collective defense against predators or parasites are all taken care of. Efficient sharing of information helps recruit workers to

accomplish these tasks, and allows coordinating their actions toward crucial sites, such as hungry brood, a rich food source, or a threat to the nest (Leonhardt et al., 2016; Yan and Liebig, 2021; Mitaka and Akino et al., 2021). Because insects rely very heavily on chemical senses to perceive the world, these sense modalities represent the substrates from which eusocial insects evolved complex communication systems. Many of these chemical signals are composed of specific chemical products that produce robust effects on conspecific perceivers and are defined as pheromones.

Detection of chemicals in the environment, chemoreception, is an ancient and ubiquitous sense modality (Nei et al., 2008; Yohe and Brand, 2018). Chemosensory systems are adapted for detecting ecologically-relevant chemicals using arrays of receptor proteins with different ligand binding properties (Nei et al., 2008). In animals, chemosensory systems that detect volatiles are considered to be olfactory, while contact chemoreception is considered to be gustatory. In many organisms, these systems work through different classes of chemosensory receptors and are housed in different sensory organs, although some sensory organs play roles in both volatile and contact chemoreception (Schneider, 1964).[1]

The social and chemical environments shape one another. Organisms that live in close proximity to one another detect one another's chemical products, whether as surface molecules, secretions, wastes, or internal fluids leaking after injury (Ben-Shaul, 2015). Intraspecific chemical communication is common in bacteria, where quorum sensing systems allow individuals to alter their gene expression in response to the challenges or opportunities presented by local population density fluctuations (Mukherjee and Bassler, 2019). Chemical emissions

[1] This thesis primarily discusses the antenna of the ant, which is one such organ (Schneider, 1964). For this reason, and because of the frequent references in the literature to 'olfactory sensory neurons' and 'odorant receptor' genes related to the ant antenna, the term 'olfaction' will be used to refer to all types of chemoreception performed by the ant antenna, unless otherwise specified.

contain information about the identity and physiological state of the organism they came from, potentially indicating the presence of potential predators, prey, competitors, or cooperators. They inform an organism's decision making, such as whether to stay put or move, or how to allocate metabolic resources. The evolution of communication systems facilitates different ways of regulating social interactions. Extant animals use a host of olfactory and gustatory cues to assess proximity, mating status, and family relationships, to name a few examples (Johansson and Jones, 2007).

Chemical signals are assumed to originate either as useful substances in their own right or as byproducts of other life processes, ancestral substrates which evolution acts upon to affect the way such chemicals are produced. When the emission of a chemical product affects the perceiver in a beneficial way (acting as a cue that somehow enables cooperation, for example), it becomes adaptive for the emitter to better modulate the intensity and temporal dynamics of the cue's release, and the cue can become a functional signal. In turn, the perceiver's chemosensory systems become under selection for better signal detection. Over time, signal molecules and signal reception systems can become unlinked from the biological processes they originally resulted from, in a process called "signal ritualization" (Tinbergen, 1952; Steiger et al., 2010).

This evolutionary model is believed to explain the origin of many signaling systems, including pheromone systems. For example, insects ancestrally produce a variety of cuticular hydrocarbon molecules that prevent desiccation (Lockey, 1988), but some of compounds now also serve as cues or signals for intra-colony communication (Martin and Drijfhout, 2009). The ratios of different cuticular hydrocarbon molecules vary between individuals and correlate with characteristics like sex, caste, colony of origin, and species, and can indicate an individual's role or status in the colony. Members of this class of molecules have been identified as fertility

signals or queen pheromones (Liebig et al., 2000; Dietemann et al., 2003; d'Ettorre et al., 2004; d'Ettorre and Lenor, 2009). Quantitative ratios of cuticular hydrocarbons are controlled primarily by genetics and secondarily by environmental factors and together create a colony gestalt odor that is recognized by nestmates, reducing aggression (Bonavita-Cougardan et al., 1987; Wagner et al., 2000; van Zweden et al., 2009). Colony gestalt odors change over time and differ from pheromones, which have deterministic molecular identities; rather, members of a given nest acquire a neuronal template of the colony gestalt odor which is compared against the odors of individuals they encounter (Leonhardt et al., 2007; d'Ettorre and Lenor, 2009).

Chemical signals for danger, alarm pheromones, are also ubiquitous among eusocial insects and are crucial for initiating collective defense of the colony. Various alarm pheromones are believed to have originated either as volatile chemicals leaking from the bodies of injured individuals, or as defensive secretions (Leonhardt et al., 2016; Stökl and Steiger, 2017). In some cases, compounds such as formic acid continue to play roles both as direct anti-predator defenses and signals that trigger alarm behavior in nestmates (Löfqvist, 1976). Understanding the neural basis for perception of alarm pheromones in ants is a major topic in this thesis.

1.3: Insect chemoreception and the antennal lobe

Insects are masters of chemoreception, and with their incredible ecological diversity and experimental tractability, insects have served as primary models for understanding this sense modality. Insect chemosensory organs contain sensory neurons expressing members of several chemosensory receptor gene families, including Ionotropic Receptors (IRs), Gustatory Receptors (GRs), and Odorant Receptors (ORs), with receptor protein sequence variation conferring different ligand binding properties. Despite the gene family names, IRs and ORs both encode

proteins with ionotropic functions, and members of both OR and GR families can be involved in volatile and contact chemoreception (Dahanukar et al., 2005; Hallem et al., 2006; Rytz et al., 2013; Butterwick et al., 2018; Benton et al., 2020; de Mármol et al., 2021). Thorough study of the vinegar fly *Drosophila melanogaster* has shown that olfactory sensory neurons (OSNs) housed in the antennae and maxillary palps each project their dendrites to chemosensory sensilla, with each OSN expressing small numbers of chemosensory receptor genes (Vosshall et al., 2000; Zhao and McBride, 2020). ORs function as heterocomplexes containing both the odorant receptor co-receptor *Orco* and a second "tuning" receptor conferring ligand specificity (Larsson et al., 2004; de Mármol et al., 2021). IRs also function as heterocomplexes with one or more co-receptors plus a tuning receptor (Abuin et al., 2011). Environmental molecules enter the sensillar lymph through pores, where they are trafficked by odorant binding proteins (OBPs) and chemosensory proteins (CSPs) before contacting receptor proteins (Campanacci et al., 2003; Dani et al., 2011; Zhao and McBride, 2020; Rihani et al., 2021). Effective binding between ligands and receptors excites or inhibits neural activity in the OSNs, transducing signals that inform the organism of the status of the external chemical environment.

Insect OSNs project their axons to the central brain, either to targets in the antennal lobe (AL) or the sub-esophageal zone (SEZ) (Vosshall et al., 2000). Based on anatomical comparisons, the structure and organization of the AL are thought to be generally conserved across insects (Anton and Homberg, 1999). In the AL, OSN axons synapse with lateral interneurons (LNs) and projection neurons (PNs), forming glomeruli (Stocker, 1994; Laissue et al., 1999; Anton and Homberg, 1999). In *Drosophila*, the AL glomeruli each receive input from typically just one functional class of OSNs, resulting in an anatomical-functional map where each glomerulus has tuning properties corresponding to associated OSN type, and odorants are

encoded as spatial activity maps across the AL (Strausfeld and Hildebrand, 1999; Gao et al., 2000; Vosshall et al., 2000; Zhao and McBride, 2020). Recent studies showed that the one-to-one matching of odorant receptor to glomeruli is an incomplete description, because ORs and IRs are co-expressed in several classes of OSNs in two *Drosophila* species and the mosquito *Anopheles coluzzii* (Task et al., 2022). The relationship breaks down further in the mosquito *Aedes aegypti*, with single OSNs frequently expressing multiple tuning receptors, as well as complex mapping between transcriptomically-defined OSN types and their glomerular targets (Herre et al., 2022). It remains to be determined how generalizable the canonical mapping rules for receptors, OSNs, and glomeruli are across insects.

The AL forms a neural network that processes olfactory signal inputs. Initially, the convergence of OSNs of the same type onto one glomerulus helps average out signal variation across individual OSNs and increases the signal to noise ratio (Laurent, 1999). This activity is modulated and transformed by both excitatory and inhibitory activity of the LN network, and information is ultimately output by PNs to the mushroom bodies and/or lateral horns (Olsen et al., 2007; Shang et al., 2007). PNs come in uniglomerular and multiglomerular varieties, with the latter projecting their dendrites into and integrating signals from multiple glomeruli (Laurent, 2002; Fuscà and Kloppenburg, 2021).

In *Drosophila*, the assortment of OSN types onto different glomeruli means that odor stimuli can be understood as odor-specific topographic activity maps across the repertoire of glomeruli (Vosshall et al., 2000; Wang et al., 2003). Studies in *Drosophila* showed that most tested odorants affect neural firing patterns (either excitatory or inhibitory) in a substantial portion of the total glomeruli, indicating that odors are usually encoded in a combinatorial manner across multiple glomeruli (Wang et al., 2003; Hallem and Carlson, 2006). The central

brain then decodes this activity pattern to interpret odorant identity, concentration, or other features of the local chemical environment. However, some ecologically important odorants like sex pheromones activate only small numbers of specialized ORs and glomeruli that do not typically respond to other odorants, using a "labeled-line" wiring system (Christensen and Hildebrand, 1987; Hildebrand and Shepherd, 1997; Sakurai et al., 2004; Dweck et al., 2007; Kurtovic et al., 2007).

1.4: Elaboration of the chemical communication system in eusocial insects

Many eusocial insects have expanded and highly subdivided olfactory systems, with larger numbers of chemosensory receptor genes and AL glomeruli than are typical for insects. Genomic analyses of several independent lineages of eusocial insects showed that they possess very large numbers of chemosensory receptor genes, with an expansion of IR genes in termites (Terrapon et al., 2014) and expansions of the OR gene family in honeybees (Robertson and Wanner, 2006) and ants (Smith et al., 2011; McKenzie et al., 2016; McKenzie and Kronauer, 2018). In the eusocial Hymenoptera, OR expansion co-occurs with expansion of the number of AL glomeruli (McKenzie et al., 2016). For example, the clonal raider ant *Ooceraea biroi* possesses approximately 500 ORs and glomeruli, in both cases 10x more than *Drosophila melanogaster* (Mysore et al., 2009; Kelber et al., 2010; Smith et al., 2011; Zhou et al., 2012; Zhou et al., 2015; McKenzie et al., 2016; McKenzie and Kronauer, 2018; Ryba et al., 2020; Trible et al., 2017; Ferguson et al., 2021). This elaboration of the chemosensory system is believed to confer greater chemical detection and discrimination abilities, facilitating perception of the large numbers of chemical cues and pheromones used in colony communication.

However, the encoding of olfactory signals across the sensory system has not been comprehensively investigated in any eusocial insect.

1.5: The chemosensory system of the ant

If you have ever watched an ant go about her business from up close, you have likely noticed that her antennae are never still; they constantly tap the area in front of her with delicate movements. In contrast to stubby *Drosophila* antennae, more akin to a nose for sensing chemicals in the air, ant antennae are long, articulated organs that sample both the air and surfaces within reach (Fig 1.1). In the clonal raider ant, the vast majority of the thousands of antennal chemosensory neurons express the conserved insect co-receptor gene *Orco* and are designated as OSNs (Trible et al., 2017), and the antennae express almost all of the OR genes found in the genome (McKenzie et al., 2016). Several types of chemosensory sensilla are found on the antennae, which are categorized as basiconic, coeloconic, and trichoid types based on their morphology. While *Drosophila* chemosensory sensilla each only house dendrites of four or fewer OSNs, in ants, up to 130 OSNs can project their dendrites into the same basiconic sensillum (Ozaki et al., 2005; Sharma et al., 2015). Basiconic sensilla have very broad odor tuning and cannot be easily separated into functional types from single sensillum electrophysiological recordings, indicating that they are innervated by heterogeneous populations of OSNs (Sharma et al., 2015). Furthermore, OSNs innervating the same sensilla may directly interact with one another via gap junctions or ephaptic feedback, suggesting that ant sensilla may perform some types of processing or computation before signals reach the antennal nerve (Takeichi et al., 2018). These features make it extremely challenging to link odor tuning properties to OSN types or OR genes from analyses of the antennae. Two studies made some

progress at this task by heterologous expression of ORs from the ponerine ant *Harpegnathos saltator* in *Drosophila* OSNs, allowing the de-orphanization of a subset of ant ORs (Slone et al., 2017; Pask et al., 2017). However, the low-throughput nature of this approach has so far only allowed examination of 47 out of 347 annotated ORs from *Harpegnathos saltator*, and the relatively narrow receptive ranges of most examined ORs have made it difficult to identify ligands for all tested receptors. (Slone et al., 2017; Pask et al., 2017).

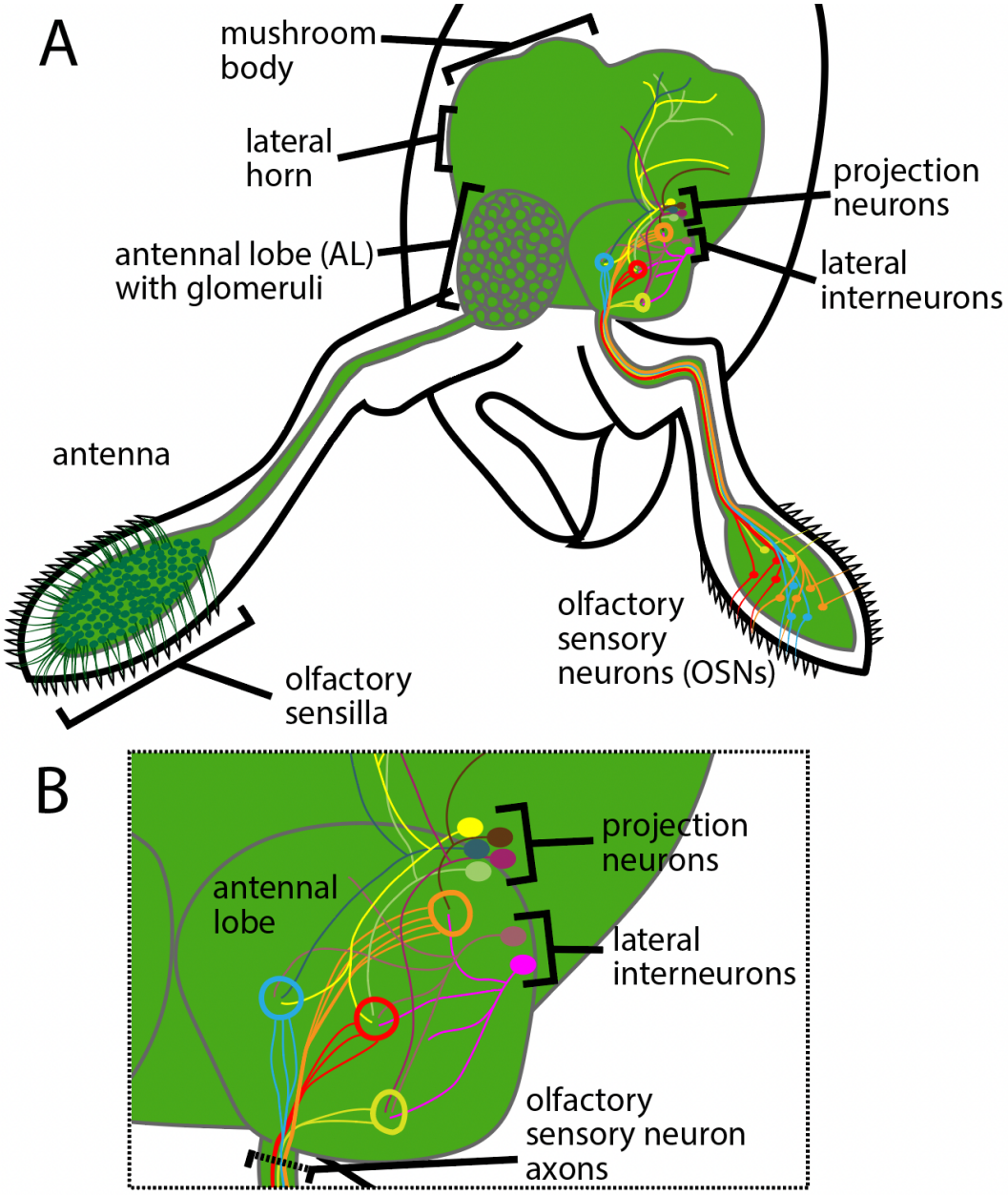

Figure 1.1: Cartoon of the clonal raider ant olfactory system. (A) Clonal raider ant head and antennae. On left, anatomical regions involved in olfaction are shown, highlighting OSN somas in the antenna and the AL glomeruli. On right, a subset of cells from key neuron types are shown, with different sub-varieties shown in different colors. (B) Magnification of the AL from (A).

Several techniques have allowed recording neural activity associated with subsets of the AL glomeruli in various species of eusocial Hymenoptera. Optical recording of odor-evoked calcium activity has been achieved in carpenter ants, leaf-cutting ants, and honeybees by first either staining the brain with diffusible fluorescent calcium dyes, or by injecting dyes into projection neurons (Joerges et al., 1997; Galizia et al., 1998; Galizia et al., 1999a-b; Sachse et al., 1999; Guerrieri et al., 2005; Zube et al., 2008; Brandstaetter et al., 2010; Kuebler et al., 2010; Brandstaetter and Kleineidam, 2011; Brandstaetter et al., 2011; Paoli et al., 2016; Paoli and Galizia, 2021). These studies most frequently used epifluorescence imaging to record calcium activity from the AL surface, or in a few cases used two-photon microscopy to image optical slices of the AL (Haase et al., 2011; Scarano et al., 2022). One study in the carpenter ant *Camponotus obscuripes* instead used electrophysiological recordings from projection neurons to identify alarm pheromone-sensitive neurons (Yamagata et al., 2006). These studies showed important features of odor encoding in ants and honeybees: odor representations have a degree of stereotypy across individuals, glomeruli have characteristic odor response functions, most odorants generated activity in multiple glomeruli, and the representations of different odorants often overlap (Joerges et al., 1997; Galizia et al., 1998; Galizia et al., 1999a-b; Sachse et al., 1999; Guerrieri et al., 2005; Yamagata et al., 2006; Zube et al., 2008; Brandstaetter and Kleineidam, 2011; Paoli et al., 2016; Paoli and Galizia, 2021).

1.6: The question of stereotypy in eusocial insect odor representation

Recent developmental studies in ants have shown that olfactory system development is considerably different from the canonical insect model. In addition to the expansion of the OR and glomerular repertoires, ant OSNs also express odorant receptors from early metamorphosis, and traffic the co-receptor Orco to their axon terminals in the AL (Ryba et al., 2020). Furthermore, ant OSNs do not survive to adulthood without functional *Orco* (Trible et al., 2017; Yan et al., 2017). Based on these differences, it has been suggested that ants, similar to mice but unlike flies, might rely on intrinsic features of ORs for OSN axon guidance and AL patterning (Duan and Volkan, 2020; Ryba et al., 2020). This in turn could translate to increased developmental plasticity in the olfactory system. In both mice and *Drosophila*, olfactory glomeruli receiving input from a defined class of OSNs are consistently located in the same anatomical region, but at the local scale, homologous mouse glomeruli vary substantially in their spatial location across individuals, and even across the left/right axis within a single individual (Schaefer et al., 2001; Strotmann et al., 2000; Lodovichi and Belluscio, 2012; Zapiec and Mombaerts, 2015). Whether the level of anatomical-functional stereotypy of the ant olfactory glomeruli more closely resembles *Drosophila* or mice has not been assessed. However, the number of glomeruli varies with sex, caste, and worker body size (Mysore et al., 2009; Kelber et al., 2010; Kuebler et al., 2010; McKenzie et al., 2016), suggesting that stereotypy may be lower in ants.

1.7: Insect pheromone detection systems

Odor encoding has been most comprehensively studied in solitary insects such as moths and the vinegar fly, which do not possess the large arrays of non-sexual pheromones that

eusocial insects employ to organize their societies. Studies have instead focused on sex pheromones, which are ubiquitous across animals. While non-pheromonal odorants often activate several glomeruli out of the dozens in the fly AL, sex pheromones typically have relatively dedicated receptor proteins and AL glomeruli (Hildebrand and Shepherd, 1997; Christensen and Hildebrand, 1987; Sakurai et al., 2004; Kurtovic et al., 2007). In some moths, sex pheromones emitted by females are detected at extremely low concentrations by specialized receptors in the antennae of males. The corresponding receptor neurons innervate male-specific, enlarged, and spatially segregated AL glomeruli referred to as 'macroglomerular complexes' (Christensen and Hildebrand, 1987; Hildebrand and Shepherd, 1997). In *Drosophila melanogaster*, sex pheromone-sensitive glomeruli are sexually dimorphic in size, but they are not anatomically differentiated from other glomeruli by gross morphology (Dweck et al., 2007; Kurtovic et al., 2007). While most components of insect olfactory systems respond to a range of odor molecules and participate in combinatorial coding, sex pheromone-sensitive receptors and glomeruli usually have narrow tuning and appear largely dedicated to detecting the presence of sex pheromones and transmitting that information to higher brain regions directly. This labeled-line wiring logic is found also in the case of non-pheromone sensory systems that detect environmental chemicals of high ecological importance, such as CO_2 and the microbial volatile geosmin (Jones et al., 2007; Stensmyr et al., 2012).

Eusocial insects use expanded arrays of pheromones to mediate many behaviors beyond sex, and studies have searched for links between pheromone mediated-behaviors and AL morphology. ALs in eusocial Hymenoptera show substantial phenotypic plasticity, with males possessing fewer glomeruli than queens or workers, and workers possessing the largest numbers of glomeruli (Kuebler et al., 2007; McKenzie et al., 2016). The ALs of leaf-cutting ant workers,

which have extreme plasticity in body size, contain variable numbers of glomeruli, with more glomeruli present in the ALs of larger workers, and some large workers also possessing additional enlarged glomeruli that appear similar to macroglomerular complexes for sex pheromones (Kelber et al., 2007; Kuebler et al, 2007). As most pheromone-mediated colony tasks are performed by workers, and task performance varies with body size, these discoveries lend credence to the idea that expansions of the olfactory systems in eusocial insects are to accommodate the perception of many types of non-sexual pheromones.

Understanding pheromone encoding in eusocial insects is a question of major interest, because such systems underlie the exchange of information that allows insect societies to function. Here, I briefly summarize findings on the molecular basis of pheromone perception in ants. In the ants *Ooceraea biroi* and *Harpegnathos saltator*, CRISPR-induced mutation of *Orco* impaired social behaviors such as trail following, aggregation, and brood care, indicating that ORs are likely involved in mediating these behaviors (Trible et al., 2017; Yan et al., 2017). Perturbing Orco-dependent chemoreception with chemical treatments also impaired aggression toward non-nestmates in the carpenter ant *Camponotus floridanus*, implicating ORs in detecting colony membership odors (Ferguson et al., 2020). In another carpenter ant species, a CSP found in basiconic sensilla was found to bind cuticular hydrocarbons, which are the source of colony-specific membership gestalt odors (Ozaki et al., 2005). Several members of the 9-exon OR subfamily from the ponerine ant *Harpegnathos saltator* were shown to be capable of responding to queen pheromone when expressed in *Drosophila* OSNs (Slone et al., 2017). This study and another together showed that *Harpegnathos* ORs have relatively narrow receptive ranges, and members of several OR gene subfamilies are capable of detecting cuticular hydrocarbons (Slone

et al., 2017). Beyond this, little is known is known about the molecular basis of pheromone perception in ants.

The functional basis of pheromone perception has also been investigated in ants. Single sensillum electrophysiological recordings from males of the ant *Harpegnathos saltator* showed that trichoid sensilla respond to alarm pheromones (Ghaninia et al., 2018). Other studies using single sensillum recordings in several ant species showed that some basiconic sensilla responded only to cuticular hydrocarbon mixtures from non-nestmates, but not nestmates, implying that processing of colony membership gestalt odors could occur in the sensilla, before olfactory information reaches the brain (Ozaki et al., 2005; Kidokoro-Kobayashi et al., 2012). However, Brandstaetter et al. (2011) contested these findings in a calcium imaging study that reported no difference in the extent of AL activation in response to nestmate vs. non-nestmate gestalt odors. A calcium dye study in the leaf-cutting ant *Atta vollenweideri* found that a macroglomerulus specific to large workers responded to a trail pheromone component (Kuebler et al., 2011). Several studies using similar methods reported that various alarm pheromone components generated multi-glomerular neural activity on the AL surface in both honeybees and ants, and these studies will be summarized in more detail in a later section (Joerges et al., 1997; Galizia et al., 1998; Galizia et al., 1999a-b; Sachse et al., 1999; Guerrieri et al., 2005; Zube et al., 2008; Brandstaetter et al., 2011; Haase et al., 2011; Carcaud et al., 2015; Paoli and Galizia, 2021; Scarano et al., 2022).

The complexity of the olfactory systems of eusocial insects has so far prevented conducting investigations of pheromone encoding in a comprehensive manner, whether at the level of molecules, ORs, or glomeruli. While the critical role of Orco for social behaviors in ants has been demonstrated, it is otherwise unclear how the sensory components that have been

linked to pheromones would fit into a more complete picture of pheromone encoding. For instance, if response functions of the entire repertoire of glomeruli were recorded from alarm pheromone stimulus, would the overall pattern more resemble combinatorial or labeled-line encoding? The same question must be asked for each pheromone system in turn, as pheromones vary widely in chemical nature and function, and there is no reason to assume the same rules apply to all.

1.8: Challenges for understanding mechanisms of social behavior in eusocial insects

Eusocial insects have featured prominently in studies of social evolution since the formalization of inclusive fitness theory by William D. Hamilton (Hamilton, 1963; Hamilton, 1964a-b). These foundational papers generated predictions related to numerous aspects of insect societies, ranging from sex investment ratios -- to worker policing -- to monogamy at the origin of eusociality. Over the past 50 years, many of these predictions have been tested empirically (Trivers and Hare, 1976; Ratnieks, 1988; Visscher, 1989; Ratnieks and Visscher, 1989; Hughes et al., 2008; Ratnieks et al., 2006; Boomsma, 2013; Kay et al., 2020).

Despite the long history of using eusocial insects as model systems for the study of social evolution, several features of eusocial insect biology limit the available experimental approaches. Most species cannot be propagated in the laboratory, reproduction is generally restricted to one or a few members of the colony (the queens), and generation times relevant for fitness measurements, i.e., from queen to queen, range from many months to years. These traits not only impede the ability to control for genetic backgrounds and conduct longitudinal experiments on feasible timescales, but also hinder genome editing. Much research into social interactions over the past two decades has therefore relied on microbial models instead (e.g. West et al., 2007;

Strassmann et al., 2011; Nadell et al., 2016; Tarnita et al., 2017;). These appealing systems display quick generation times, clonal reproduction, and can be used for mutagenesis or transgenics experiments to empirically examine the mechanisms of social evolution.

Studies using microbes have highlighted key features that determine whether and how cooperative behavior can evolve. Due to the risk posed by non-cooperating "cheater" lineages, microbes ranging from bacteria to amoebae limit the circumstances where they perform costly social behaviors by discriminating against non-relatives (Queller et al., 2003; Santorelli et al., 2008; Benabentos et al., 2009; Strassmann et al., 2011) or employing systems in which non-contributors cannot benefit from the social product (Xavier et al., 2011; Boyle et al., 2015; Boyle et al., 2017; Yan et al., 2019). They also highlight the importance of features that favor cooperative interactions, including a spatial population structure with high relatedness, diminishing returns on cooperation or competition, and lower growth rates (Strassmann et al., 2000; Foster et al., 2004; Kreft et al., 2004; Griffin et al., 2004; Gilbert et al., 2007; Xavier et al., 2007; Nadell et al., 2008; Nadell et al., 2009; Chuang et al., 2009; Strassmann and Queller, 2011). These studies have been greatly aided by the ability to visually differentiate interacting genotypes of microbes by transgenic expression of reporter genes (Dingermann et al., 1989; Smukalla et al., 2008; Xavier et al., 2011).

Many important topics in the study of sociality cannot be studied in microbes, especially the behavioral and neural adaptations for eusocial living. It is clear that the evolution of behaviors for social living, including brood care, division of labor, collective defense, food collection and extensive pheromone communication, required modification of the nervous system. Despite interest in uncovering the neural bases for these adaptations, few molecular or neural mechanisms for these phenomena have been identified and none have been characterized

in detail. This is due both to the complexity of these systems and the near-absence of neurogenetic tools that facilitated neuroscience in canonical model systems, such as *Drosophila melanogaster*.

Today's considerable understanding of olfactory development and function in *Drosophila* were enabled by neurogenetic tools, especially through neural recordings using genetically encoded calcium indicators such as GCaMP targeted to OSNs (Fig. 1.2; Wang et al., 2003, Stökl et al., 2010; Stensmyr et al., 2012). GCaMP is advantageous compared to calcium dye studies because of the possibility of consistent cell type-specific labeling, higher signal-to-noise ratios, and obviating the need to stain each brain before imaging. Among the Hymenoptera, transgenic lines expressing GCaMP have recently been established in honeybees, although GCaMP was expressed broadly across neurons and the reported calcium imaging data appear to be of a similar quality to dye-based studies (Carcaud et al., 2022). Transgenics methods have so far not been established in any other eusocial or Hymenopteran species. Finally, because eusocial Hymenoptera possess hundreds of glomeruli which are arranged in layers, understanding odor encoding will require higher throughput methods for linking odors to responding glomeruli. Conventional calcium imaging using a stationary objective only allows recording from a fraction of the glomeruli from a single trial (typically imaging 10-25% of total glomeruli). Single neuron electrophysiological recording studies have even lower throughput. As a result, most of the glomeruli have never been functionally characterized in any Hymenopteran species. Coming to a more complete understanding of pheromone encoding in eusocial insects, especially identifying functional elements of the olfactory system that drive social behaviors, will depend on implementing additional experimental tools to overcome the complexity of the olfactory systems in these species.

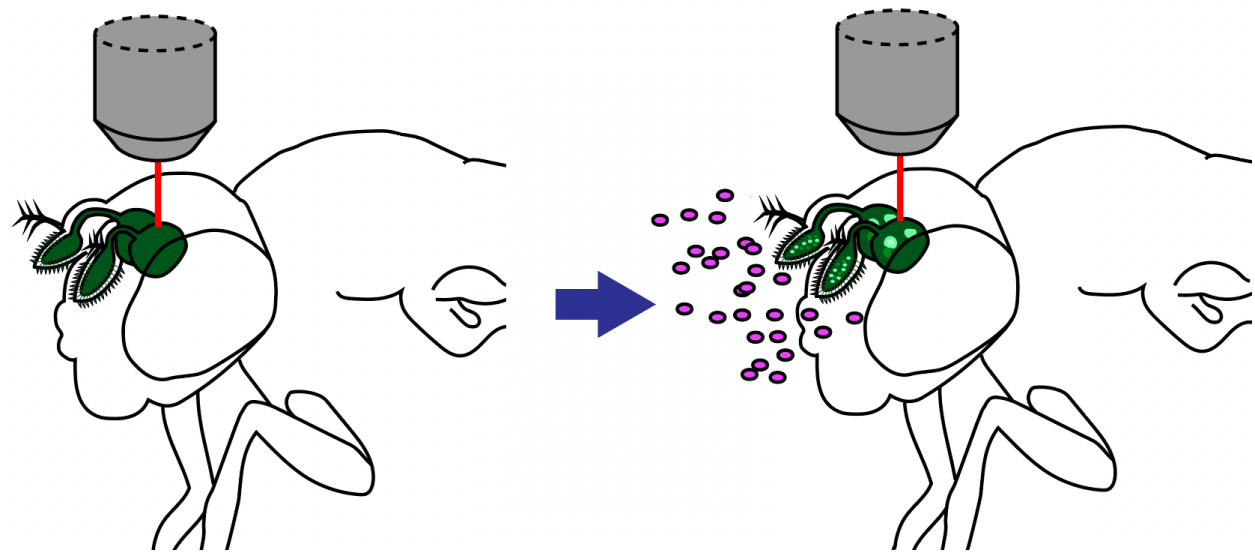

Figure 1.2: GCaMP imaging of odor-evoked neural activity in the antennal lobe. Cartoon of an experiment in *Drosophila melanogaster* expressing GCaMP in OSNs. Before odor presentation, OSN calcium levels are at baseline and GCaMP fluorescence is low (left). After odor presentation (magenta ellipses), a subset of OSNs respond, allowing detection of calcium increases in their associated AL glomeruli using fluorescence microscopy (right).

1.9: Alarm pheromones

Out of numerous types of pheromones used by social insects, alarm pheromones, chemical signals for danger, are especially well characterized. Alarm pheromone systems are found in both solitary and social animals, but systems in eusocial insects are specialized for activating collective defense (Wilson and Regnier, 1971; Verheggen et al., 2010; Enjin and Suh, 2013). Stimulating individuals with alarm pheromone volatiles is experimentally simple and quickly leads to behavioral responses, which makes them attractive models for studying the neurobiological basis of chemical communication. Upon perception of the pheromone, locomotion usually increases and aggression or "panic" commences (Wilson and Regnier, 1971). The alarm response can culminate in nest evacuation, where ants leave the nest carrying brood (Duffield et al., 1976; Smith and Haight, 2008). Specific features of alarm behavior vary with context, species, and specific mixtures and concentrations of chemicals, but in eusocial insects

frequently include either frenzied panic responses or attraction to the alarm source, as well as changes in the posture of antennae, mandibles, and the sting (Blum, 1969; Vander Meer and Alonso, 1998).

Despite a wealth of behavioral and chemical ecology data on alarm pheromones, the neural representation of alarm pheromones is not well understood in eusocial insects. Alarm pheromone representation has been investigated using calcium dyes to record activity from the AL surface in several carpenter ant species (Galizia et al., 1999b; Zube et al., 2008; Brandstaetter et al., 2011) and in honeybees (Joerges et al., 1997; Galizia et al., 1998; Galizia et al., 1999a; Sachse et al., 1999; Guerrieri et al., 2005; Carcaud et al., 2015; Paoli and Galizia, 2021; Haase et al., 2011; Scarano et al., 2022). These studies found broad, multi-glomerular activation patterns after alarm pheromone presentation without evidence for specialized glomerulus clusters, similar to the combinatorial representation of non-pheromonal odors in *Drosophila* (Joerges et al., 1997; Laurent, 1999; Hallem and Carlson, 2006; Wang et al., 2003; Carcaud et al., 2015; Münch and Galizia, 2016).

Under such a broadly tuned, combinatorial model, the expansion of the glomerular repertoire implies that odor mixtures could potentially activate combinations of hundreds of glomeruli. Because the number of potential combinations of glomeruli grows super-linearly with each additional glomerulus, increasing the number of glomeruli by 10x from *Drosophila* to ants could amplify the possible glomerular ensembles by many orders of magnitude. This scenario poses enormous challenges for higher order neurons in decoding multicomponent olfactory signals, detecting and identifying pheromones, and activating appropriate behavioral responses. This is especially true for small insect brains like those of ants, which have a similar number of neurons to *Drosophila*. In contrast, narrower tuning, where most odorants only activate a small

number of glomeruli as is typically the case for sex pheromones (Dweck, Kurtovic et al., 2007; Christensen and Hildebrand, 1987; Sakurai et al., 2004; Hildebrand and Shepherd, 1997), could simplify the neural architecture necessary for processing odor information in the complex olfactory environment of an ant colony and ensure that pheromone signals remain salient.

1.10: The clonal raider ant: a model system for mechanistic study of social behaviors in eusocial insects

The clonal raider ant is an experimentally tractable relative of the army ants that lives in small colonies and preys on other ant species (Oxley et al., 2014; Trible et al., 2017; Chandra et al., 2021). This species has unusual potential as a model system for the study of social interactions, because it provides an opportunity to combine the rich natural history knowledge of eusocial insects with some of the experimental advantages of model systems like microbes and the vinegar fly. Unlike other eusocial insects, colonies of clonal raider ants are queenless, all workers can reproduce clonally (Tsuji and Yamauchi, 1995; Ravary and Jaisson, 2004; Kronauer et al., 2012), and offspring are produced as age-synchronized cohorts during reproductive cycles lasting approximately 34 days (Fig. 1.3; Ravary and Jaisson, 2002; Ravary et al., 2006). Different wild type clonal genotypes can be collected in the field and propagated indefinitely in the laboratory (Trible et al., 2020). They can then be mixed in experimental colonies, allowing researchers to control colony size, age structure, and genotypic composition. Despite lacking a queen caste, clonal raider ants exhibit two distinct morphotypes: the regular workers and intercastes, which have queen-like characteristics including larger size, possession of eye-spots, and more ovarioles (Ravary and Jaisson, 2004; Teseo et al., 2014a). They also exhibit behavioral and task performance changes with age (age polyethism), like other eusocial insects (Ravary and

Jaisson, 2004; Teseo et al., 2014b; Ulrich et al., 2021). These features have allowed direct tests of the roles of colony demographic properties in colony fitness and division of labor (Teseo et al., 2014a; Ulrich et al., 2018; Ulrich et al., 2021). Crucially, some of the pheromone molecules used in chemical communication by clonal raider ants have been identified, including two alarm pheromone components (Lopes et al., 2022). CRISPR-induced mutant lines can be generated in clonal raider ants (Trible et al., 2017), which are very difficult to achieve in most eusocial insects due to long generation times, worker sterility, and difficulty with laboratory crosses. Thus, the clonal raider ant makes an especially good experimental system among eusocial insects, and implementing transgenic tools in this species would open a wide range of new possibilities, especially using neurogenetic tools for functional neuroscience in eusocial insects.

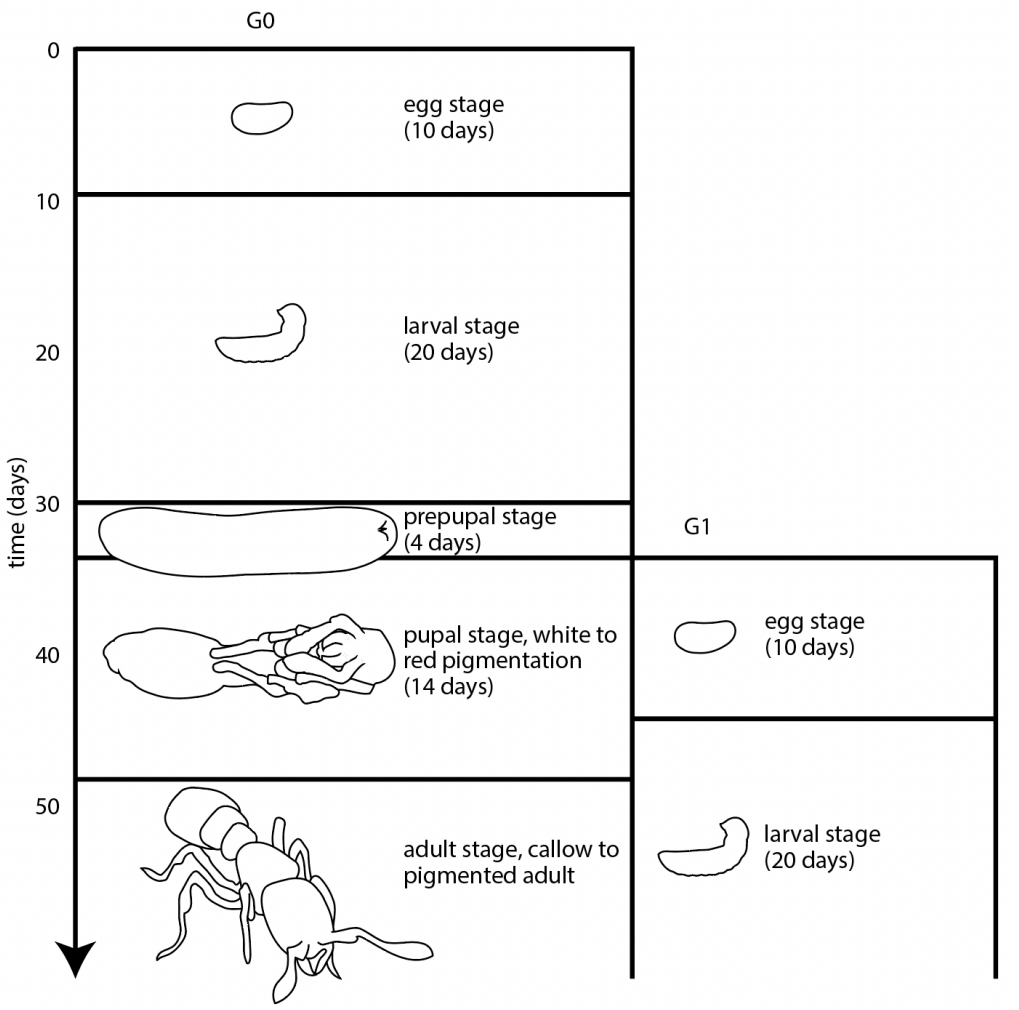

Figure 1.3: Reproductive cycles of the clonal raider ant. Adapted from Ravary and Jaisson (2002).

1.11: Summary of conclusions

Chapter 2 describes the implementation of the first transgenic tools in ants, where we report the development of a piggyBac transgenesis protocol for the clonal raider ant, and characterize several transgenic lines. We validate a suite of transgenic tools in clonal raider ants, including the easily detectable fluorescent reporter gene ie1-DsRed, the promoter/enhancer fragment ObirOrco that drives transgene expression in clonal raider ant OSNs, the QF2/QUAS binary expression system, and the genetically encoded calcium indicator GCaMP.

Chapter 3 describes the development of a GCaMP-based imaging method for recording odor-evoked neural activity in vivo from the clonal raider ant AL. Together with volumetric two-photon imaging, this neurogenetic system made it possible to study the representation of olfactory signals in the ALs of a eusocial insect with unprecedented completeness and precision. We found that general odorants generate disparate glomerular response patterns, with most odorants evoking spatially restricted activity patterns, but very broad across-glomerulus patterns for another. We then tested a panel of five ant alarm pheromones in a colony alarm behavior bioassay, and then characterized their neural representation in the AL. This revealed that alarm pheromone representation is sparse and stereotyped across individuals. We also found that three panic-inducing pheromones activate a single shared glomerulus, suggesting the presence of a neural circuit for panic alarm behavior mediated through this glomerulus.

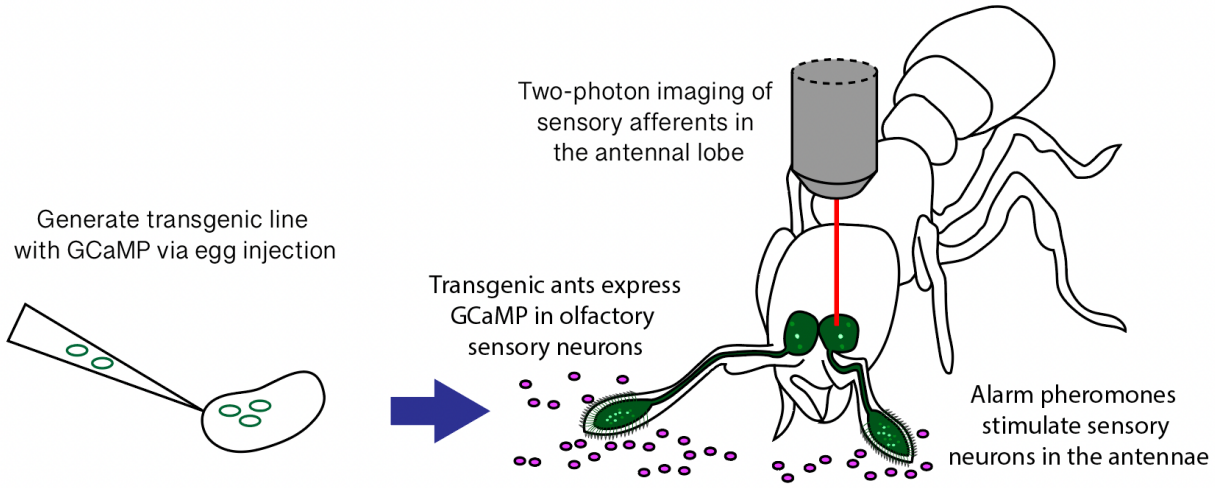

Figure 1.4: Cartoon of project designs in this thesis. Generate a transgenic line with GCaMP expressed in olfactory sensory neurons, then record alarm pheromone-evoked calcium responses in the AL.

CHAPTER 2: DEVELOPMENT OF A PIGGYBAC TRANSGENICS METHOD FOR THE CLONAL RAIDER ANT

2.1: piggyBac transgenesis

Protocols for transgenics, the integration of foreign DNA into genomes, have not yet been reported in any ant species. This has prevented establishing the transgenic and neurogenetic tools that facilitated mechanistic studies in other systems such as microbes and the vinegar fly. Several methodologies for generating transgenic organisms have been developed, making use of various enzymes such as transposons, integrases, and CRISPR (Largaespada, 2003; Groth et al., 2004; Jasin and Haber, 2016). After taking into consideration expected transformation efficiencies from experiments in other organisms, as well as the low hatch rates associated with CRISPR DNA cutting in the clonal raider ant (Gregory et al., 2016; Trible et al., 2017), we decided to attempt transgenesis using piggyBac transposons. This approach involves injection into the embryo of a mix containing a source of the piggyBac transposase enzyme (mRNA or plasmid) and a plasmid vector carrying the transgene construct with appropriate transposase recognition sites, called terminal repeats. The method has potential drawbacks because of the pseudorandom insertions, which cannot be targeted, and the possibility for multiple integrations, which could increase the potential for disruption of endogenous genes. However, the method has been successful in a wide range of insect species, including honeybees, the only Hymenopteran in which transgenesis has been achieved (Schulte et al., 2014; Gregory et al., 2016; Otte et al., 2018). Furthermore, new variants of the piggyBac transposase sequence have improved integration rates (Otte et al., 2018), giving us hope that we could develop a protocol for the clonal raider ant. We built on the previously described methods for embryo injections and larva rearing that were designed for CRISPR mutagenesis in the clonal raider ant (Trible et al., 2017) and adapted them for piggyBac transgenesis.

2.2: Transgene constructs

It is unknown how the clonal raider ant olfactory system encodes alarm pheromones. Previous work from our group demonstrated that the odorant receptor co-receptor *Orco* is expressed specifically in all OSNs (Ryba et al., 2020; Trible et al., 2017), and we reasoned that transgenic ants expressing GCaMP under control of an *Orco* promoter could allow optical recording of neural activity in OSN afferents in the ALs, as has been done in other insects (Stensmyr et al., 2012; Stökl et al., 2010; Wang et al., 2003; Zhao et al., 2022). To achieve this, we cloned a 2.4 kb genomic fragment upstream of the clonal raider ant *Orco* gene, including intergenic sequence and the entire 5' UTR, which presumably contained promoter and enhancer elements sufficient to drive expression in clonal raider ant OSNs (fragment ObirOrco). We constructed two piggyBac vector plasmids based on this fragment: The first construct used ObirOrco to drive expression of GCaMP6s (Chen et al., 2013) using the QF2 and 15xQUAS binary expression driver and effector elements (Riabinina et al., 2015). We assembled QF2 and 15xQUAS in tandem and directly between ObirOrco and GCaMP6s, under the assumption that the strong binding between QF2 and the QUAS promoter elements would amplify transgene expression compared to using ObirOrco alone (Fig. 2.1A). Because we did not know if GCaMP6s would be detectable in live animals, we included an expression construct with the baculovirus-derived ie1 enhancer/promoter element to drive broad expression of the red fluorescent protein DsRed (Fig. 2.1A) (Anderson et al., 2010). Similar regulatory elements based on baculovirus ie1 sequences drive strong, broad expression of transgenes in both *Drosophila melanogaster* and *Bombyx mori* (Suzuki et al., 2003; Masumoto et al., 2012), and we hypothesized that they might produce a similar, easily detectable phenotype in clonal raider ants. We also cloned an additional, minimal construct containing ObirOrco-jGCaMP7s (Dana et al.,

2019) as a possible alternative for imaging experiments (Fig. 2.1B). Finally, we cloned a construct with ie1-DsRed alone which could be used in experiments requiring an easily detectable, heritable phenotype (Fig. 2.1C).

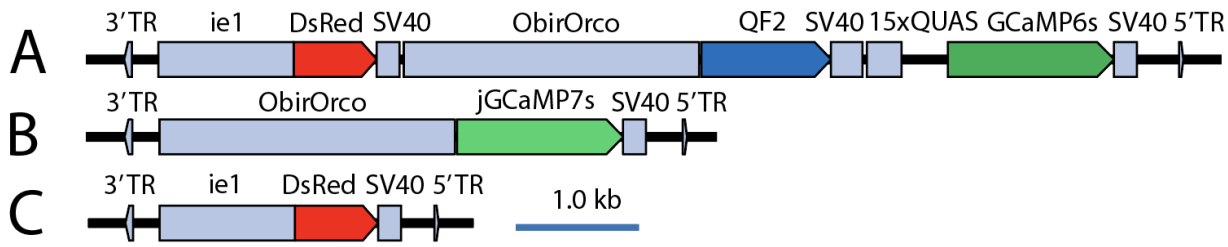

Figure 2.1: Transgene constructs. (A) pBAC-ie1-DsRed, ObirOrco-QF2, 15xQUAS-GCaMP6s. (B) pBAC-ObirOrco-jGCaMP7s. (C) pBAC-ie1-DsRed.

2.3: Injection parameters

For each construct, we injected ant eggs with a mix of plasmid DNA and transposase mRNA (transcribed in vitro from the hyperactive transposase hyPBase[apis]; Otte et al., 2018) and reared the resulting G0 individuals using protocols modified from Trible et al., 2017 (see methods for details, Table 2.1). For the GCaMP6s construct, we varied the age of eggs and the concentration of transposase mRNA in the injection mix. Higher rates of fluorescent G0s were obtained when eggs were <3 hours old rather than <5 hours old at the time of injection. Mixes with >110ng/µL mRNA concentrations produced low hatch rates and no fluorescent G0s (Table 2.1). Based on the precedent for mutagenesis in clonal raider ants from Trible et al. (2017), our injection protocol was initially developed using only clonal line B eggs (Table 2.1). However, in a later experiment where we injected the ie1-DsRed construct, we tested separate batches of clonal line A eggs in addition to the clonal line B condition (Table 2.1).

2.4: Rearing transgenic lines

Adults arising from the injected eggs (G0 adults) were reared in groups, and their clonally produced eggs were fostered into colonies of wild type clonal raider ants and reared to G1 adults (Fig. 2.2A). G1 adults with visible fluorescence were isolated and individually placed in colonies of wild type ants. Because individuals were injected as G0 eggs and then experienced a single-nucleus bottleneck between the G0 and G1 generations, all descendants of a single G1 individual have identical transgene insertion sites. Eggs produced by these colonies were removed and fostered into new colonies, from which fluorescent individuals (G2 and subsequent generations) were returned to the nest containing their G1 parent (Fig. 2.2B). Once colonies had reached stable sizes, wild type ants were removed (Fig. 2.2C). This procedure yielded isogenic colonies of fluorescent individuals derived from single founders. Although we generated several separate transgenic lines, we only reared the line deriving from the first set of injections to large population sizes, and this line was used for all later characterization of the [ie1-DsRed, ObirOrco-QF2, 15xQUAS-GCaMP6s] phenotypes (first four rows, Table 2.1). We also generated a line carrying [ObirOrco-jGCaMP7s] which we maintained at a smaller population size, and generated a total of three lines from treatments with ie1-DsRed. We inferred the presence of two distinct lines of clonal line A ants carrying ie1-DsRed due to distinct, heritable differences in baseline DsRed fluorescence (Table 2.1). We expanded the ie1-Dsred, clonal line B ants to a large isogenic population, and did the same for one of the two ie1-DsRed, clonal line A transgenic lines.

Injected construct	Clonal line	Treatment $\frac{\frac{pmol}{\mu L} DNA}{\frac{ng}{\mu L} RNA}$	Egg age at injection (hours)	# eggs injected	# G0 eggs hatched	# G0 adults eclosed	# G0 adults eclosed with fluorescence	Minimum # of lines generated	Overall efficiency	Transformation efficiency
ie1-DsRed, ObirOrco-QF2, 15xQUAS-GCaMP6s	B	27.8/110	<5	1945	155 (8.0%)	14	3	1	0.00021	0.018
ie1-DsRed, ObirOrco-QF2, 15xQUAS-GCaMP6s	B	27.8/220	<5	1367	72 (5.3%)	16	0			
ie1-DsRed, ObirOrco-QF2, 15xQUAS-GCaMP6s	B	27.8/440	<5	739	6 (0.8%)	0	0			
ie1-DsRed, ObirOrco-QF2, 15xQUAS-GCaMP6s	B	27.8/110	<3	637	15 (2.4%)	25	5			
ie1-DsRed, ObirOrco-QF2, 15xQUAS-GCaMP6s	B	27.8/110	<3	353	44 (12.5%)	17	2	1	0.0028	0.059
ObirOrco-jGCaMP7s	B	27.8/110	<3	803	67 (8.3%)	24	2	1	0.0012	0.042
ie1-DsRed	A	27.8/110	<3	258	41 (15.9%)	16	3	2	0.0078	0.125
ie1-DsRed	B	27.8/110	<3	660	37 (5.6%)	5	2	1	0.0015	0.20

Table 2.1: Injection parameters and results. The "Treatment" column indicates the concentrations of plasmid DNA and transposase mRNA used in the injection mix. G0 adults from the first four treatments were reared as a group, and we therefore cannot determine which treatment generated the single line that was propagated from that group. Overall efficiency was calculated by dividing the minimum number of lines generated by the number of eggs injected; transformation efficiency was calculated by dividing the minimum number of lines generated by the number of G0 adults eclosed.

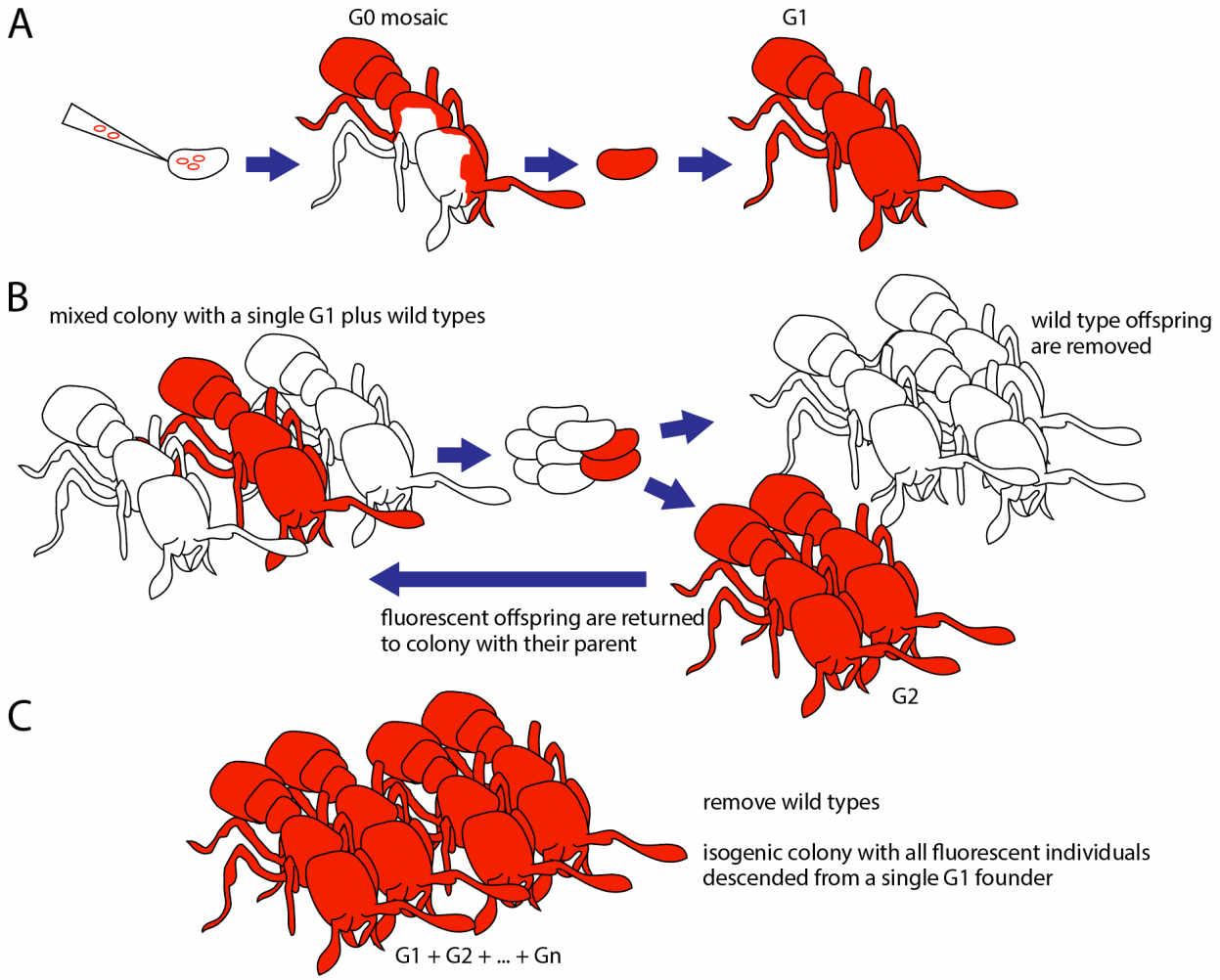

Figure 2.2: Rearing procedure for generating isogenic colonies of transgenic ants. (A) Transgenesis is achieved through egg microinjection, and transgenic animals are identified by fluorescent protein expression visible under epifluorescence (red individuals). The initial transgenesis process can yield mosaic G0 animals. In the subsequent G1 generation, mosaicism is eliminated. (B) Single G1 animals are placed in mixed colonies with wild types and allowed to lay eggs. These eggs may be cross-fostered by chaperone ants. The resulting offspring are then checked for fluorescence, with fluorescent G2 individuals returned to the colony containing their parent, while wild type offspring are removed. (C) After several reproductive cycles, the expanded population of transgenic individuals becomes self-sustaining. Wild types are then removed, leaving only transgenic individuals descended from a single G1 founder.

2.5: Phenotypes of ie1-DsRed

We initially identified the presence of transgenic animals among the G0 ants by examining live animals under an epifluorescence microscope and visually confirming

fluorescence. The simplest means of doing so was to look for DsRed fluorescence from ie1-DsRed, which was possible in all transgenic lines except for ObirOrco-jGCaMP7s due to the absence of that transgene. As expected from experiments in other insects (Suzuki et al., 2003; Masumoto et al., 2012), ie1-DsRed led to a broad fluorescence pattern that was detectable from larvae through adults (Fig. 2.3A). Because the strongest DsRed fluorescence was detected from the gaster, we dissected gasters from both clonal line B transgenic animals and wild type animals to identify the source of the fluorescence. DsRed most strongly labels a pair of bilateral, elongated structures that appear to be the poison gland filaments (Fig. 2.3B-C; Billen, 1986; Hölldobler and Wilson, 1990). The malpighian tubules are also labeled (Fig. 2.3B). DsRed label is also found in cells associated with the fat body (Fig. 2.3D-F). To see if ie1-DsRed might impact neuroscience experiments, we checked whether fluorescence was visible in the brain. No fluorescence was detectable in this organ (Fig. 2.4).

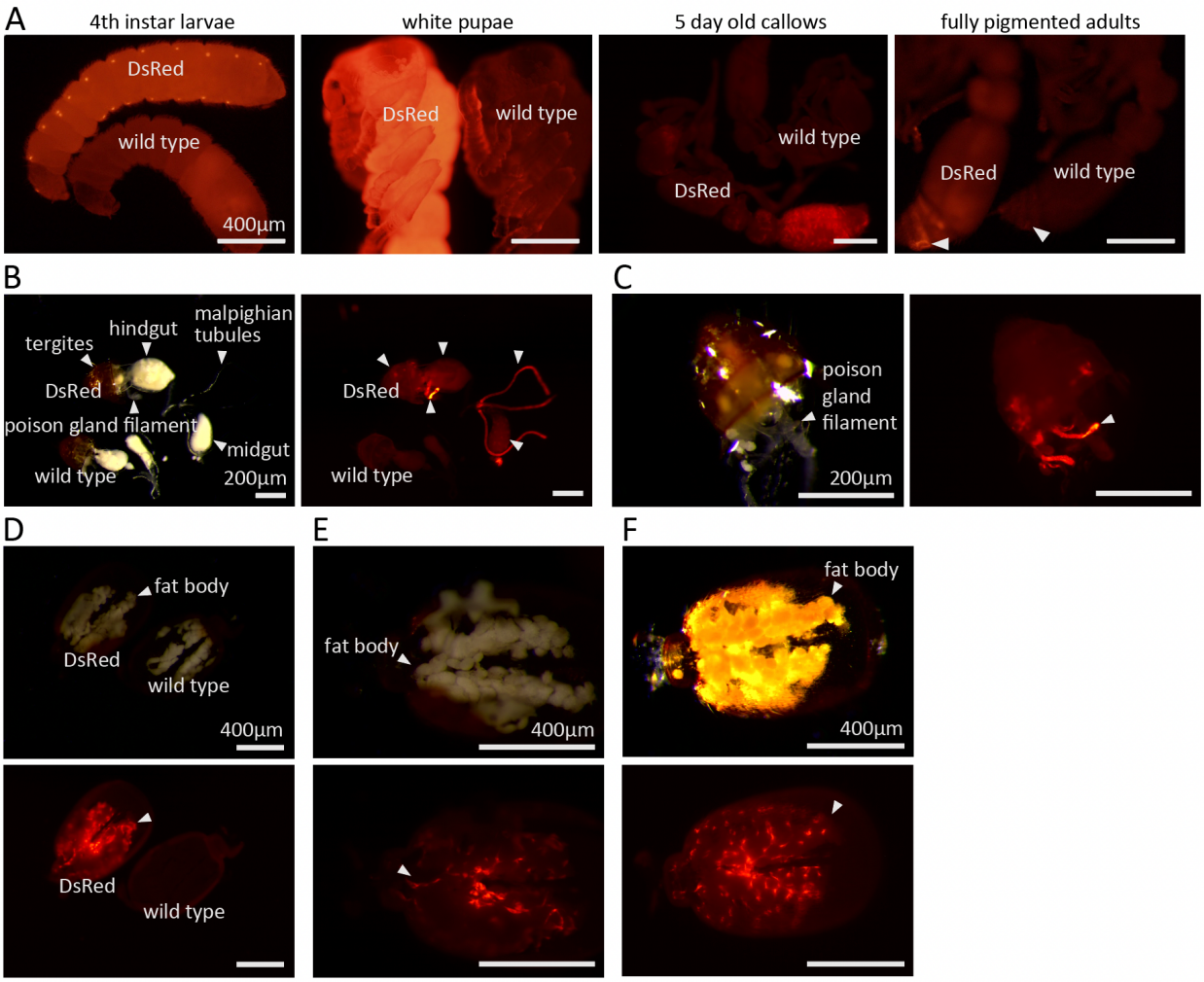

Figure 2.3: Fluorescence phenotypes of ie1-DsRed in the clonal raider ant. (A) Fluorescence is visible in 4th instar larvae (left); pupae (middle left); 5 day old callows (middle right); and fully pigmented adults (right). Images were taken using an epifluorescence microscope. All individuals were from clonal line B. (B-F) Dissection of the gaster of a callow reveals the localization of ie1-DsRed signal. In B and D, clonal line B transgenic and wild type animals are shown side by side. (B) DsRed fluorescence intensely labels the poison gland filaments and malpighian tubules. (C) Close-up on what appears to be the poison gland filaments. (D-F) DsRed labels cells associated with the fat body, showing the inner side of the cuticle (D-E), and looking through the transparent cuticle (F). Anatomy is labeled only on dissections of transgenic individuals to reduce clutter.

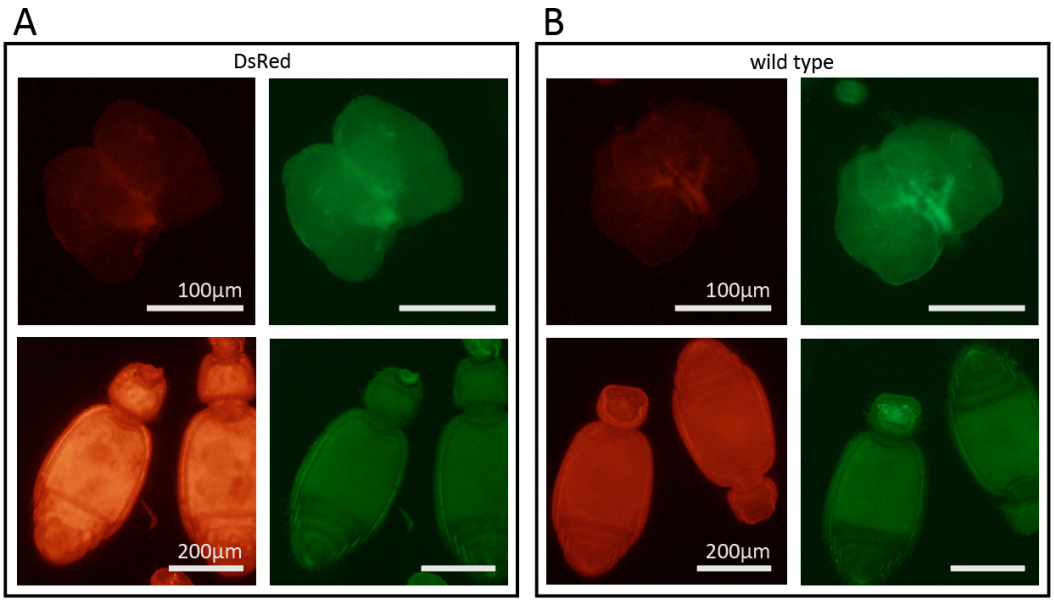

Figure 2.4: Comparison of ie1-DsRed fluorescence in brains and gasters. In transgenic clonal line B ants with ie1-DsRed, DsRed fluorescence is detectable in gasters, but only autofluorescence is detectable in brains. (C) Comparison showing red and green channel autofluorescence in wild type animals.

2.6: Phenotypes of ObirOrco-GCaMP

Fluorescence from GCaMP6s and DsRed were highly visible and consistent in pupae with [ie1-DsRed, ObirOrco-QF2, 15xQUAS-GCaMP6s] before pigmentation begins (Fig. 2.5). GCaMP was always most strongly detected in the pupal antennal club, consistent with expression in OSNs (Figs. 2.5-2.6A). However, the signal intensity in pupae carrying ObirOrco-jGCaMP7s was dramatically weaker than in pupae carrying [ie1-DsRed, ObirOrco-QF2, 15xQUAS-GCaMP6s], and we inferred that expression amplification from QF2/QUAS led to higher levels of GCaMP expression in the latter line (Fig. 2.6A). We decided to use this line for imaging experiments (from here on referred to as "GCaMP6s ants") and did not further characterize the ObirOrco-jGCaMP7s line.

We also found that DsRed is expressed at a low level in the AL in this the GCaMP6s ants, possibly due to leaky expression from ObirOrco (Fig. 2.6B). We assessed the expression of GCaMP6s in OSNs in the antennal club using immunohistochemistry and found that GCaMP6s labels the great majority of Orco-positive cells (Fig. 2.6C). Examination of brains from GCaMP6s ants showed high levels of GCaMP6s in the ALs, where it co-localizes with Orco, which labels OSN afferents (Fig. 2.6D). GCaMP6s is also expressed in parts of the sub-esophageal zone and central complex (Fig. 2.6E-F).

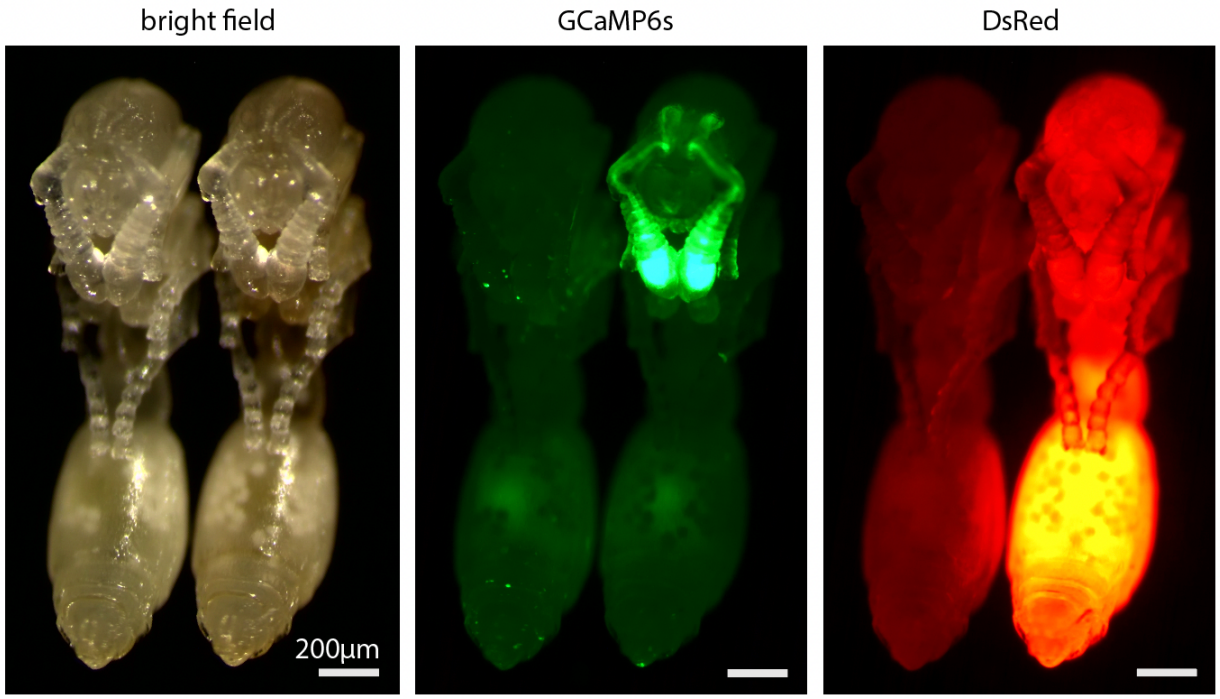

Figure 2.5: Fluorescence phenotypes of ObirOrco-GCaMP6s versus wild type pupae. The same two clonal line B pupae, one wild type and one transgenic, were imaged under bright field (left) and epifluorescence, with filters set to detect GCaMP6s (middle) and DsRed (right). Pupae were imaged 10 days after pupation.

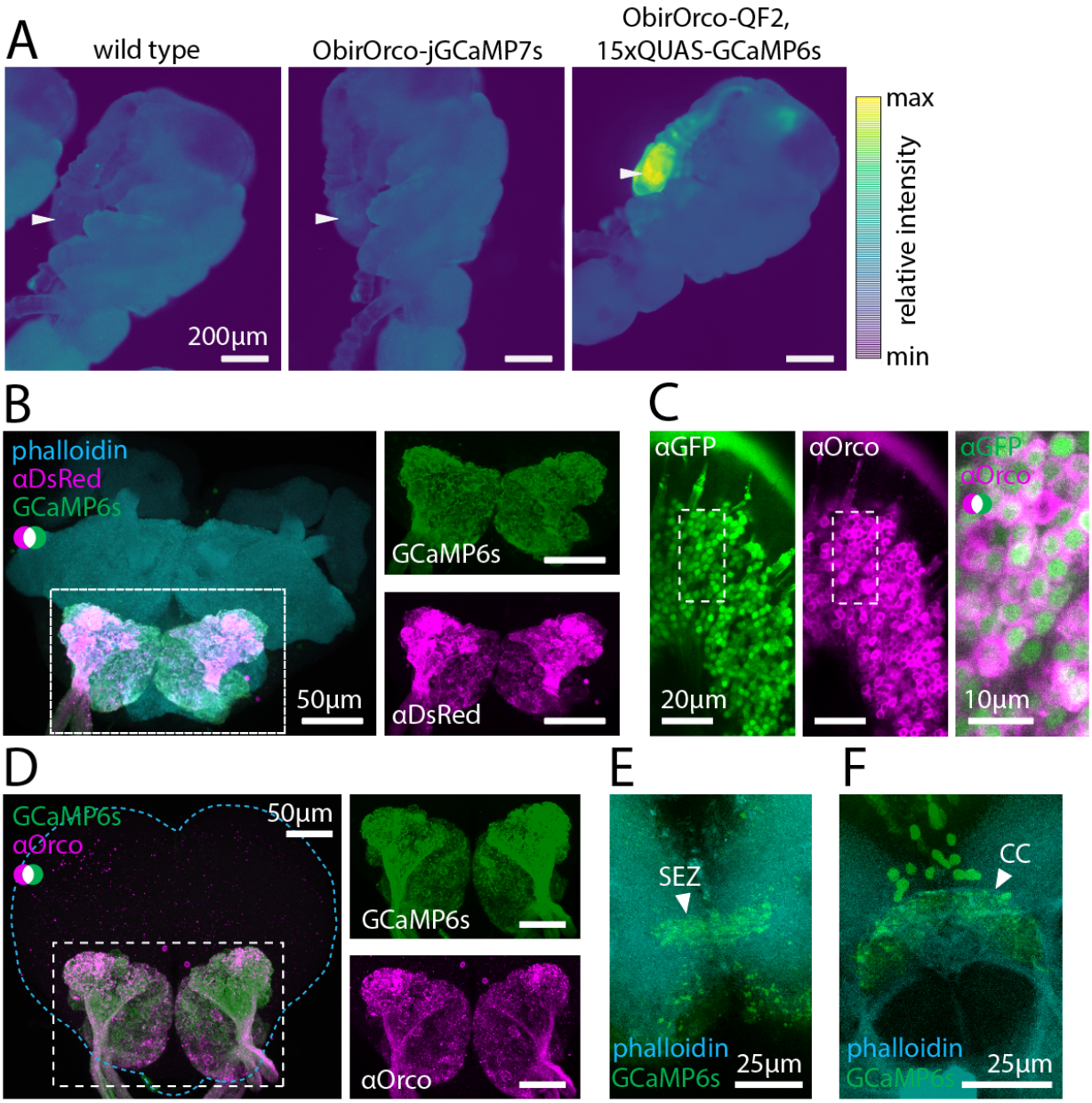

Figure 2.6: Additional fluorescence phenotypes of ObirOrco-GCaMP. (A) Comparison of GCaMP fluorescence levels in wild type, ObirOrco-jGCaMP7s, and [ObirOrco-QF2, 15xQUAS-GCaMP6s] individuals under epifluorescence. The images show pseudocolor of pixel intensity. Animals were imaged ~7 days after pupation, when GCaMP fluorescence becomes visible in the transparent pupal antennal club (arrowheads), but before melanization begins. Fluorescence is detectable in both transgenic lines but is much brighter in the line carrying the QF2/QUAS system. (B) Anti-DsRed (magenta) labels the ALs, indicating co-expression of DsRed with GCaMP6s (green; endogenous fluorescence) in ants carrying [ie1-DsRed, ObirOrco-QF2, 15xQUAS-GCaMP6s]. Phalloidin stains actin (cyan). (C) Anti-GFP (green, cytoplasmic) and anti-Orco (magenta, membrane bound) densely label OSNs in the antennal club (max z-projection through 3 1µm slices of whole-mounted tissue). (D) GCaMP6s and anti-Orco signal co-localize in the ALs (max z-projection through the AL); brain contour is shown with cyan line.

(E) GCaMP6s fluorescence (green) is detectable in the subesophageal zone (SEZ). (F) GCaMP6s fluorescence (green) is also visible in processes innervating part of the central complex (CC) as well as in a nearby cluster of somas. Images show max z-projections through the imaged brain regions.

Examination of GCaMP6s brains stained with anti-Orco revealed that all Orco-positive glomeruli were also GCaMP6s-positive (GCaMP6s+) (Fig. 2.7). The ~6 glomeruli of the T7 cluster are the only Orco- glomeruli (Mckenzie et al., 2016; Ryba et al., 2020), and GCaMP6s labeling in the area mapping to the T7 cluster was weak or absent, supporting specific expression of the transgene (Fig. 2.7). The antennal mechanosensory and motor center (AMMC), another adjacent Orco- structure (Habenstein et al., 2020; Ryba et al., 2020), was also GCaMP6s- (Fig. 2.7). This indicates that our transgenic line in principle allows us to detect calcium responses from all olfactory glomeruli of the AL (about 99% of total glomeruli) with high specificity. To see whether GCaMP6s is expressed by cells other than OSNs in the ALs, we performed unilateral antennal ablations on transgenic animals to sever the antennal nerve and examined their brains after allowing the fluorescent proteins to be cleared for one month (n=3 brains). GCaMP6s and anti-Orco signal was greatly reduced across the entire AL connected to the ablated antenna, and no clear glomerular labeling remained (Fig. 2.8A). This indicates that GCaMP6s signal in the AL derives from the antennae and is likely to be exclusive to sensory neuron axons. GCaMP6s signal in the sub-esophageal zone and central complex was not affected by the antennal ablation (Fig. 2.8B).

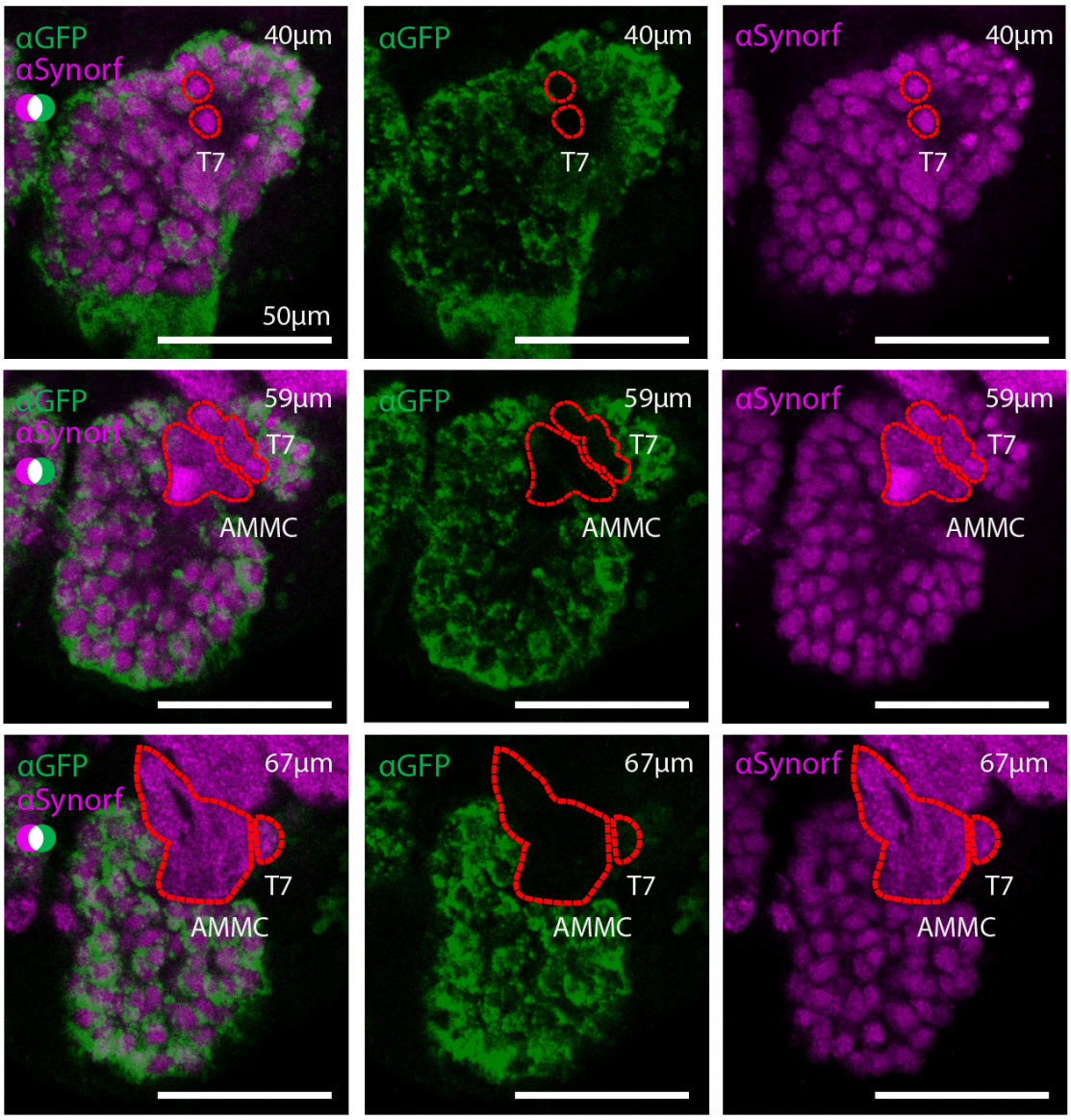

Figure 2.7: ObirOrco-GCaMP6s specifically labels olfactory glomeruli. All glomeruli are visible with anti-Synorf, which stains neuropil (magenta). At 40µm (top row), 59µm (middle) and 67µm (bottom) (single z-slices), the T7 glomerulus cluster is visible. Whereas anti-GFP labeling of GCaMP6s (green) is strong in the rest of the AL glomeruli, this signal is very weak or absent in the T7 glomeruli and absent in the antennal mechanosensory and motor center (AMMC).

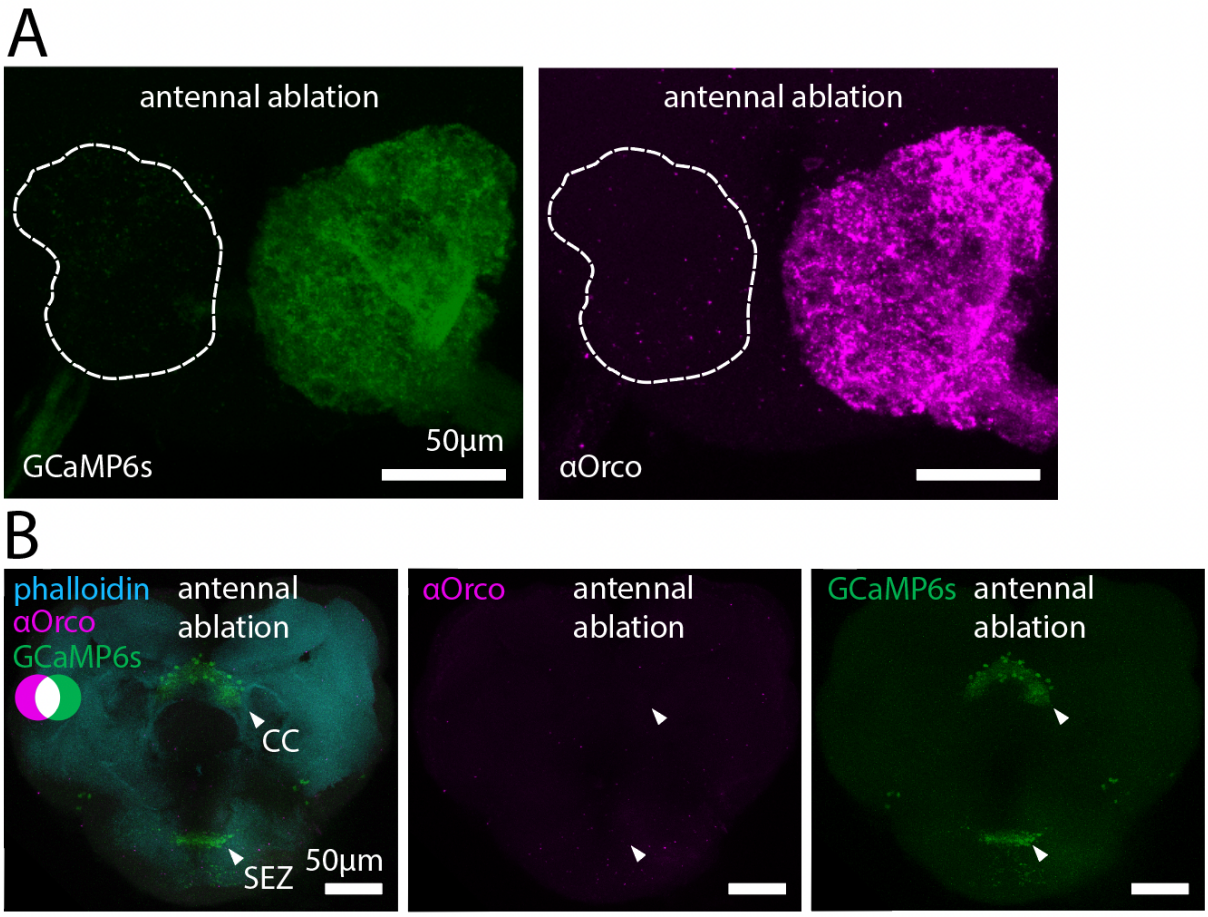

Figure 2.8: Unilateral ablation of the antenna eliminates GCaMP6s signal in the antennal lobe. Right antenna was ablated from the scape, with brain fixation and staining occurring one month later. (A) Signal from GCaMP6s (left) and anti-Orco signal (right) is eliminated from the antennal lobe (max z-projections of confocal z-stacks). (B) Bilaterally symmetrical GCaMP6s signal is still detectable in the central complex (CC), as well as the subesophageal zone (SEZ). No anti-Orco signal was detected in these brain regions. Images show max z-projections through the imaged brain regions.

Introduction of transgenes can sometimes disrupt endogenous sequences, and expression of genetically encoded calcium indicators can alter cellular calcium buffering and affect behavior (Ferkey et al., 2007; Bellen et al., 2011; Tian et al., 2012). We therefore examined whether the GCaMP6s ants had defects that could be relevant to the study of odor encoding. To confirm normal anatomy of the AL, we manually reconstructed glomeruli from a GCaMP6s ant and

counted a total of 505 glomeruli, which is within the range of counts in wild type ants (493-509 glomeruli; McKenzie et al., 2016; Trible et al., 2017; Ryba et al., 2020) (Fig. 2.9).

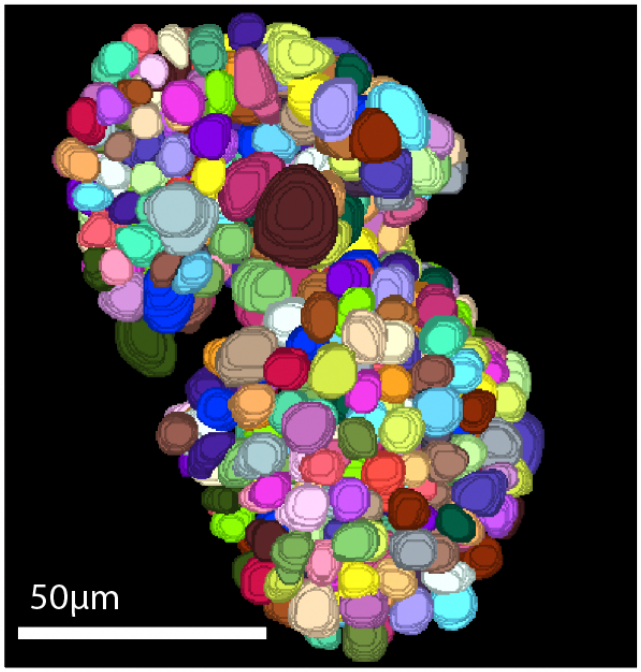

Figure 2.9: GCaMP6s ants have anatomically normal antennal lobes. 505 glomeruli were manually reconstructed from the right AL of a GCaMP6s ant stained with anti-Synorf.

2.7: Genomic analyses of transgenic lines.

To count transgene insertions and map their positions within the genome, we conducted whole genome resequencing for one individual each from the GCaMP6s line, and the clonal line A and clonal line B transgenic lines. We aligned reads separately to the *O. biroi* reference genome (McKenzie and Kronauer, 2018) and to the transgene sequence and compared the average read depths to infer the number of transgene insertions. For the GCaMP6s line, reads mapping to the ObirOrco and the rest of the transgene insert were aligned separately due to homology between ObirOrco and the reference genome. In all three transgenic lines, the distribution of read depths across the transgene insert (excluding the ObirOrco region) was close to 0.5x that of the inferred genome-wide average. Because these sequences derive from diploid

O. biroi workers, we infer that the transgene is present in only a single copy for the GCaMP6s line, ie1-DsRed clonal line A, and ie1-DsRed clonal line B (Fig. 2.10A). For the ObirOrco region, read depth was approximately 1.5x the genome-wide average, indicating one additional copy was added to the two endogenous *Orco* alleles (Fig. 2.10A).

We then identified reads that aligned to both the transgene insert and the *O. biroi* reference genome (Guttikonda et al., 2016; Park et al., 2017). The identified positions for all three lines contained 'TTAA' motifs, which are expected at the insertion site for the piggyBac transposon (Cary et al., 1989; Fraser et al., 1996; O'Brochta et al., 2003). In the GCaMP6s line, the insertion was localized to occur between positions Chr2:3,870,844-3,870,847, and predicted to lie within an intron of LOC105285027 (trace amine-associated receptor 9) (Fig. 2.10B-C). In ie1-DsRed clonal line A, the transgene was inserted between positions Chr6:10,206,218-10,206,219, within a predicted exon of LOC113562179 (uncharacterized protein), and within an intron of LOC105286974 (CCR4-NOT transcription complex subunit 6-like) (Fig. 2.10B-C). The insertion in ie1-DsRed clonal line B was located between positions Chr9:8,810,280-8,810,281, which is not within any predicted gene model (Fig. 2.10B-C).

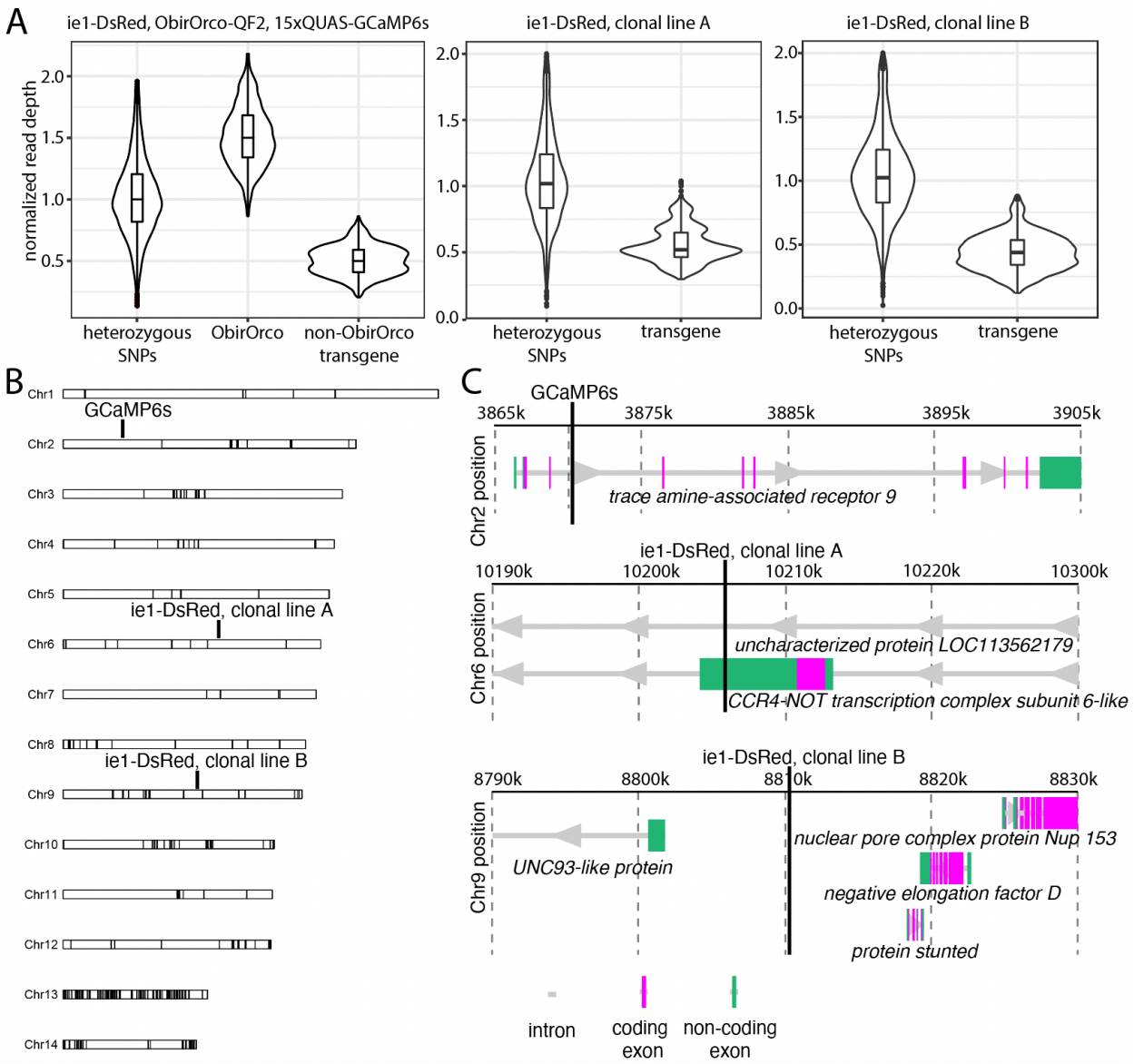

Figure 2.10: Genomic analyses of transgenic lines. (A) Normalized read depth at a panel of heterozygous sites in the *O. biroi* reference genome compared to read depth for the transgene insert sequence based on whole genome resequencing of a single transgenic ant from [ie1-DsRed, ObirOrco-QF2, 15xQUAS-GCaMP6s] (GCaMP6s; left), ie1-DsRed, clonal line A (middle), and ie1-DsRed, clonal line B (right), Normalized read depth for ObirOrco is ~1.5, corresponding to a single additional copy of ObirOrco inserted into the genome (added to the two endogenous copies). Normalized read depth of ~0.5 at the rest of the insert and the other two transgenes is also consistent with a single copy (haploid) insertion. (B) The transgene insertions were localized to sites on chromosomal scaffolds. Black bars indicate breaks between contigs. (C) Close-up of the insertion loci for the GCaMP6s line (top), ie1-DsRed, clonal line A (middle), and ie1-DsRed, clonal line B (bottom), recreated from the NCBI Genome Data Viewer (NCBI, 2022).

2.8: Conclusions on transgenesis in the clonal raider ant

We implemented the first protocol for transgenesis in ants, and developed several transgenic lines in clonal raider ants. Because of the reasonable efficiency of the piggyBac-based methodology and the advantages of rearing and maintaining clonal raider ant colonies, generating and using transgenic lines in this system is feasible for many experiment plans. For all three lines that were sequenced, we identified only single transgene integrations rather than multiple integrations. This reduces the likelihood of disruption of endogenous sequences from the transgene insertions. The transgene constructs that we characterize here represent the beginnings of an experimental toolkit for transgenics in clonal raider ants. Using ie1-DsRed as a marker for transgenesis facilitates identification of newly-generated transgenic lines and transgenic individuals within mixed colonies, without the need for extensive molecular genotyping. ObirOrco labels OSNs with high specificity, which has potential uses for studying the development of the ant olfactory system. Finally, we achieved very strong GCaMP expression using ObirOrco in combination with QF2/QUAS, facilitating the recording of odor-evoked neural activity as we demonstrate in the next chapter. Together, these tools vastly expand experimental possibilities in the clonal raider ant, opening many new avenues for dissecting the underlying mechanisms of social behaviors in eusocial insects.

CHAPTER 3: ALARM PHEROMONE ENCODING IN THE CLONAL RAIDER ANT ANTENNAL LOBE

3.1: Behavioral analysis of alarm pheromones in the clonal raider ant

With the aim of linking alarm pheromone-evoked behaviors to their sensory representation in the AL, we assembled a panel of alarm pheromone stimuli for our study. The alarm pheromones 4-methyl-3-heptanone and 4-methyl-3-heptanol have previously been extracted from clonal raider ants and verified to elicit panic alarm responses in a colony bioassay, both alone and as a blend of the two at a 9:1 ratio that mimics on their relative abundance in ant head extracts (Fig. 3.1A-B, Table 3.1; Lopes et al., 2022). Two chemically related compounds, 4-methyl-3-hexanol and 6-methyl-5-hepten-2-one, act as alarm pheromones in other ant species but have not been found in clonal raider ant chemical extracts (Bernardi et al., 1967; Duffield et al., 1977; Han et al., 2022; Keegans et al., 1993; Lopes et al. 2022; McGurk, 1968; Morgan et al., 1992; Oldham et al., 1994; Pasteels et al., 1980; Pasteels et al., 1981) (Fig. 3.1, Table 3.1). A third, chemically unrelated compound, undecane, has been found in clonal raider ant chemical extracts and acts as an alarm pheromone in other species (Fig. 3.1A, Table 3.1; Ayre and Blum, 1971; Bergström and Löfqvist, 1970; Hillery and Fell, 2000; Lenz et al., 2013; Löfqvist, 1976; Lopes et al., 2022; Maschwitz, 1964; Regnier and Wilson, 1968, 1969).

Using the same bioassay and analyses that we previously used to study 4-methyl-3-heptanone and 4-methyl-3-heptanol (Fig. 3.1B; Lopes et al., 2022), we behaviorally characterized the three compounds 4-methyl-3-hexanol, 6-methyl-5-hepten-2-one, and undecane. All three compounds caused ants to leave the nest pile, and both 4-methyl-3-hexanol and 6-methyl-5-hepten-2-one caused ants to leave the initial nest chamber, while none of the three

compounds attracted the ants to the pheromone source behind the porous wall (Fig. 3.1C-E). However, the behavioral responses were qualitatively distinct from one another, prompting additional analyses. Blinded categorization of the major behavioral response to each pheromone, including re-analysis of videos from our previous study (Lopes et al., 2022), showed that 4-methyl-3-heptanone, 4-methyl-3-heptanol, the 4-methyl-3-heptanone/4-methyl-3-heptanol blend, and 4-methyl-3-hexanol all caused "immediate panic alarm" in at least 80% of trials, while the most common response to 6-methyl-5-hepten-2-one was "ants leave nest," i.e. the majority of ants slowly walking away from the nest, and undecane primarily led to "increase in activity," which indicated that some but fewer than half of the ants slowly walked away from the nest (Fig. 3.2A).

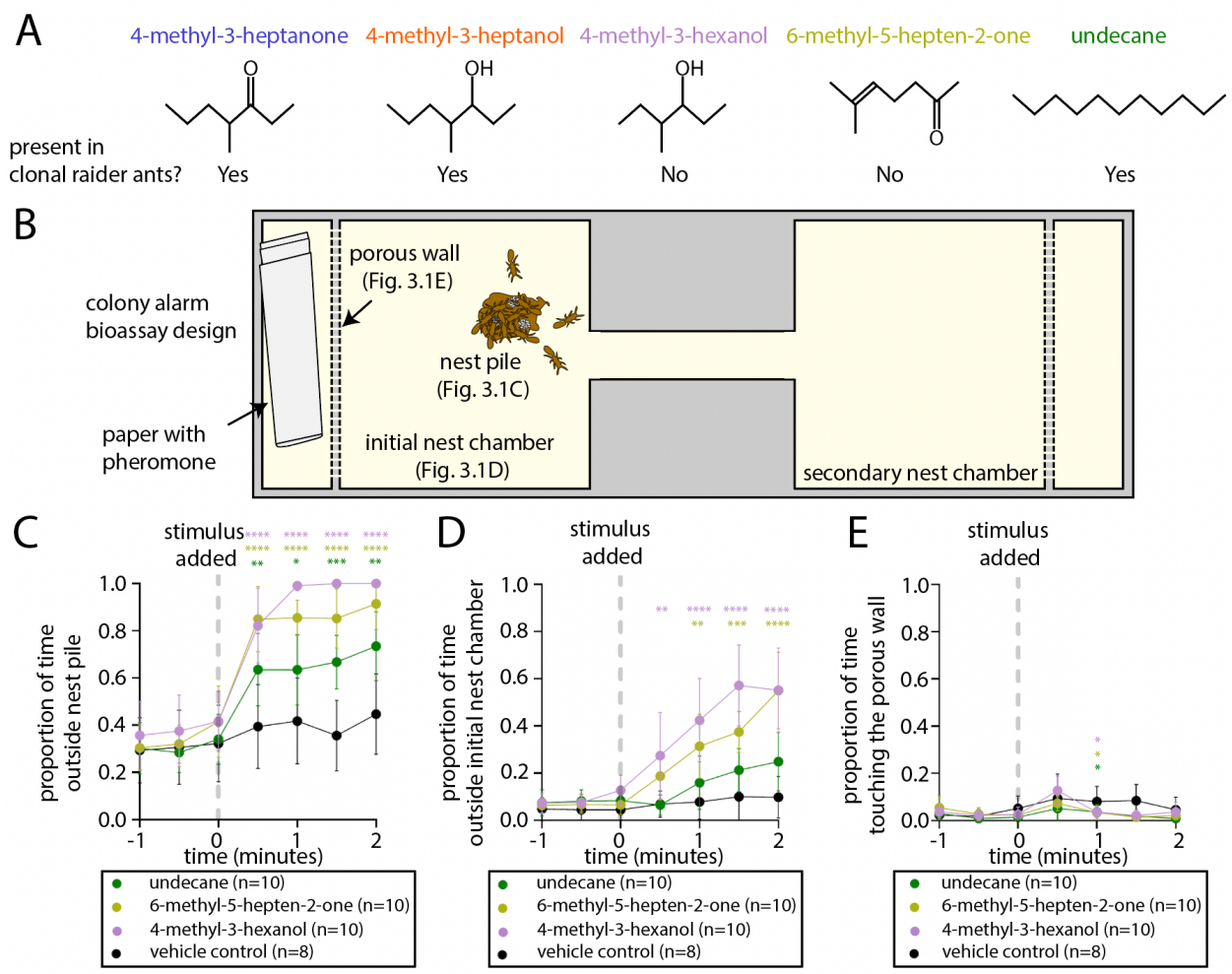

Figure 3.1: Colony alarm bioassays for additional alarm pheromones in the clonal raider ant. (A) Chemical structures for five ant alarm pheromones used in this study obtained from the PubChem database (National Institute for Biotechnology Information: https://pubchem.ncbi.nlm.nih.gov). (B) Experimental design for the colony alarm bioassay (Lopes et al., 2022). (C-E) Time series of colony responses to alarm pheromones vs. control, measuring three parameters (mean±SEM): the proportion of ants outside the nest (C); the proportion of ants leaving the nest chamber (D); the proportion of ants touching the porous wall, indicating attraction to the pheromone source (E). * = p<0.05; ** = p<0,01; *** = p<0.001; **** = p<0.0001, compared to vehicle control. Only comparisons that are statistically different from the vehicle control are indicated.

In many of our behavioral trials, the original nest pile (defined here as the pile of eggs plus at least two workers) was disassembled, which is consistent with nest evacuation as part of a panic alarm response. In other cases, the ants moved away from the nest pile while leaving it at

least partially intact, which reflects a disturbance among the ants but not a clear evacuation or panic response. We analyzed the length of time that the original nest remained intact for each odorant and found that treatment with 4-methyl-3-hexanol led to similarly rapid disassembly of the nest as 4-methyl-3-heptanone, 4-methyl-3-heptanol, and the blend (Fig. 3.2B, Table 3.1). In contrast, treatment with 6-methyl-5-hepten-2-one produced a wide range of outcomes, while treatment with undecane predominantly left the nest pile intact. In both cases, the average response was significantly different from responses to clonal raider ant alarm (Fig. 3.2B, Table 3.1). In summary, 4-methyl-3-hexanol elicits panic alarm behavior similarly to the native clonal raider ant alarm pheromones 4-methyl-3-heptanone, 4-methyl-3-heptanol. 6-methyl-5-hepten-2-one and undecane, on the other hand, lack panic alarm activity and do not normally cause nest evacuation in our bioassay. The occasional alarm responses to 6-methyl-5-hepten-2-one could represent secondary responses, in which an ant emits actual alarm pheromone in response to the stimulus compound.

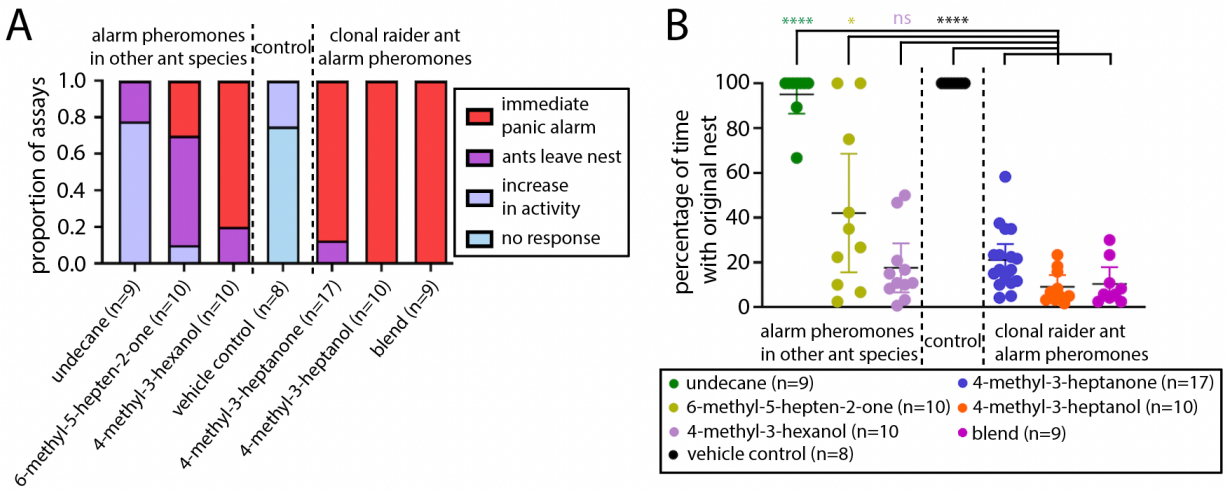

Figure 3.2: Three ant alarm pheromones elicit panic alarm behavior in the clonal raider ant. (A) Categorical analysis of major behavioral responses to alarm pheromone stimuli. (B) Quantification of the length of time that the original nest pile remained intact in the bioassays from Fig. 3.1C-E; see Table 3.2 for details. * = p<0.05; ** = p<0,01; *** = p<0.001; **** = p<0.0001, non-*O. biroi* alarm pheromones were compared to known *O. biroi* alarm pheromones; see Table 3.1 for details.

Chemical name	Example ant taxa using the compound as alarm pheromone	Major behavior in *O. biroi* (Fig. 3.2B)	Extracted from *O. biroi*? (Lopes et al., 2022)
4-methyl-3-heptanone	*Atta texana* (Moser et al., 1968); *Pogonomyrmex* sp. (McGurk et al., 1966); *Neoponera villosa* (Duffield and Blum, 1973); Myrmicinae subfamily (Blum and Brand, 1972); *Atta* sp. (Hughes et al., 2001); *Eciton burchellii* & *E. hamatum* (Lalor and Hughes, 2011)	Immediate panic alarm	Yes
4-methyl-3-heptanol	*Pogonomyrmex barbatus* (McGurk, 1968); *Atta sexdens* (Bento et al., 2007); Dolichoderinae subfamily (Blum and Hermann, 1978); *Harpegnathos saltator* (do Nascimento et al., 1993)	Immediate panic alarm	Yes
4-methyl-3-hexanol	*Tetramorium impurum* (Morgan et al., 1992; Pasteels et al., 1980; Pasteels et al., 1981)	Immediate panic alarm	No
6-methyl-5-hepten-2-one	*Formica* sp. (Duffield et al., 1977); *Iridomyrmex purpureus* (Han et al., 20222); *Aenictus rotundatus* (Oldham et al., 1994); *Eciton burchellii* (Keegans et al., 1993); *Pogonomyrmex barbatus* (McGurk, 1968); *Lasius fuliginosus* (Bernardi et al., 1967)	Ants leave nest	No
undecane	*Lasius fuliginosus* (Maschwitz, 1964); *Formica argentea* (Lenz et al., 2013); *Camponotus pennsylvanicus* (Hillery and Fell, 2000); *Acanthomyops claviger* (Regnier and Wilson, 1968); *Lasius alienus* (Regnier and Wilson, 1969); *Camponotus* sp. (Ayre and Blum, 1971); *Lasius* sp. (Bergström and Löfqvist, 1970); *Formica rufa* (Löfqvist, 1976)	Increase in activity	Yes

Table 3.1: Background information on the five ant alarm pheromones used in this study.

Šidák's multiple comparisons test	Mean diff.	95% CI of diff.	Adjusted P value
4-methyl-3-hexanol (n=10) vs. 4-methyl-3-heptanone (n=17)	-3.575	-23.50 to 16.40	>0.99 (ns)
4-methyl-3-hexanol (n=10) vs. 4-methyl-3-heptanol (n=10)	8.485	-14.00 to 31.00	0.98 (ns)
4-methyl-3-hexanol (n=10) vs. blend (n=9)	7.199	-15.90 to 30.30	>0.99 (ns)
6-methyl-5-hepten-2-one (n=10) vs. 4-methyl-3-heptanone (n=17)	20.92	0.40 to 41.40	0.042 (*)
6-methyl-5-hepten-2-one (n=10) vs. 4-methyl-3-heptanol (n=10)	32.98	10.00 to 56.00	0.0008 (***)
6-methyl-5-hepten-2-one (n=10) vs. blend (n=9)	31.69	8.00 to 55.40	0.0022 (**)
undecane (n=9) vs. 4-methyl-3-heptanone (n=17)	73.98	52.80 to 95.20	<0.0001 (****)
undecane (n=9) vs. 4-methyl-3-heptanol (n=10)	86.04	62.40 to 109.70	<0.0001 (****)
undecane (n=9) vs. blend (n=9)	84.76	60.5 to 109.00	<0.0001 (****)
vehicle control (n=8) vs. 4-methyl-3-heptanone (n=17)	78.87	56.80 to 100.90	<0.0001 (****)
vehicle control (n=8) vs. 4-methyl-3-heptanol (n=10)	90.93	65.50 to 115.40	<0.0001 (****)
vehicle control (n=8) vs. blend (n=9)	86.64	64.60 to 114.70	<0.0001 (****)

Table 3.2: Detailed statistical comparisons for the effects of alarm pheromones on the length of time that the original nest pile remained intact in the alarm behavior colony bioassay. Related to Fig. 3.2B.

3.2: Alarm behavior analysis in GCaMP6s ants

To further validate our GCaMP approach for the study of alarm pheromone representation, we then tested whether the GCaMP6s ants had defects in alarm behavior by subjecting them to our alarm behavior bioassay. While the ants left the nest in response to 4-methyl-3-heptanone, 4-methyl-3-heptanol and the blend as expected (Fig. 3.3A), the effect on leaving the nest chamber was only significantly different from control for 4-methyl-3-heptanone and the blend (Fig. 3.3B), and there was no initial attraction as we previously reported in wild type ants (Fig. 3.3C, Lopes et al., 2022). GCaMP6s ants thus perceive both alarm pheromones and respond behaviorally, similar to wild types. However, these findings could also reflect minor behavioral differences between GCaMP6s and wild type ants or could result from the smaller colony and sample sizes used in this experiment due to lower availability of GCaMP6s animals.

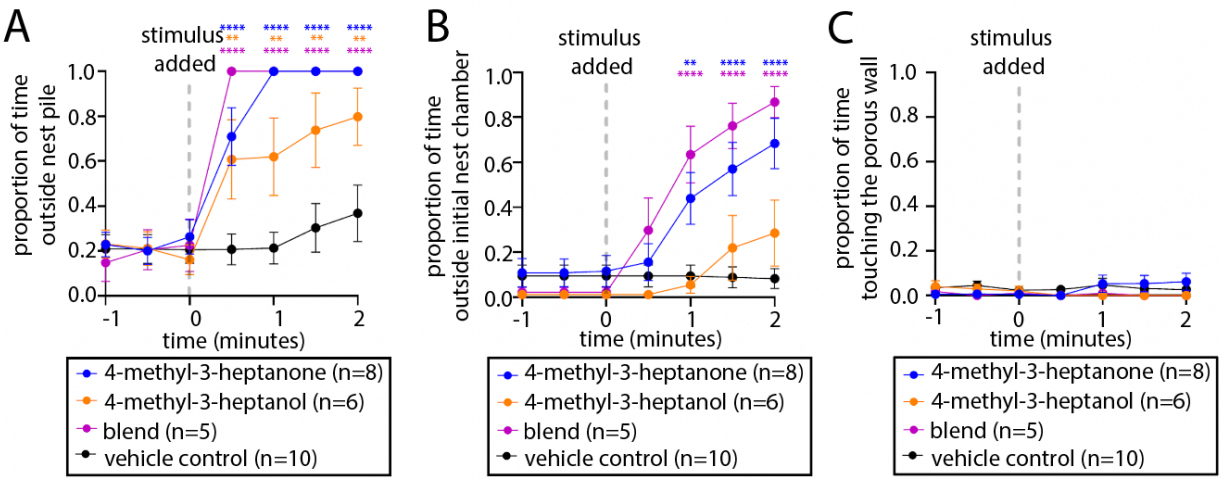

Figure 3.3: Alarm pheromones elicit behavioral responses in GCaMP6s ants.
Colony alarm bioassay using GCaMP6s animals, showing mean±SEM; only comparisons that are significantly different from the vehicle control are indicated. GCaMP6s animals leave the nest in response to 4-methyl-3-heptanone, 4-methyl-3-heptanol, and a 9:1 blend of the two; (C) ants leave the nests chamber in response to 4-methyl-3-heptanone and the blend; (D) but are not attracted toward the source of any treatment. *: $p<0.05$; **: $p<0.01$; ***: $p<0.001$; ****: $p<0.0001$, compared to vehicle control.

3.3: Volumetric two-photon imaging allows recording odor-evoked calcium responses across the entire ant antennal lobe

We implemented several new approaches for recording neural activity in eusocial insects. First, we used OSN-specific GCaMP6s, which allows detection of calcium responses from all OSNs without possible confounding signals from projection neurons, lateral interneurons, or glia. Second, we used a volumetric imaging approach that allowed us to record from the entire AL during a single odor stimulus trial. We developed an in vivo two-photon imaging preparation for clonal raider ants, where animals are head-fixed and a small imaging window is excised from the cuticle covering the ALs (Fig. 3.4A-B). Ants are then exposed to reproducible odor stimuli via a computer-controlled olfactometer (Galizia et al., 1997; Wang et al., 2003; Zube et al., 2008) and the resulting changes in GCaMP6s fluorescence are captured at 27.5fps, and across the entire volume every 1.2s (Fig. 3.4C-D). We imaged 33 z-planes at 5µm increments, which was sufficient to capture all glomeruli in multiple planes, as most clonal raider ant glomeruli are 10-20µm in diameter (the entire AL has approximate dimensions of 65µm x125µm x150µm). We could clearly detect the boundary at the ventral surface of the AL where GCaMP6s signal disappeared, indicating that we imaged all GCaMP6s-positive AL glomeruli. Individual glomeruli were often discernible from baseline GCaMP6s fluorescence and always from calcium responses due to spatially clustered correlated pixels (Fig. 3.4C). This approach allowed us to detect the glomerular activation pattern across the entire AL from a single odor stimulus trial, without concerns that our imaging method biased detection of calcium responses to particular regions of the AL (Fig. 3.4E).

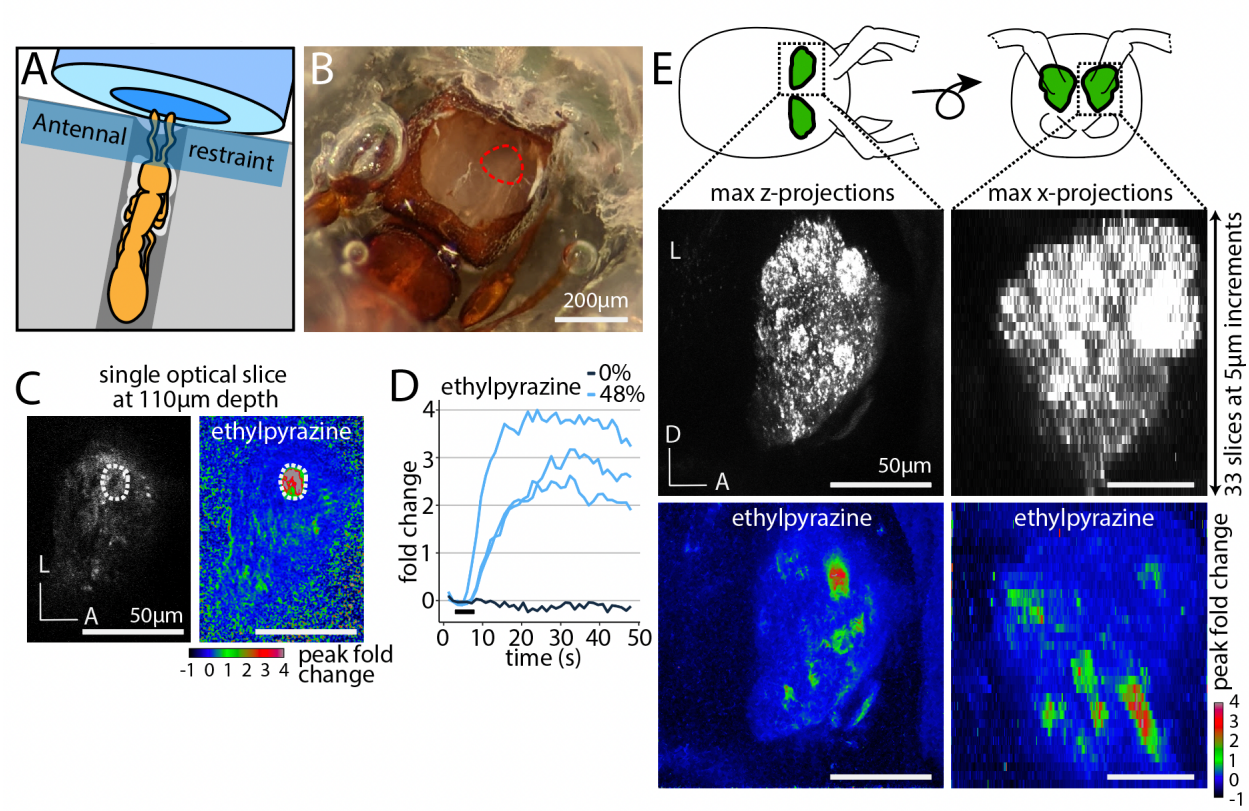

Figure 3.4: Imaging odor-evoked calcium responses in the clonal raider ant antennal lobe. (A) Whole animal is adhered to a plastic base with glue (white) applied to the ventral side of the head and thorax. Antennae are restrained with a strip of parafilm directly in front of the air tube (B). Preparation after dissection, with cuticle and glandular tissue removed to expose the right AL. (C) Appearance of a single optical slice through the AL using two-photon microscopy (brightness and contrast enhanced, one glomerulus of interest circled). (D) Peak fold change of calcium response after 5s od presentation. (E) Time series of calcium responses in the glomerulus from (C-D) from several trials with ethylpyrazine or paraffin oil vehicle (0%); black bar indicates the 5s odor presentation. (F) Volumetric imaging of clonal raider ant ALs. GCaMP6s fluorescence is visible throughout the lobes in max z-projection (left) and max x-projection (right). (G) The same as (F) but showing peak fold change of fluorescence after presentation with ethylpyrazine (48%). D: dorsal; L: lateral; A: anterior.

To test our GCaMP imaging approach and obtain a basic overview of odor representation in the clonal raider ant AL, we presented ants (n=6) with a panel of 11 general (non-pheromone) volatile odorants and recorded whole-AL calcium responses. The general odorants were prepared to the same concentration (48% v/v), but the intensity of the stimulus varied because the odorants spanned a range of vapor pressures (Table 6.1). Five of the odorants generated robust calcium

responses, and odorants with lower volatility/vapor pressure did not generate calcium responses. To simplify the display of calcium responses while considering the entire AL, we calculated the peak fold change of fluorescence in each slice of the volumetric videos and then flattened them using max z-projection. Viewed this way, it was apparent that that the ant AL exhibits properties of odor encoding that have been shown in other insects: each odorant activated a unique combination of glomeruli, and responses to the same odorant occurred in similar regions of the AL in different individuals, indicating that on a qualitative level, odor representation is stereotyped across individuals (Fig. 3.5A; Sachse et al., 1999; Wang et al., 2003). We also found that the breadth of the activity varied dramatically across odorants, with most odorants activating zero or a few glomeruli, while 3-hexanone activated large regions of the AL (Fig. 3.5A-C). The range of results demonstrates that our imaging approach can detect both sparse and broad calcium response patterns if they occur.

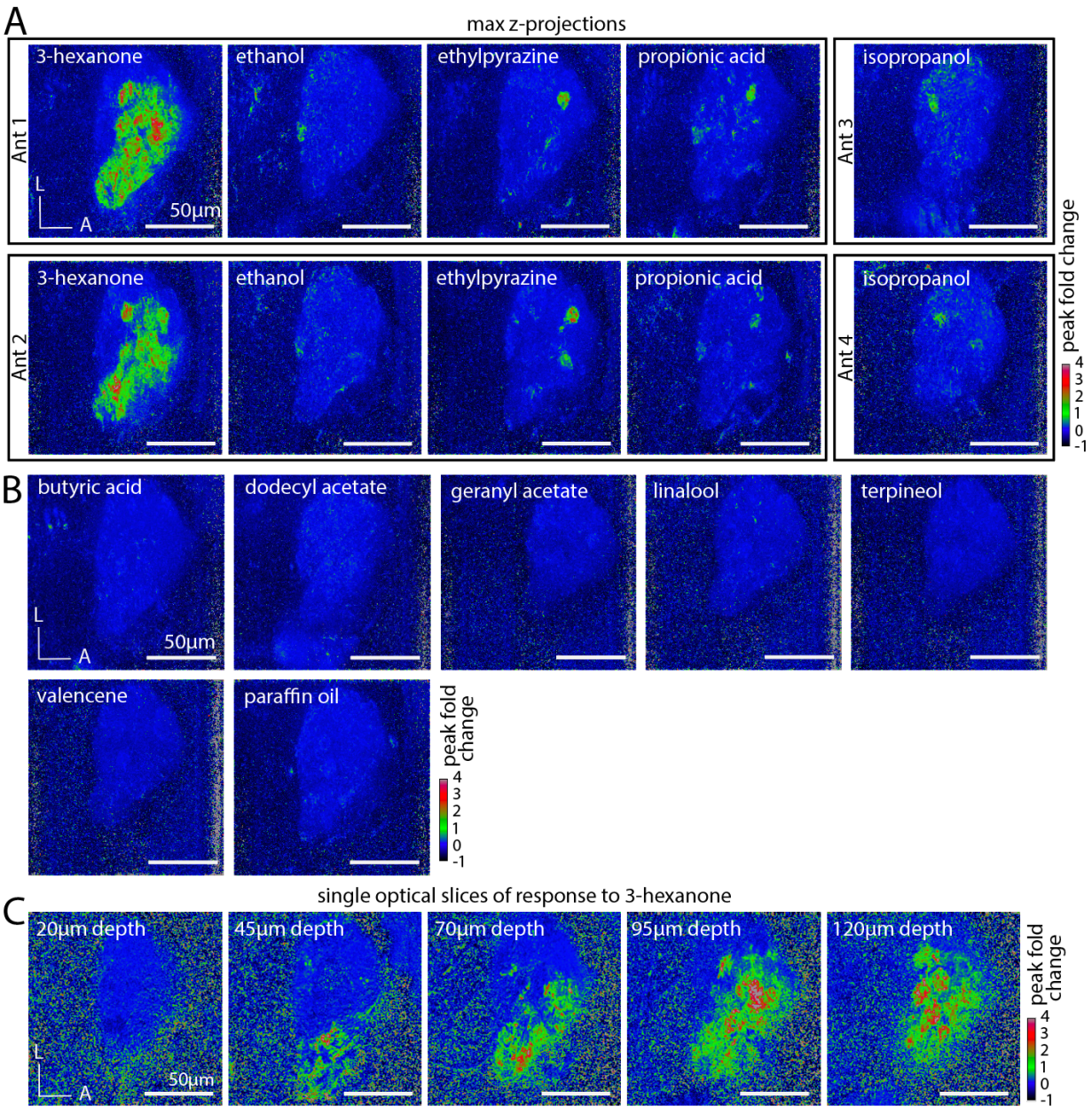

Figure 3.5: Whole-antennal lobe calcium response patterns to general odorants are spatially stereotyped. (A) Images show representative max z-projections of peak fold change to five general odorants that generated robust calcium responses. (B) Six additional general odorants, and the paraffin oil vehicle, do not generate robust calcium responses. (C) Analysis of single optical slices of responses to 3-hexanone show that responding glomeruli are primarily located in the ventral/medial AL.

3.4: Alarm pheromone representation is sparse and spatially stereotyped in the ant antennal lobe

To describe the encoding of alarm pheromones in clonal raider ant ALs, we presented each ant (n=13 ants) with the five alarm pheromones in a random sequence, each at two concentrations out of four that were tested in total (Fig. 3.6A). Each 5-pheromone sequence at a particular concentration was repeated three times, for a total of 30 alarm pheromone presentations per individual (Fig. 3.6A). For four of the odors tested, examination of max z-projections of the peak calcium response revealed a sparse, unique subset of responding AL glomeruli, while undecane generated no responses (Fig. 3.6B). Several of the odors activated glomeruli in similar positions in the AL (Fig. 3.6B). Fluorescence increases were frequently large (1-2-fold change) and remained elevated above baseline for longer than the 5s odor presentation. The response patterns to the same pheromone in different individuals were qualitatively similar, in accordance with what we observed for general odorants (Fig. 3.5, Fig. 3.6C). We did not observe any fluorescence decreases in response to odor, although we did detect small, non-specific decreases in fluorescence as a persistent artifact in our imaging setup, as small changes in AL position and photobleaching gradually decreased detectable fluorescence. This artifact did not affect our ability to detect calcium responses, which remained highly consistent after normalization for the duration of the experiment (Fig. 3.7). Comparison of calcium traces from two adjacent glomeruli showed high specificity of the response functions, without evidence for weak or transient calcium responses that might not be visible from analysis of peak fold change (Fig. 3.7).

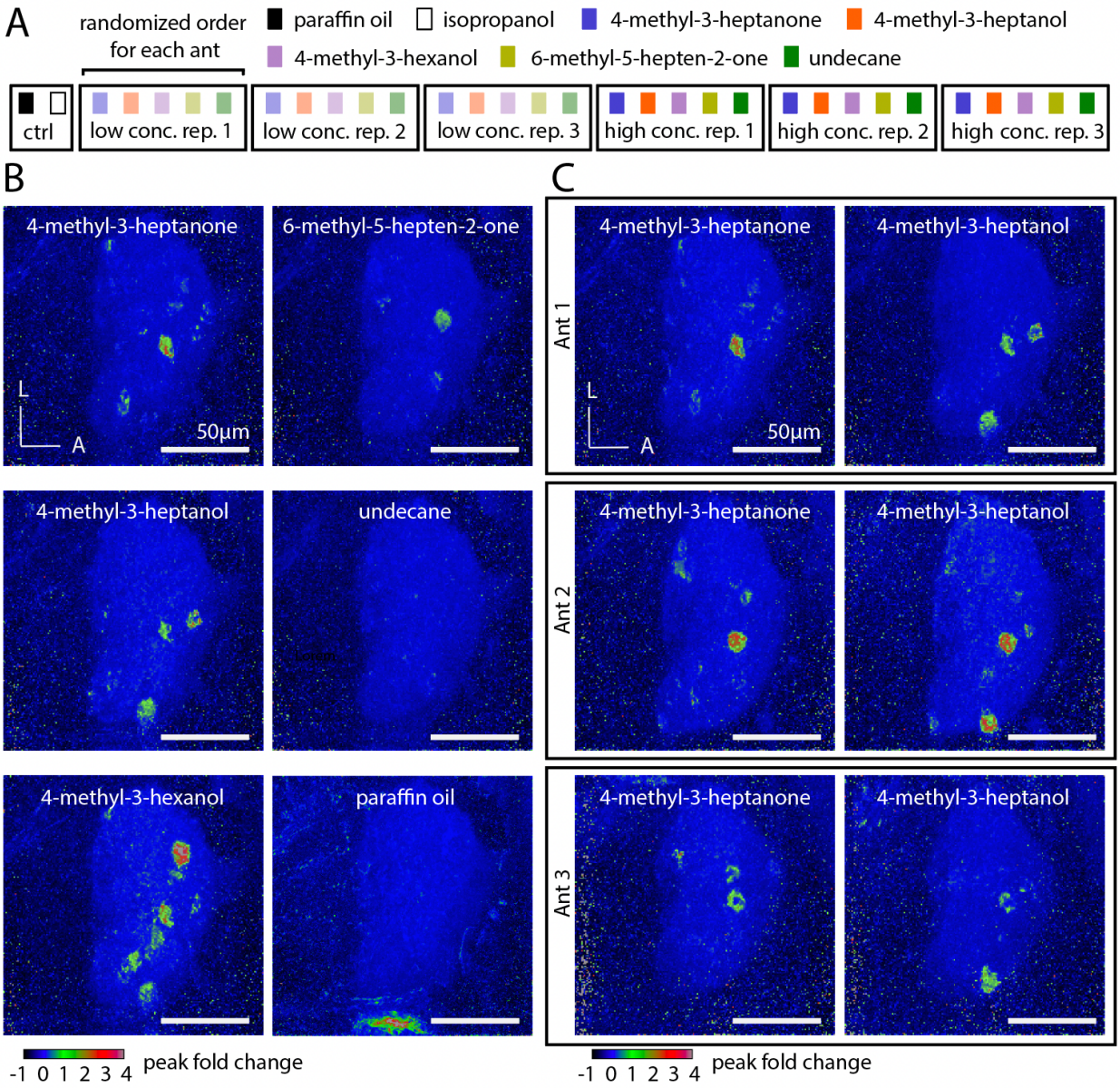

Figure 3.6: The representation of alarm pheromones in the clonal raider ant antennal lobe. (A) Pheromone stimulus regime. (B) Representative max z-projections of peak fold change from a single ant for five alarm pheromones (48% concentration) and the paraffin oil vehicle. No responses to undecane were detected. (C) Three different individuals were stimulated with 4-methyl-3-heptanone (left) and 4-methyl-3-heptanol (right) at 48% concentration, producing qualitatively similar activation patterns. L: lateral; A: anterior.

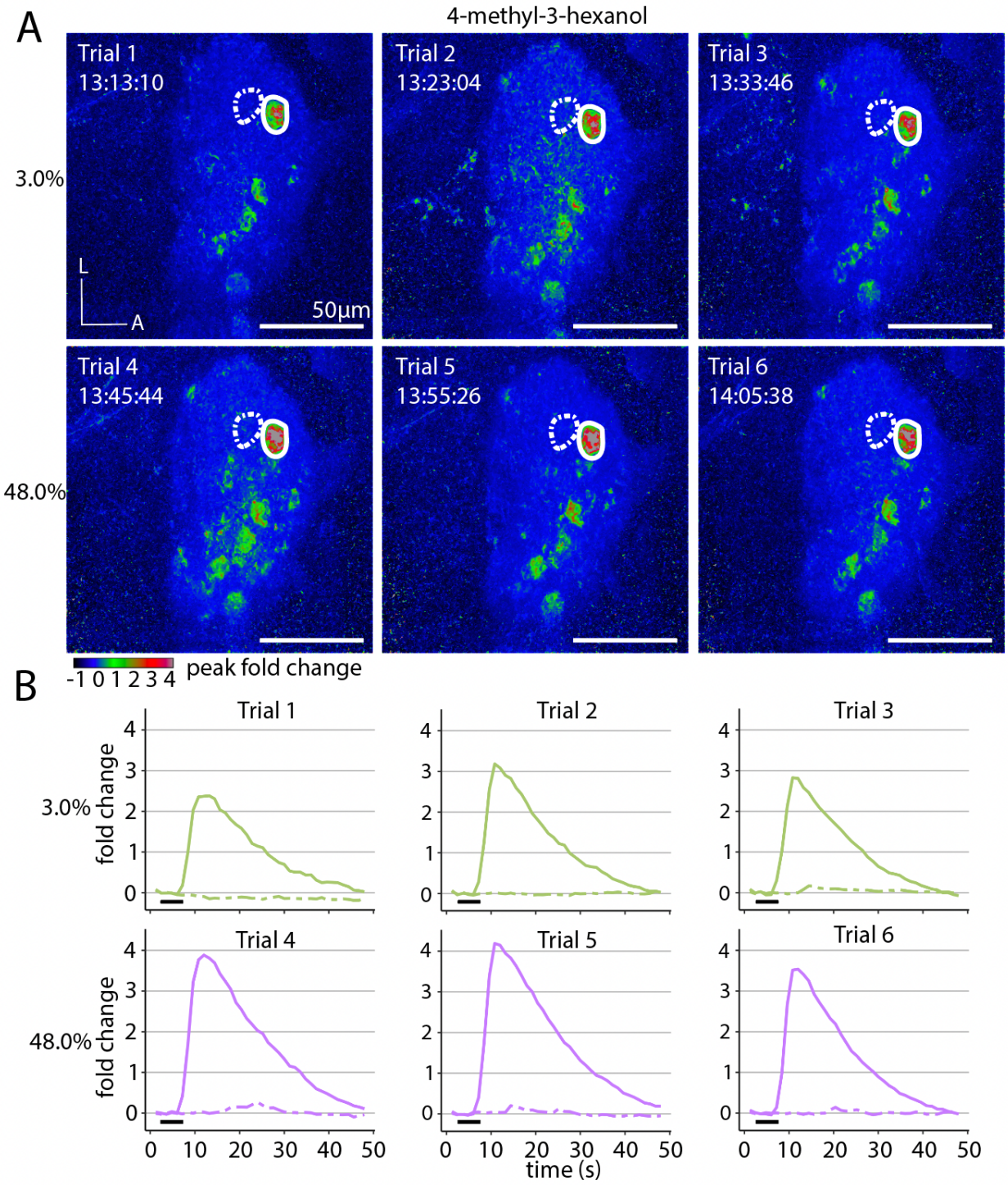

Figure 3.7. Calcium responses are robust across trials. (A) Max z-projections of peak fold change from a single ant after presentation with 4-methyl-3-hexanol. Three trials were performed at 3.0% concentration (top), and three additional trials were performed at 48.0% concentration (bottom). Timestamps for each trial demonstrate that responses are robust over the duration of a full experiment. Two adjacent focal glomeruli are circled. (B) Time series of calcium responses from each trial in (A) for the two adjacent glomeruli; responses in the left glomerulus are shown

as alternating short and long dashes and responses in the right glomerulus are shown as solid lines; black bars indicate the 5s odor presentations. Responses are quantified from max z-projections of three slices centered on 105µm z-depth.

3.5: Three panic-inducing pheromones activate a single shared glomerulus

We sought to determine how many of the ~500 glomeruli responded to each alarm pheromone by examining the max z-projections of the calcium response. Undecane was excluded from this analysis because it did not elicit calcium responses. We identified all regions of interest (ROIs) corresponding to activated glomeruli from any of the four analyzed pheromone, quantified the mean peak fold change from each pheromone stimulus/concentration, and used a threshold of ≥0.2 mean peak fold change to find robust odor-evoked responses (Fig. 3.8A). The four odorants always activated 12 or fewer glomeruli, even at the highest concentration tested (Fig. 3.8A). Despite the small number of responding glomeruli, we observed consistent partial overlap in the response patterns activated by the three compounds eliciting panic alarm responses, 4-methyl-3-heptanone, 4-methyl-3-heptanol, and 4-methyl-3-hexanol, with a single glomerulus activated by all three (Fig. 3.8B). In contrast, while we sometimes observed responses to 6-methyl-5-hepten-2-one and either 4-methyl-3-heptanone or 4-methyl-3-hexanol in an overlapping region, those occurrences were rare and inconsistent (Fig. 3.8C). We outlined a conceptual schematic based on the median number of responding glomeruli for each pheromone and pheromone combination, and their behavioral output (Fig. 3.8D). The three chemically related pheromones with overlapping response patterns all robustly elicited panic alarm behavior, while among the two pheromones that did not elicit panic alarm behavior, the chemically related 6-methyl-5-hepten-2-one generated a non-overlapping response pattern, and the chemically unrelated undecane did not generate a response (Fig. 3.8D). We named the single glomerulus that responded to 4-methyl-3-heptanone, 4-methyl-3-heptanol, and 4-methyl-3-

hexanol the "panic glomerulus, broad" (PG_b). Our findings point to a shared pathway for eliciting panic alarm response, centered on PG_b.

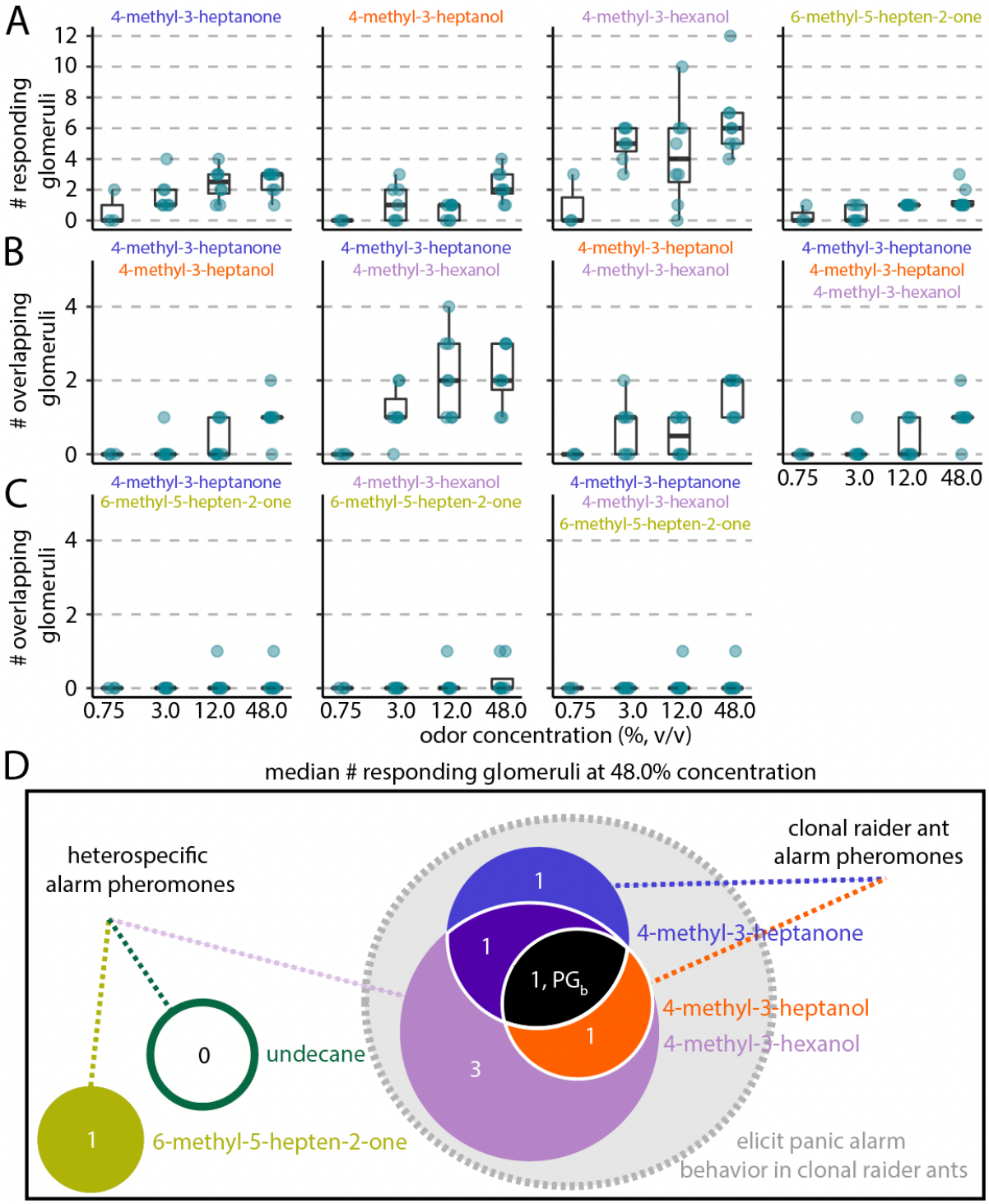

Figure 3.8: Increased odor concentration results in more responding glomeruli. Counts of the number of responding glomeruli from max z-projections; boxes enclose the first to third quartile range, with bold line showing the median and whiskers enclosing the min and max values that fall within 1.5x the interquartile range. Data points show the mean number of responding glomeruli for a given ant across all trials for a particular odorant/concentration. n=13 ants total, 3 ants presented with 0.75% and 12.0% odor concentrations; 2 ants with 3.0% and 12.0%; 3 ants with 12.0% and 48.0%; and 5 ants with 3.0% and 48.0%. Single pheromones each activated a small number of glomeruli (A), whereas 4-methyl-3-heptanone, 4-methyl-3-heptanol, and 4-methyl-3-hexanol activated overlapping sets of glomeruli (B). 6-methyl-5-hepten-2-one only rarely activated glomeruli shared with the other pheromones (C). All pheromones were presented separately, rather than as blends. Only pheromones and pheromone combinations that activated at least one glomerulus are shown. Because undecane never generated robust responses it was not included in this analysis. (D) Conceptual schematic for the representation of alarm pheromones in the clonal raider ant AL, showing the median number of responding regions for each pheromone combination, using the highest concentration tested (48%; n=8 ants tested at this concentration). The three pheromones that elicit panic alarm responses, 4-methyl-3-heptanone, 4-methyl-3-heptanol, and 4-methyl-3-hexanol, activate mutually overlapping sets of glomeruli, while 6-methyl-5-hepten-2-one activates a mutually exclusive response in a separate glomerulus. Undecane generates no detectable response. See Figs. 3.10-3.11 for calcium response quantification and time series in three focal glomeruli.

3.6: Alarm pheromones activate distinct combinations of three neighboring, spatially stereotyped glomeruli

Examining max z-projections of the calcium responses revealed that several glomeruli activated by combinations of alarm pheromones, including PG_b, were located in similar regions of the AL across individuals (Fig. 3.9A). As 4-methyl-3-heptanone and 4-methyl-3-heptanol elicit slightly different forms of alarm behavior (Lopes et al., 2022), this finding is consistent with the expectation that these pheromones might share sensory pathways while also activating distinct sets of glomeruli (Fig. 3.9A). To better understand these alarm pheromone-sensitive glomeruli, we decided to localize PG_b within the AL more precisely, and to characterize its local environment. Inspection of the raw recordings revealed that PG_b is located in the anterior AL, next to a region without glomeruli, approximately halfway between the dorsal and ventral AL surfaces (Fig. 3.9A-B). PG_b is neighbored by two additional glomeruli that respond to alarm

pheromones, with all three visible in the same optical plane (Fig. 3.9B). While PG_b responds to 4-methyl-3-heptanone, 4-methyl-3-heptanol, and 4-methyl-3-hexanol, a nearby glomerulus responds to 6-methyl-5-hepten-2-one, which we refer to as the "6-methyl-5-hepten-2-one glomerulus" (6G). Both glomeruli were identified in 13/13 individuals. In 11/13 individuals, we identified a third neighboring glomerulus that responds to 4-methyl-3-heptanol and 4-methyl-3-hexanol, which we termed the "panic glomerulus, alcohol" (PG_a). Examination of the position of the three glomeruli in the z-stack and comparison with a previous segmentation of the AL (McKenzie et al., 2016) showed that they are part of the T6 glomerulus cluster, which is innervated by OSNs from basiconic sensilla on the ventral surface of the ant antennal club that mostly express members of the 9-exon OR subfamily (McKenzie et al., 2016) (Fig. 3.9B). In gross anatomy, PG_b, PG_a, and 6G look like typical glomeruli, rather than anatomically differentiated or enlarged macro glomeruli. To validate our initial finding that these three glomeruli are functionally distinct from one another, we aligned them across individuals and quantified glomerulus-specific odor responses. This demonstrated that, while PG_b, PG_a, and 6G are spatially adjacent, they each reliably respond to unique combinations of odorants (Figs. 3.10, 3.11). Importantly for its potential role in mediating alarm behavior, PGb did not respond to 6-methyl-5-hepten-2-one, showing selectivity in its receptive tuning (Figs. 3.9B, 3.10, 3.11).

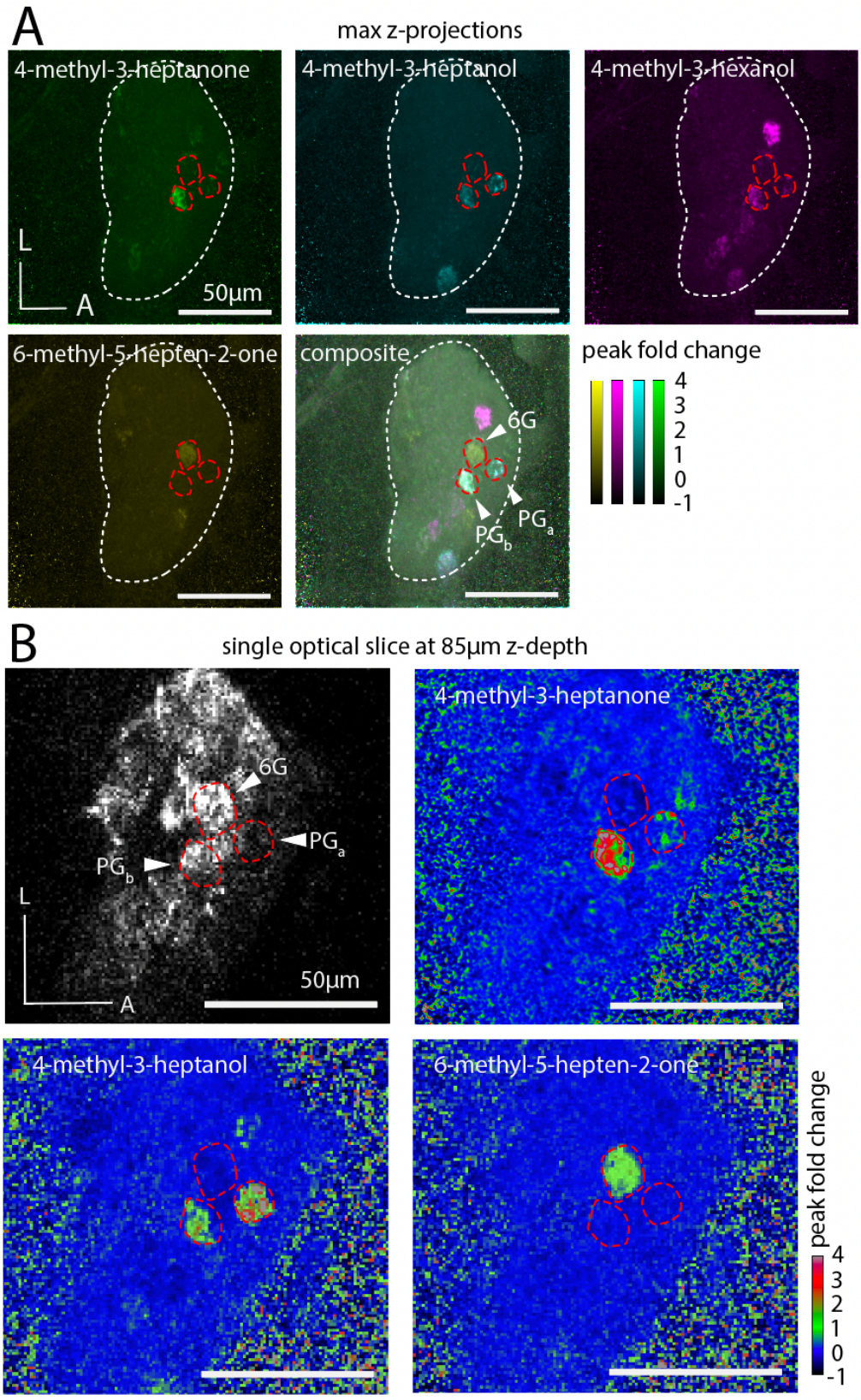
A
max z-projections
4-methyl-3-heptanone
4-methyl-3-heptanol
4-methyl-3-hexanol
L
A
50µm
6-methyl-5-hepten-2-one
composite
6G
PG_a
PG_b
peak fold change
4
3
2
1
0
-1
B
single optical slice at 85µm z-depth
6G
PG_a
PG_b
L
A
50µm
4-methyl-3-heptanone
4-methyl-3-heptanol
6-methyl-5-hepten-2-one
peak fold change
4
3
2
1
0
-1

Figure 3.9: A glomerulus cluster with stereotyped spatial organization and robust responses to alarm pheromones. (A) Whole-AL activation patterns for alarm pheromones overlap in several glomeruli. Three focal glomeruli are outlined. (B) Single optical slice through the AL with the three focal glomeruli (outlined). Fluorescence with enhanced brightness/contrast (left). Peak fold change in response to odors (middle, right). L: lateral; A: anterior.

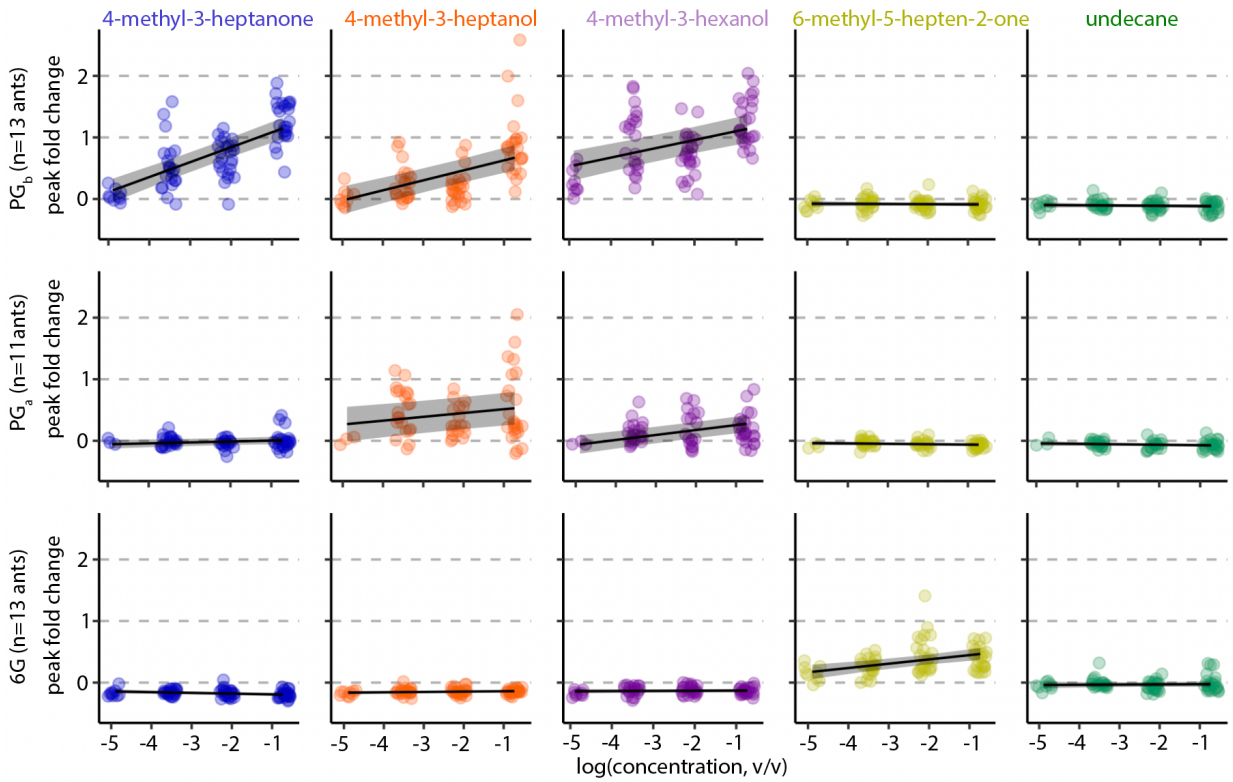

Figure 3.10: Quantification of peak fold change in three focal glomeruli. PG_b (top), PG_a (middle), and 6G (bottom). Three trials per ant for each odorant/concentration; n=13 ants total, 3 ants presented with 0.75% and 12.0% odor concentrations; 2 ants with 3.0% and 12.0%; 3 ants with 12.0% and 48.0%; and 5 ants with 3.0% and 48.0%. PG_a could not be identified in two ants. Graphs show outputs of linear models (with 95% confidence) for dose/response to each odorant in each glomerulus, with a random effect for individual. Concentrations were log transformed to show the linear relationship.

Calcium responses had slow temporal dynamics, and in some cases fluorescence changes lasted beyond the duration of a single 48s recording trial. We therefore examined the temporal dynamics of alarm responses in PG_b, PGa, and 6G (Fig. 3.11A). While responses in PG_b and PG_a had a relatively sharp peak and then declined close to baseline by the end of the 48s recording, calcium responses in 6G, which only responds to 6-methyl-5-hepten-2-one, were extremely slow,

with a fluorescence plateau of tens of seconds that sometimes remained elevated by the end of the recording (Fig. 3.10A). We therefore performed additional odor presentations with 6-methyl-5-hepten-2-one with an extended recording period (144s) and found that calcium responses did eventually return to baseline, although in some trials the fluorescence remained elevated for >100s (Fig. 3.11B). At higher odor concentrations, all calcium responses lasted substantially longer than the 5s pheromone presentation (Fig. 3.11A). Quantifying time to response onset and time to response maximum for the different pheromones in the three focal glomeruli showed that different combinations had distinct temporal dynamics, as has been shown in other species (Fig. 3.12; Laurent, 1999; Hallem et al., 2004, Hallem and Carlson, 2006; Su et al., 2011).

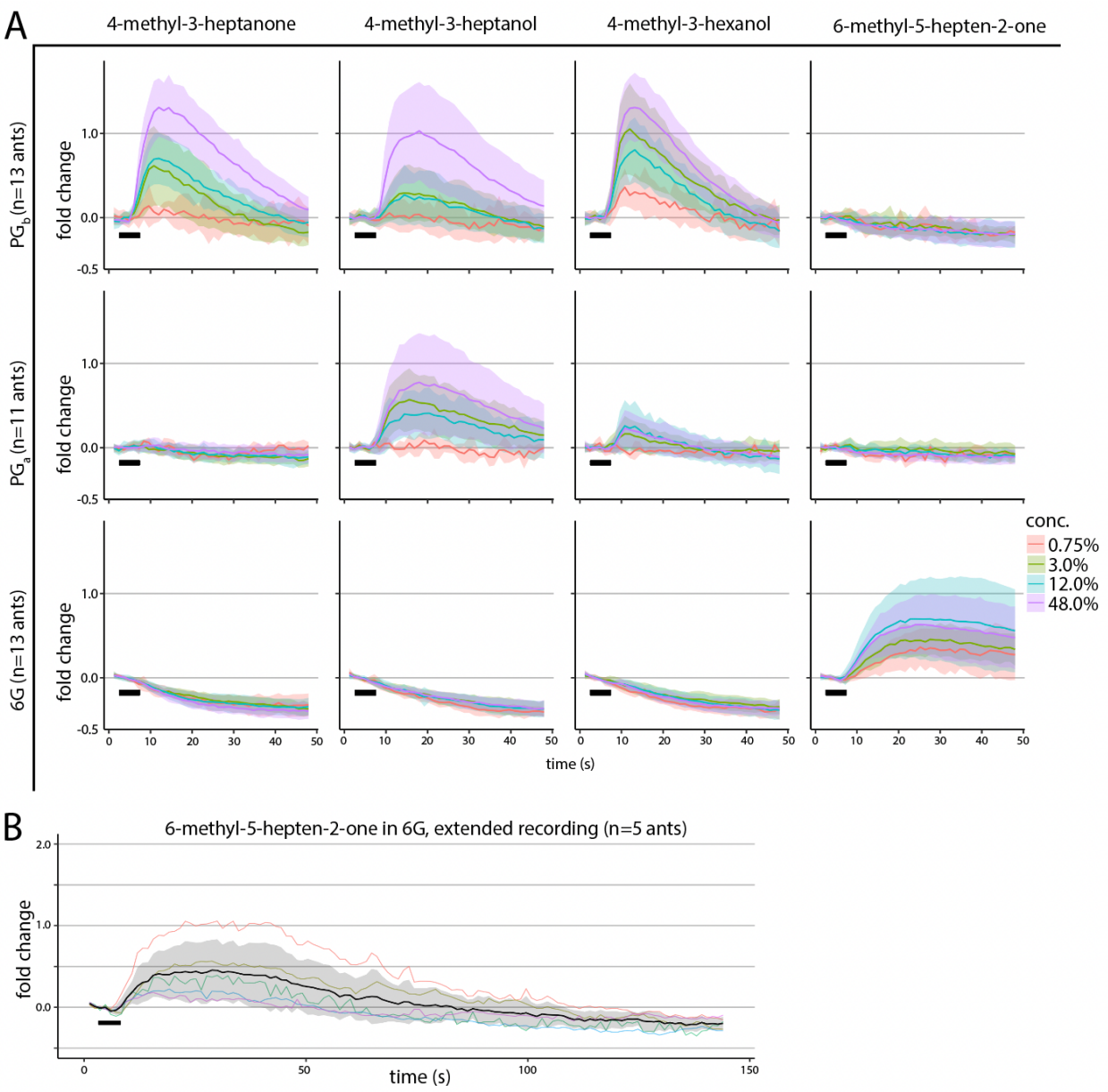

Figure 3.11: Time series of odor-evoked calcium responses in three focal glomeruli. (A) Time series of calcium responses in PG_b (top), PG_a (middle) and 6G (bottom). Only alarm pheromones that generated calcium responses are shown. Responses to 4-methyl-3-heptanone, 4-methyl-3-heptanol, and 4-methyl-3-hexanol (occurring in PG_b and PG_a) rose quickly and then declined to baseline by the end of the 48s recording. Responses to 6-methyl-5-hepten-2-one in 6G rose slowly and then plateaued for tens of seconds. Black bars indicate the 5s odor presentation. Plots show mean±SD, calculated from three trials per individual at each concentration. (B) Extended time series for the response to 6-methyl-5-hepten-2-one in 6G. Data were collected separately from (A): Single trials each from five different individuals at 48% concentration (colored traces); mean±SD (black line and gray ribbon). Fluorescence plateaued for ~30s before declining and returning to baseline ~80s after odor presentation.

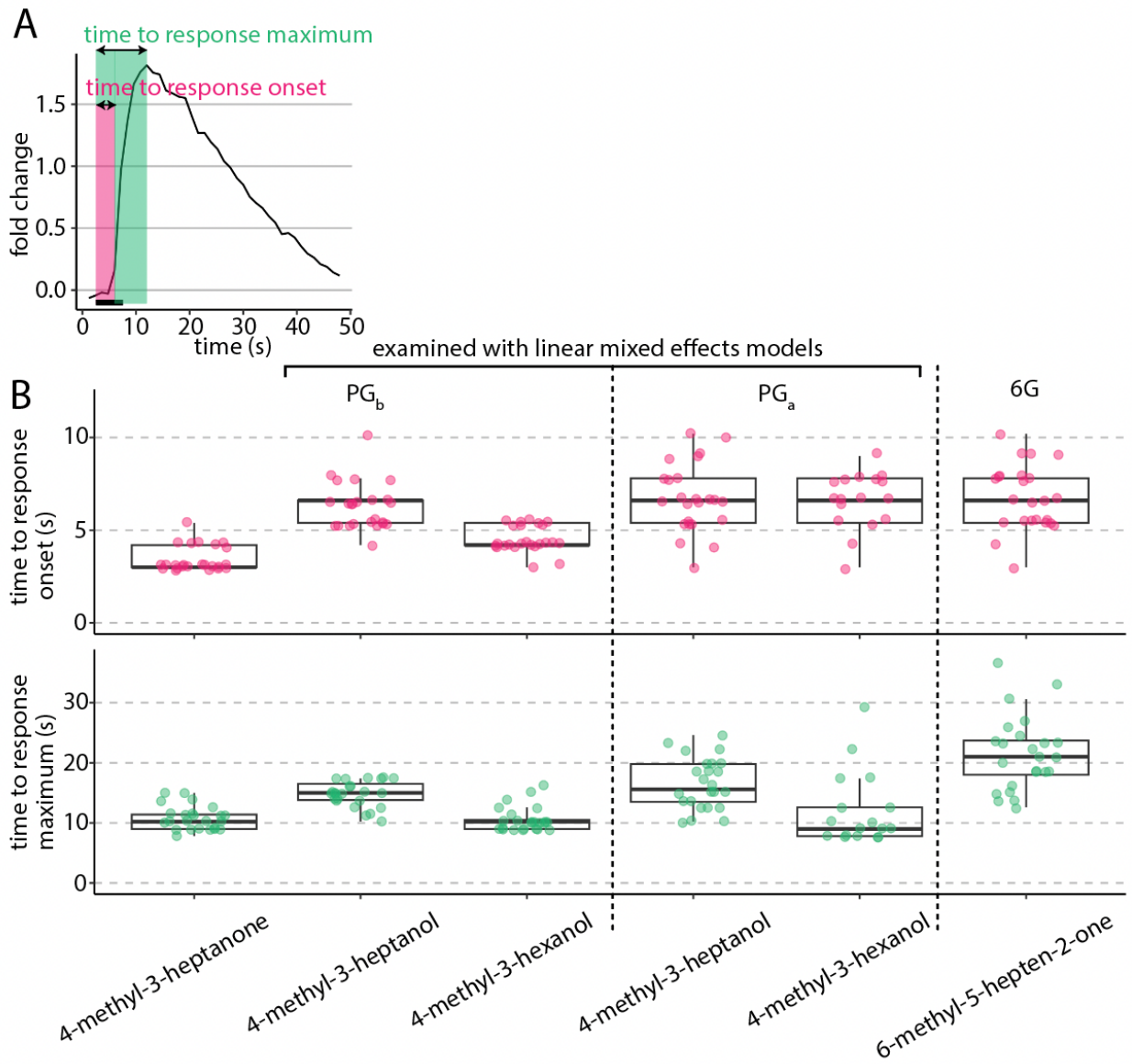

Figure 3.12: Quantification of temporal dynamics in focal glomeruli. (A) Two parameters of temporal dynamics extracted from glomerulus-specific calcium response traces. (B) Quantification of time to response onset (top) and time to response maximum (bottom) in the three focal glomeruli PG_b, PG_a, and 6G in response to stimuli at 48% concentration (n=8 ants, three trials per condition per ant). Only glomerulus/pheromone combinations with typically robust responses are shown. Boxes enclose the first to third quartile range, with bold lines showing the median and whiskers enclosing the min and max values that fall within 1.5x the interquartile range. For PG_b and PG_a in response to 4-methyl-3-heptanol and 4-methyl-3-hexanol, linear mixed effects models were used to test for effects of pheromone, glomerulus, and a pheromone/glomerulus interaction on the time parameters. Time to response onset: significant effects of pheromone ($p=0.0034$), glomerulus ($p<0.0001$) and the interaction ($p=0.0030$). Time to response maximum: significant effects of pheromone ($p<0.0001$) and glomerulus ($p=0.047$), but not the interaction ($p=0.88$).

Our analyses thus far show that alarm pheromones evoke qualitatively similar calcium responses across individuals, and that the number of activated glomeruli is consistent for a given odor. However, they do not answer the question of whether the activated glomeruli are located in fixed positions within the AL as in *Drosophila*, or whether there is significant local variation as in mice. To quantify the level of stereotypy across individuals in clonal raider ants, we examined the relative spatial positioning between PG_b, PG_a, and 6G in the medial-lateral and anterior-posterior axes (spatial resolution along the dorsal-ventral axis was insufficient for this analysis, especially given that these glomeruli are located at similar z-depths). We never observed large positional differences of these glomeruli across individuals, and the spatial organization of the three glomeruli was consistent. We found that PG_a was always located anterior (mean distance: 12.9±1.9SD μm), and slightly lateral (mean distance: 5.1±2.9SD μm) to PG_b (Fig. 3.13). In comparison, 6G was always lateral to PG_b (mean distance between centers: 13.1±2.6SD μm), and in a similar position on the A-P axis (mean distance: 0.6±2.2SD μm) (Fig. 3.13). The standard deviation values are much smaller than the typical diameter of a glomerulus (10-20μm). We therefore conclude that these three glomeruli occupy stereotyped positions even within their local glomerular cluster, and show stereotyped odor response functions across individuals.

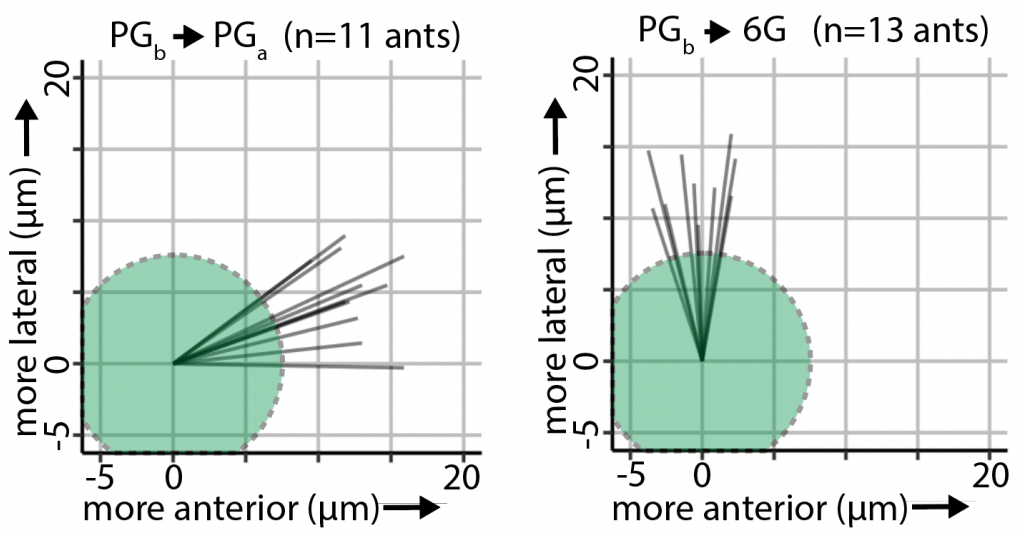

Figure 3.13: Precise, stereotyped spatial organization among three focal glomeruli. Vectors of the spatial displacement between the centers of the PG_b and PG_a (left), and between the PG_b and 6G (right) glomeruli show that the spatial relationships are conserved across individuals. Green circles show the size of a typical 15µm-diameter glomerulus.

3.7: Conclusions on calcium imaging in the clonal raider ant antennal lobe

We developed a protocol for whole-AL calcium imaging of odor-evoked neural activity, using volumetric two-photon GCaMP imaging. For the first time in a eusocial insect, this approach allowed us to detect calcium responses across all olfactory glomeruli from a single odor presentation. Our results showed that odor encoding is in most cases quite sparse, with most general odorants and all alarm pheromones robustly activating small numbers of glomeruli out of the total repertoire of ~500. Comparison of activity patterns for three panic-inducing alarm pheromones showed that one single glomerulus is activated by any of the three, while remaining inactivated after presentation with two other alarm pheromones that did not elicit panic alarm behavior. This suggests the existence of a core sensory pathway for mediating panic alarm, centered on this glomerulus. We also found that odor encoding is spatially stereotyped across individual clonal raider ants, suggesting that OSN axon targeting to AL glomeruli is not

patterned by activity dependent processes. Together, these results reveal patterns in odor and alarm pheromone encoding that could not be determined from partial imaging of the AL, notably identifying a putative core component for panic alarm behavior. The methodologies represent an experimental foundation for understanding odor encoding in eusocial insect ALs and identifying core components of the olfactory system that mediate social behaviors.

CHAPTER 4: DISCUSSION

4.1: New tools and protocols for studying the mechanisms of social behavior

We implemented several transgenic and imaging tools in ants for the first time. Our efficient piggyBac transgenesis protocol for the clonal raider ant opens new experimental possibilities for the study of social behavior in eusocial insects. Until now, the honeybee was the eusocial species in which transgenesis had been reported (Schulte et al., 2014; Carcaud et al., 2022). In addition to allowing comparison of results between two independent eusocial lineages, expanding transgenics to the clonal raider ant has several advantages for conducting experiments using transgenic lines. Compact colonies, the absence of a need for large amounts of foraging space, and asexual reproduction from totipotent workers all reduce the resource and maintenance costs of maintaining transgenic lines over the long term. Indeed, we have maintained three transgenic lines in the lab for more than four years at the time of writing.

The transgenic lines reported here represent a suite of experimental tools, each with many potential applications. The highly visible ie1-DsRed marker gene makes identification of transgenic individuals simple at all life stages, excluding eggs. This experimental tool could facilitate the study of colony reproductive dynamics in the clonal raider ant by allowing matching parents to offspring from inheritance of the fluorescence phenotype. This approach would allow simple measurement of the fitness of individual lineages in a clonal colony context, similar to studies in social microbes (Dingermann et al., 1989; Smukalla et al., 2008; Xavier et al., 2011)

We also targeted GCaMP6s to OSNs with high specificity using the ObirOrco fragment, which was cloned from the clonal raider ant genome. The success of this approach suggests that generating new transgenic lines with transgenes targeted to other cell populations using genomic

fragments is feasible, presenting the possibility of answering diverse questions in social insect neurobiology using a collection of lines with GCaMP targeted to narrow neural populations. Finally, the OSN-targeted GCaMP6s transgenic line we generated for this study is not only useful for studying alarm pheromone representation but has many potential applications for studying odor representation in ants.

Our imaging approach successfully overcomes the challenges posed by the complex ant olfactory system. GCaMP expression was highly consistent and specific to OSNs, allowing robust detection of odor-evoked sensory signals without the need to stain the brain. Together with volumetric two-photon imaging, we were able to record activity from all ~500 olfactory glomeruli from a single odor presentation, which made it feasible to characterize the whole-AL response profile with replication for many stimulus conditions. This approach greatly reduces the impact of inter-trial variation, brain motion, and sensory habituation, which could otherwise dramatically impact the results due to the typically small number of responding glomeruli.

Recording of odor-evoked neural activity from honeybees with pan-neuronal GCaMP was recently reported (Carcaud et al., 2022). This report demonstrated the ability to record activity from multiple brain areas simultaneously in a eusocial insect, a useful approach for understanding sensory information processing and other questions in eusocial insect neurobiology. However, the reported odor-evoked fluorescence deflections are low amplitude, potentially hindering detection of calcium responses, and the pan-neuronal expression could lead to higher noise when imaging AL glomeruli compared to our OSN-specific approach. Resolving potential technical issues with imaging in transgenic honeybees could facilitate interesting comparative experiments on olfaction and pheromone communication between ants and honeybees.

Because alarm pheromones are represented sparsely across glomeruli in clonal raider ants, it should be possible to identify the key neuronal elements through which alarm behavior is elicited, from odorant receptors to central brain regions. Dye filling from pheromone-responsive glomeruli could be used to trace the anatomy of alarm pheromone neural circuits. Identifying and gaining genetic access to specific receptor neuron populations could allow direct tests of causality between glomerular activation and alarm behavior, using e.g. targeted ablation or neural modulators such as kir2.1 and optogenetic approaches (Johns et al., 1999; Deisseroth et al., 2006; Deisseroth, 2015). Extending calcium imaging to other brain areas by generating GCaMP lines with different cell type specificity will aid the identification of the downstream elements of alarm behavior circuits. Over the longer term, combining these approaches could eventually allow linking pheromone sensory channels to motor areas, and to reconstruct the neural circuits that generate alarm and other behaviors.

4.2: Odor and pheromone representation in the clonal raider ant antennal lobe

Using our newly implemented neurogenetic and imaging tools, we characterized the behavioral and sensory correlates of alarm pheromone stimuli in the clonal raider ant. Our study presents the first description of odor response functions across essentially the entire AL of a eusocial insect. These data provide insight into the functional organization of the large and complex olfactory systems of eusocial insects and identify putative components of neural mechanisms through which alarm response behavior is elicited.

Out of our panel of 11 general odorants, we only detected robust responses to five stimuli. As there is currently no data on what compounds the clonal raider ant encounters in its natural environment, other than its own pheromones and cuticular hydrocarbons, it is not

surprising that some of the compounds on our panel were not effective stimuli in this context. Our general odorant experiment paradigm, in which mostly plant-derived volatiles were presented as short pulses of perfumed air, was informed by the insect olfactory literature, which have focused on the detection of floral and fruit volatiles by *Drosophila melanogaster* (Wang et al., 2003; Hallem et al., 2004; Hallem and Carlson, 2006; Pelz et al., 2006; Schlief et al., 2007; Münch and Galizia, 2016). Because *Drosophila* consume yeast living on decaying fruit and also lay their eggs at these locations, plant-derived odorants are of high ecological importance to this species (Hansson et al., 2009). These flies navigate between different potential sites for feeding or egg laying using environmental volatiles in the air as sources of information. Ants, on the other hand, only fly during dispersal and mating and otherwise are ground-based, typically living in underground nests. Workers are entirely earth-bound. Many are primarily or entirely subterranean, including the clonal raider ant (Chandra et al., 2021). Contact chemoreception also plays an especially important role in the close quarters of nest chambers and tunnels that the clonal raider ant typically inhabits. Furthermore, the general odorants that failed to generate calcium responses all had lower vapor pressures compared to the stimuli that caused robust responses, suggesting that the ant olfactory system has low sensitivity to many lower volatility compounds (Table 6.1). Some of the compounds that we tested were also used to examine response functions of ORs from the ant *Harpegnathos saltator*, but robust responses were also rare in that context (Slone et al., 2017). Experiment designs in ants must therefore consider that the clonal raider ant olfactory system is adapted for very different olfactory environments compared to flying insects like the vinegar fly. Future studies of odor representation in the clonal raider ant should identify ecologically relevant odorants, and also explore a wider range of

parameters for odor concentration, stimulus presentation length, and volatile vs. contact presentation.

It has been proposed that the complex ant olfactory system may involve receptor-dependent processes for patterning the glomeruli, similar to mice (Duan and Volkan, 2020; Ryba et al., 2020). While olfactory glomeruli in *Drosophila* are developmentally specified, mouse OSNs lack hard-wired spatial targets in the olfactory bulb, and there is significant local variation in the spatial representation of odors across individuals. We examined the level of stereotypy across individuals for a cluster of three AL glomeruli in the clonal raider ant, and found that they have consistent positions, spatial organization, and odor-evoked response functions. PG_b, PG_a, and 6G always had the same relative position and occurred at similar distances from one another. In contrast, molecularly defined glomeruli have locally variable positions across individuals in mice, and two nearby glomeruli have variable orientation and distance between them (Strotmann et al., 2000; Schaefer et al., 2001). Our results show that ant ALs possess a high degree of spatial conservation at the scale of individual glomeruli, similar to *Drosophila*, axon targeting by ant OSNs can be stereotyped, despite the vastly increased complexity of the olfactory system. However, given that we only performed this analysis on three focal glomeruli, additional work is required to determine whether receptor this level of stereotypy is conserved across other parts of the AL.

We described behavioral and neural responses for two clonal raider ant alarm pheromones and three additional alarm pheromones from other ant species. Of these compounds, 4-methyl-3-hexanol is not produced by clonal raider ants but nonetheless elicits panic alarm behavior. 4-methyl-3-hexanol also activates most of the same glomeruli as the two native alarm pheromones, 4-methyl-3-heptanone and 4-methyl-3-heptanol. Thus, 4-methyl-3-hexanol

represents a chemical cue emitted by other species that affects behavior (i.e., a kairomone), probably by mimicking the native pheromones via activating the same receptors and neural circuits. In contrast, 6-methyl-5-hepten-2-one is neither produced by clonal raider ants nor does it robustly cause panic alarm behavior, while still eliciting robust and extremely long-lasting calcium responses. We showed that the glomerular response pattern for 6-methyl-5-hepten-2-one is distinct from those of the panic inducing alarm pheromones, which aligns with previous work in moths and mice, showing that pheromones and kairomones with different behavioral activity are usually detected through distinct olfactory channels (Isogai et al., 2011; Cattaneo et al., 2017). Interestingly, an ant-hunting spider uses 6-methyl-5-hepten-2-one as an "eavesdropping" kairomone to locate its prey, the meat ant *Iridomyrmex purpureus* (Allan et al., 1996). Given that *O. biroi* is a specialized predator of other ants, our observation that this heterospecific alarm pheromone evokes a distinct pattern of behavioral and neural activity raises the possibility that *O. biroi* may also employ kairomones to detect prey.

In addition to 4-methyl-3-heptanone and 4-methyl-3-heptanol, clonal raider ants produce the common ant alarm pheromone undecane (Lopes et al., 2022). However, this compound generated neither alarm behavior nor calcium responses in our experiments. The ants did increase locomotion after stimulation with undecane compared to control, however, suggesting that they either sense this compound via sensory channels distinct from the GCaMP6s-positive AL glomeruli, or that glomeruli only respond after extended presentations or very high concentrations, higher than what we supplied during calcium imaging. In *Camponotus* carpenter ants, which use undecane as an alarm pheromone, undecane does generate neural activity in the AL (Galizia et al., 1999b; Zube et al., 2008, Yamagata et al., 2006; Mizunami et al., 2010). The

apparent sensory difference between the two species could thus reflect the ecological and chemosensory diversity across the ants.

In both mice and *Drosophila*, olfactory glomeruli with similar chemical receptive ranges are clustered into functional subdomains, a pattern that can result from the duplication and gradual divergence of ancestral chemosensory receptors and their associated glomeruli (Uchida et al., 2000; Fishilevich and Vosshall, 2005; Prieto-Godino et al., 2016). In our experiments, all four pheromones that generated calcium responses (4-methyl-3-heptanone, 4-methyl-3-heptanol, 4-methyl-3-hexanol, and 6-methyl-5-hepten-2-one), which share structural similarities, activated combinations of spatially adjacent glomeruli, despite the sparse representation of alarm pheromones. This suggests that the ant olfactory system also tends to map proximity in chemical space to actual spatial proximity in the AL. Here we focused on glomeruli in the T6 cluster, which are mostly innervated by OSNs expressing ORs in the 9-exon subfamily (McKenzie et al., 2016). This subfamily is particularly highly expanded via gene duplications and undergoes rapid evolution in ants (McKenzie et al. 2016; McKenzie & Kronauer 2018). Accordingly, many 9-exon ORs show similar chemical tuning (Pask et al., 2017; Slone et al., 2017). Our results are thus consistent with a model in which recently duplicated ORs are not only activated by chemically related compounds but are expressed in OSNs innervating adjacent AL glomeruli. An electrophysiological study of subsets of randomly selected olfactory projection neurons in carpenter ants also found spatially clustered responses. However, these responses came from two chemically distinct alarm pheromone components, suggesting that spatial patterning in the ant AL may also reflect pheromone social functions in addition to chemical similarity (Yamagata et al., 2006).

The proportion of glomeruli that robustly responded to any alarm pheromone was very small, with a maximum of only 6 glomeruli displaying robust activation out of ~500 total. Contrary to previous studies on social insects (Joerges et al., 1997; Galizia et al., 1998; Galizia et al., 1999b; Sachse et al., 1999; Guerrieri et al., 2005; Zube et al., 2008; Brandstaetter et al., 2011; Haase et al., 2011; Carcaud et al., 2015; Paoli and Galizia, 2021), this sparse activation shows that alarm pheromones are in fact encoded by small numbers of glomeruli, similar to ecologically relevant chemicals in Drosophila and moths, such as sex pheromones and aversive compounds including CO2 and the microbial odorant geosmin (Christensen and Hildebrand, 1987; Hildebrand and Shepherd, 1997; Sakurai et al., 2004; Dweck et al., 2007; Kurtovic et al., 2007; Jones et al., 2007; Stensmyr et al., 2012). This sparse encoding logic could be advantageous by reducing the computational task for responding to molecules indicative of danger, despite the complex olfactory environment of an ant colony. With the exception of 3-hexanone, the general odorants that we tested also only activated small numbers of glomeruli. This finding is consistent with narrow tuning of individual ant ORs (Pask et al., 2017; Slone et al., 2017), and suggests that ant olfactory systems might compensate for the greater potential signal complexity implied by an expanded olfactory system by narrowing the tuning of glomeruli. Using sparse encoding for sensory signals could decrease the probability of odor mixtures activating hundreds of glomeruli simultaneously, reducing the need for vast numbers of neural connections for decoding highly combinatorial signals. We also found that the temporal dynamics of calcium responses differed by odor and glomerulus. These features provide additional information that olfactory systems can use to interpret sensory inputs, including mixtures of odors (Laurent, 1999; Hallem et al., 2004, Hallem and Carlson, 2006; Su et al., 2011).

Ant pheromone communication employs diverse chemical substrates, including compound mixtures (Hölldobler, 1995; Morgan, 2009). These mixtures can be complex, as is the case for the cuticular hydrocarbon blends that serve as nest membership gestalt odors (Bonavita-Cougourdan et al., 1987). While ant ALs could in principle use broad encoding to represent such complex blends, insect olfactory systems can have an impressive capacity to reduce the complexity of ecologically relevant signal inputs. Mosquito ALs, for example, encode critical features of complex host odor mixtures using only a few glomeruli (Zhao et al., 2022). Future work should investigate whether the sparse encoding we reported here holds true for other types of chemical cues used by ants. This will help develop a general understanding of how glomerular tuning evolves in the context of chemical cues with high ecological relevance, complex chemical communication, and expanded olfactory systems.

CHAPTER 5: MATERIALS AND METHODS

Alarm pheromones. We purchased 96% 4-methyl-3-heptanone from Pfaltz and Bauer (Item #: M19160) and ≥99% 4-methyl-3-heptanol from Sigma-Aldrich (Item #: M48309). 99% 6-methyl-5-hepten-2-one was purchased from Sigma-Aldrich (Item #: M48805-100ML). ≥99% undecane was purchased from Sigma-Aldrich (Item #: U407-25ML) and 95% 4-methyl-3-hexanol was purchased from Enamine (CAS# 615-29-2). Paraffin oil was purchased from Hampton Research (cat. #HR3-421).

General odorants. 98% 3-hexanone, 97% dodecyl acetate, 97% linalool, and ≥70% (+)-valencene were purchased from Aldrich Chemistry (Item numbers 103020-10G, D221953-25G, L2602-5G, and 75056-10G-F, respectively). ≥99% butyric acid, 98% ethylpyrazine, 99% propionic acid, and 97% terpineol were purchased from Sigma-Aldrich (Item numbers W222119-SAMPLE-K, 250384-5G, W292419-SAMPLE-K, and 86480-250ML, respectively). 100% ethanol was purchased from Decon Laboratories (Item #: 2716). ≥99.5% Isopropanol was purchased from Fisher Chemical (Item #: A416SK-4). General odorants were selected from *Drosophila melanogaster* studies (3-hexanone, isopropanol, ethanol, (+)-valencene; Münch and Galizia, 2016); an olfactory study in the ant *Harpegnathos saltator* (dodecyl acetate, ethylpyrazine, geranyl acetate, linalool, terpineol; Slone et al., 2017); or soil volatile organic compounds (butyric acid and propanoic acid; Insam and Seewald, 2010).

Colony alarm bioassay. Alarm behavior assays were performed as described previously (Lopes et al., 2022). For experiments with 4-methyl-3-hexanol, 6-methyl-5-hepten-2-one, and undecane, 30 mixed-age ants from clonal line B were introduced without brood into each arena. For behavioral experiments with GCaMP6s ants, due to limited numbers, 15-20 ants were introduced into each arena. Prior to beginning behavioral experiments, ants were allowed to settle for at

least 5 days, until they had laid eggs and spent most of their time within a tightly packed nest pile.

Each compound (pure compounds for 4-methyl-3-heptanone, 4-methyl-3-heptanol, 4-methyl-3-hexanol, 6-methyl-5-hepten-2-one, undecane, or 9:1 4-methyl-3-heptanone:4-methyl-3-heptanol blend) was freshly diluted 1:20 with 100% pentane each day of experiments. After recording baseline activity for 4 minutes and 30 seconds, 50 µL of each compound was added to a ~1 cm^2 piece of filter paper and allowed to evaporate for 30 seconds before folding and placing into the stimulus chamber. Behavioral responses were recorded for another 5 minutes.

Data were analyzed as described previously, scoring three metrics of interest by hand: (1) the number of ants outside the nest pile, (2) the number of ants outside the nest chamber, and (3) the number of ants touching the mesh wall (indicating attraction to the pheromone source). We limited statistical analyses to the time window starting 1 minute prior to adding the stimulus and 2 minutes after. To evaluate the effect of the stimulus over time, we performed a two-way repeated measures ANOVA, and to determine the effect of the stimulus at each timepoint we used Dunnett's multiple comparisons test.

Categorical analysis of the major behavioral response to each odorant (4-methyl-3-hexanol, 6-methyl-5-hepten-2-one, undecane, and the vehicle control, plus reanalysis of responses to 4-methyl-3-heptanone, 4-methyl-3-heptanol, and the blend from experiments in Lopes et al. 2022) was performed by visually classifying each video as one of the following in a blinded manner: During "immediate panic alarm," the nest pile was disassembled within the first minute of the five-minute-long stimulus exposure. For "ants leave nest," the nest pile persisted for at least one minute but over half of the ants left the region of the nest pile within the first minute. For "increase in activity," the nest pile persisted for at least one minute, and some but

fewer than half of the ants left the region of the nest pile within the first minute. For "no response," the nest pile persisted for the first minute and no additional ants left the region of the nest pile during that time window. We also identified the time when the initial nest pile disappeared after addition of the stimulus. The nest pile was defined as the area containing the eggs and at least two adult ants. We calculated the percentage of time during which the initial nest pile remained present for the first two minutes after addition of the stimulus. We evaluated the effect of the compounds on the nest pile dissipating using a one-way ANOVA and Šidák's multiple comparisons test to compare each additional alarm pheromone to each of the two known *O. biroi* alarm pheromones (4-methyl-3-heptanone, 4-methyl-3-heptanol, and a 9:1 blend of the two compounds).

Generation of transgenic ants

Cloning and plasmid assembly. We assembled plasmids pBAC-ie1-DsRed, pBAC-ie1-DsRed-ObirOrco-QF2-15xQUAS-GCaMP6s, and pBAC-ObirOrco-jGCaMP7s using multiple rounds of PCR for generating fragments, restriction digestion with gel purification for backbones, and Gibson assembly cloning (Gibson et al., 2009; Gibson et al., 2010). Following each Gibson assembly step, correct assembly was verified using restriction digests and by sequencing PCR amplicons spanning across each of the fragment boundaries.

pBAC-ie1-DsRed

[1] piggyBac backbone from pBAC-ECFP-15xQUAS_TATA-SV40 (Addgene, ID #104875) (Riabinina et al., 2016), from double restriction digest with SpeI (New England Biolabs [NEB] #R3133S) and EcoRV (NEB #R0195S).

[2] ie1: An enhancer/promoter from pGL3-IE1 (a gift from Zach Adelman, Addgene ID #52894) (Anderson et al., 2010) (primers: forward 5'-ttatcgaattcctgcagcccgggggatccaACTAGTTGTTCGCCGAGCTCTTACGCGC -3', reverse 5'-ctcggaggaggccatCCGCGGCGAACAGGTCACTTGGTTGTTCACGATCTTG -3').

[3] DsRed from pBac-DsRed-ORCO_9kbProm-QF2 (a gift from Christopher Potter, Addgene ID #104877) (Riabinina et al., 2016) (primers: forward 5'-acctgttcgccgcggATGGCCTCCTCCGAGAA -3', reverse 5'-ttattatatatatttttcttgttatagatGGCGCGCCCGAACACATATGCGAACAACAAACCACAACTAGAATGCAGTG -3').

[4] pBAC-ie1-DsRed from Gibson assembly of piggyBac backbone, ie1-A, and DsRed fragments, transformed into NEB 10-beta competent cells (item # C3019H).

pBAC-ie1-DsRed-ObirOrco-QF2-15xQUAS-GCaMP6s

[1] ObirOrco: A 2.4kb promoter/enhancer fragment from clonal raider ant genomic DNA, clonal line B (NCBI LOC105284785) (primers: forward, 5'-tagttgtggtttgttgttcgcacaTATGTCACGTAATCAGCTTTTGACG -3', lowercase shows Gibson homology region; reverse 5'- gcgcttgggtggcatgttgcaTCATATGTCTGCGAGCAAATGGAACG -3').

[2] QF2 from pBac-DsRed-ORCO_9kbProm-QF2 (primers: forward 5'-aaccaagtgacctgttcgggccggACATATGCAACATGCCACCCAA -3', reverse 5'-acccagtgacacgtgaccgCGAGCGCTGGATCTAAACGAGTTTTTAAGC -3').

[3] 15xQUAS from BAC-ECFP-15xQUAS_TATA-SV40 (a gift from Christopher Potter, Addgene ID #104875) (Riabinina et al., 2016) (primers: forward 5'- cggtcacgtgtcact -3', reverse 5'- tgagaacccatcgaacaagcGTTTAAACAGATCTGTTAACGAATTGATC -3').

[4] GCaMP6s from pGP-CMV-GCaMP6s (a gift from Douglas Kim & GENIE Project, Addgene ID # 40753) (Chen et al., 2013), (primers: forward 5-gggccggcctgttcgAGCGCTTGTTCGATGGGTTCTCATCATCATC -3', reverse 5'-atatattttcttgttatagatggCGCGCCGTAGCCCTAAGATACATTGATGAGTTTG -3')

[5] ie1-B from pBAC-ie1-DsRed, (primers: forward 5'-ctgcattctagttgtggtttgttgttcgcaCATATGTGTTCGCCGAGCTCTTACGCG -3', reverse 5'-catcgaacaagcgctcgaacaggccggcccGAACAGGTCACTTGGTTGTTCAC -3')

[6] pBAC-ie1-DsRed-ie1-GCaMP6s from Gibson assembly of pBAC-ie1-DsRed (linearized using double restriction digest with NdeI [NEB #R0111S] and AscI [NEB #R0558S]), ie1-B, and GCaMP6s.

[7] pBAC-ie1-DsRed-ie1-QF2-15xQUAS-GCaMP6s from Gibson assembly of pBAC-ie1-DsRed-ie1-GCaMP6s (linearized using double restriction digest with FseI [NEB #R0588S] and AfeI [NEB # R0652S]), QF2, and 15xQUAS.

[8] pBAC-ie1-DsRed-ObirOrco-QF2-15xQUAS-GCaMP6s from Gibson assembly of pBAC-ie1-DsRed-ie1-GCaMP6s (linearized and second ie1 copy removed using restriction digest with NdeI) and ObirOrco.

pBAC-ObirOrco-jGCaMP7s

[1] ObirOrco-B from pBAC-ie1-DsRed-ObirOrco-QF2-15xQUAS-GCaMP6s (primers: forward 5'- tgttgttcgcatatgtgttcgggCACGTAATCAGCTTTTGACGA -3', reverse 5'- attttcttgttatagatggAGCGCTGCGAGCAAATGGAAC -3').

[2] jGCaMP7s from pGP-CMV-jGCaMP7s (Addgene ID #104463) (primers: forward 5'- cgttccatttgctcgcagcGCTATGGGTTCTCATCATCATCATC -3', reverse 5'- tatattttcttgttatagatggagcGTTTAAACAGTGAAAAAAATGCTTTATTTGTGAAATTTG -3').

[3] spanning-fragment from dimerization of primers (forward 5'- cttttatcgaattcctgcagcccgggggatccaacCGCGGTGTGTTC -3', reverse 5'- gtttctcgtcaaaagctgattacgtgcccgaacacaCCGCGGTTG -3').

[4] pBAC-ie1-DsRed-ObirOrco from Gibson assembly of pBAC-ie1-DsRed-ObirOrco-QF2-15xQUAS-GCaMP6s (linearized using restriction digest with AscI) and ObirOrco-B.

[5] pBAC-ie1-DsRed-ObirOrco-jGCaMP7s from Gibson assembly of pBAC-ie1-DsRed-ObirOrco (linearized using restriction digest with AfeI) and jGCaMP7s.

[6] pBAC-ObirOrco-JGCaMP7s from Gibson assembly of pBAC-ie1-DsRed-ObirOrco-jGCaMP7s (linearized and ie1-DsRed removed using double restriction digest with NdeI and SpeI) and gap closed with spanning-fragment.

Preparation of injection mixes. Plasmid DNA for injection was purified using a Machery-Nagel endotoxin-free midiprep kit (item #740420.10). The final pellet was washed under RNAse-free conditions and dissolved in nuclease-free water. To remove precipitated DNA from injection mixes, the dissolved plasmid mix was spun in a microcentrifuge at top speed for 5 minutes, and the top 90% of the supernatant was recovered. This step was repeated at least 5 times to produce injectable mix with negligible precipitate, which was stored at -20°C until injection.

We generated mRNA from the hyperactive piggyBac variant hyPBase^{apis} (Otte et al., 2018). A DNA template was generated by PCR amplification of the transposase coding sequence, with addition of a T7 promoter on the forward PCR primer, then purified using Beckman Coulter RNAClean SPRI XPBeads (item #A63987). In vitro transcription was performed with the NEB HiScribe T7 Arca mRNA kit (with tailing) (item #E2060S) to produce poly(A) tailed mRNA encoding hyPBase^{apis}. The mRNA was purified using RNAClean beads (using 1.5x volume of beads compared to the reaction mix) and stored in nuclease-free water at -80°C. Template and RNA were handled under RNAse-free conditions, and a sample of mRNA was examined on an Agilent Bioanalyzer to verify RNA length and confirm absence of degradation. All DNA and RNA concentrations were measured using a Thermofisher Nanodrop.

Egg collection, microinjection, and larval rearing. Eggs were collected as described previously (Trible et al., 2017), with a modified schedule for treatments with eggs <3 hours old. We tested the effect of injecting even younger eggs than our previous protocol which used eggs <5 hours old (Trible et al., 2017) so that hyPBase^{apis} mRNA could be translated to active transposase while embryos still had very few nuclei, potentially reducing mosaicism. For these treatments, old eggs were removed from nests from 9am-10am, and then eggs for injection were collected from 11am-11:30am, 1pm-1:30pm, 3pm-3:30pm, and 5pm-5:30pm. Injections were performed from 11:30am-12:30pm, 1:30pm-2:30pm, 3:30pm-4:30pm, and 5:30pm-6:30pm. This schedule meant that the vast majority of eggs were less than 3 hours old when injected.

Microinjections were performed as described previously (Trible et al., 2017), with the following changes: On each injection day, final injection mixes were produced by thawing and combining stored aliquots of plasmid DNA and hyPBase^{apis} mRNA under RNAse-free conditions in nuclease-free water, into a final concentration of 27.8pmol/µL plasmid and the desired

concentration of hyPBase^{apis}. The final mix was spun at top speed in a microcentrifuge for 5 minutes, and the top 90% of supernatant was used for injection. The initial mix was split into 4 aliquots and kept on ice for the day. A different aliquot was used for each round of injections. On occasions where the needle clogged, the mix was spun at top speed in a microcentrifuge before loading a new needle. The injection pressure was initially set to 3600kpa, but was adjusted throughout the course of injections to maintain a consistent flow of liquid into the embryos.

Larvae were reared as described previously (Trible et al., 2017). Briefly, G0 larvae were hatched and placed in small colonies housed in 5cm diameter Petri dishes with a moist plaster of Paris floor to be reared by adult ants from clonal line A, which we refer to as "chaperones" when we use them to rear offspring transferred from other colonies (Trible et al., 2017). For experiments in which the injected construct included ie1-DsRed, the colonies were examined under an epifluorescence microscope to confirm that some larvae expressed DsRed, indicating uptake of the plasmid. For the ObirOrco-jGCaMP7s line, we looked for GCaMP fluorescence in the antennal club of the pupa to confirm expression of the transgene.

Rearing initial transgenic populations. G0 individuals were reared to adulthood. For cohorts of sufficient size (~20 individuals), chaperones were removed. When the number of G0s was too small to form a robust colony, they were supplemented with wild type clonal line A ants to obtain a population of ~20 individuals. One hind leg was removed from each wild type ant to reduce their egg-laying rate compared to the G0 ants in the nest. Then, the colonies were allowed to produce G1 eggs, which were usually collected twice a week. Collected eggs were transferred to a small colony of ~20 chaperones. G1 individuals were reared to adulthood in these nests and were examined for fluorescence. Different G1 individuals potentially resulted from independent transgene insertion events. To ensure that future transgenic populations were genetically

homogeneous, each fluorescent G1 adult was separated soon after eclosion, and transferred to a new transgenic line-founding colony with ~19 clonal line A ants. Eggs were collected about twice a week from these nests and given to chaperones. Fluorescent adults produced from these colonies were then returned to the transgenic line-founding colony of origin. Through several cycles of this process, genetically homogenous transgenic populations were raised and non-fluorescent individuals were removed, yielding pure colonies.

Phenotyping transgenic ants

Fluorescence microscopy. Confocal microscopy of antibody-stained tissue was conducted using Zen image acquisition software on a Zeiss LSM 880 and a Zeiss LSM 900 equipped with 405nm, 488nm, 561nm and 633nm laser lines. Images were obtained using either a Zeiss LD LCI Plan-Apochromat 40X / 1.2NA or a Zeiss LD LCI Plan-Apochromat 25X / 0.8NA multi-immersion objective lens depending on the tissue sample and Zeiss Immersol G immersion medium (Zeiss # 462959-9901-000). Z-projection images were produced from stacks taken at 1µm steps using ImageJ/FIJI (Schindelin et al., 2012). Two-photon fluorescence microscopy was performed using a Bruker Investigator with a Coherent Axon laser tuned to 920nm, equipped with dual GaAsP detectors, resonant scanning galvanometer, Z-piezo module for high-speed Z-positioning, PrairieView software, and an Olympus 40X 0.9NA water-immersion objective lens. Images of transgenic pupae were produced on an Olympus BX53 epifluorescent microscope equipped with an X-Cite Series 120 light source and Olympus DP73 camera (Figs. 2.4, 2.6A), or on an Olympus SZX16 epifluorescent microscope equipped with an X-Cite XYLIS light source and Olympus EP50 camera (Figs. 2.3, 2.5), using the appropriate filter cubes.

Immunohistochemistry. Antibody staining of ant brains was performed essentially as reported previously (McKenzie et al., 2016). Briefly, the brains of female ants of a single-age cohort were

dissected in cold phosphate-buffered saline (PBS) and fixed in 4% paraformaldehyde for 2 hours at room temperature. For antenna staining, a small section of cuticle was mechanically separated prior to fixation in order to enhance access. Blocking was performed for at least 2 hours using fresh PBS containing 0.1% or 0.5% Triton X-100 and 5% donkey serum albumin. Samples were incubated with the appropriate dilution of primary antibody in fresh blocking solution on an orbital shaker table at room temperature. Following primary incubation, samples were washed and incubated with fluorescently tagged secondary antibody diluted in fresh blocking solution. The following antibodies were used: chicken anti-GFP (Abcam #ab13970), rabbit anti-RFP (Rockland #600-401-379), mouse anti-Synorf (DSHB #3C11), mouse anti-Orco (gift from V. Ruta), goat anti-chicken Alexa 488 (Invitrogen #A-11039), donkey anti-mouse Alexa 647 (Invitrogen #A32787), and donkey anti-rabbit Alexa 594 (Invitrogen #A32787). For some experiments, DAPI (Invitrogen #D1306) and fluorescently tagged phalloidin (Invitrogen #A34055) were included during the secondary antibody incubation step. Stained tissue was mounted in SlowFade mounting media on silane-coated microscopy slides (VWR #63411-01) and stored at 4°C. For AL reconstruction, a confocal stack of the right AL from a GCaMP6s+ brain stained with anti-Synorf was manually segmented using the LABKIT plugin for ImageJ, at 1µm z-axis resolution (Arzt et al., 2022; Schindelin et al., 2012).

Microscopy and dissections. To image intact animals, movement was reduced by placing them at -20°C for 5 minutes before imaging under epifluorescence. For the comparison of DsRed fluorescence between brains and gasters, five individuals each from clonal line B and clonal line B wild type were removed from cycling colonies approximately one month after eclosion. Individuals were placed in ethanol for 10s and then dissected in PBS. Brains were dissected and bodies were cut between the thorax and gaster. Brains and gasters were fixed in 4% PFA for 30

minutes, washed 3x in PBS with 0.1% Triton, and mounted in Dako mounting medium. Whole-mounted antennal clubs were permeabilized by making an incision on one side with a razor before fixation. Brains and gasters were imaged in the red and green fluorescence channels using an epifluorescence microscope to detect DsRed and autofluorescence. For imaging dissected gasters, callows 5 days post eclosion were cooled at -20°C for 5 minutes, placed under ethanol for 10s, dissected in PBS, and immediately imaged using an epifluorescence microscope.

Genome sequencing and genomic analyses. A single ant body was disrupted with a Qiagen TissueLyser II, and genomic DNA was extracted using a Qiagen QIAmp DNA Micro Kit. Libraries were prepared using Nextera Flex, and paired end, 150 base pair reads were sequenced on an Illumina NovaSeq S1 Flow Cell. Raw reads were trimmed using Trimmomatic 0.36 (Bolger et al., 2014) and aligned using bwa mem (Li et al., 2013) to both the *O. biroi* reference genome (Obir_v5.4, GenBank assembly accession: GCA_003672135.1) (McKenzie and Kronauer, 2018) and a linearized plasmid reference genome created by "cutting open" the plasmid sequence at an arbitrary location on the backbone, and pasting 150 bp from the end at the front of the sequence and 150 bp from the front at the end of the sequence to accommodate any reads that might align to the vicinity of the "cut". Reads were sorted and deduplicated using Picard (http://broadinstitute.github.io/picard/), and read depth was recorded at all sites using "samtools depth -aa" (Li et al., 2009) (obtaining approximately 44x coverage for the GCaMP6s individual, 54x coverage for the clonal line A ie1-DsRed individual, and 41x coverage for the clonal line B ie1-DsRed individual). To infer the read depth of well-assembled genomic regions, we obtained all heterozygous SNPs with read depth less than 2x the genome-wide median, which excluded the fewer than 0.5% of such SNPs which likely resulted from errors in genome

assembly. We then randomly selected an equal number of heterozygous SNPs as the number of base pairs in the transgene insert, and calculated read depth at those sites. For analysis of the GCaMP6s line, read depth was calculated separately along both the portion of the transgene insert sequence that aligned to ObirOrco, and the rest of the transgene insert.

Junction reads that aligned to both the transgene insert and the *O. biroi* reference genome were identified using the Integrative Genomics Viewer (Robinson et al., 2011), and alignments were queried by each junction read name using "samtools view" (Li et al., 2009). We performed multiple sequence alignment on these junction reads from each end of the insert using CLUSTAL 2.1 in the R package 'msa' (Larkin et al., 2007; Bodenhofer et al., 2015) and generated consensus sequences. To obtain the sequence of the insertion site in the reference genome, the portion of the sequence that was identical to the end of the transgene insert sequence was removed from the junction read consensus sequences. BLAST (Morgulis et al., 2008) searches of the partial consensus sequence identified a position consistent with the position these junction reads had aligned to in the *O. biroi* reference genome. The insertion locus was examined in the NCBI Genome Data Viewer to check for the presence of predicted gene models (NCBI, 2022a).

In vivo calcium imaging

Ant husbandry and maintenance. Ants were kept at 25°C in nests constructed by lining 5cm Petri dishes with plaster of Paris. Nests were kept humidified and supplied with frozen fire ant pupae as food, ~3 times per week. Colonies with developing eggs or pupae were not fed. Petri dishes held 20-80 workers each. GCaMP6s ants were propagated by cross-fostering GCaMP6s eggs to colonies with clonal line A adults (Trible et al., 2017), which were separated into

isogenic GCaMP6s colonies after eclosion. Isogenic colonies can easily be assembled in this species because *O. biroi* reproduces clonally (Kronauer et al. 2012; Oxley et al. 2014). We separated transgenic animals at the G1 stage and returned all offspring of a particular G1 individual to the same nest as their parent. For live imaging experiments, stock colonies for experiments were assembled by moving cohorts of cross-fostered GCaMP6s ants that eclosed within 2 weeks of one another into fresh Petri dish nests.

Specimen preparation. Adult female worker ants were selected from stock colonies for GCaMP imaging experiments. Ants were 55-60 and 90-104 days post eclosion for the general odorant and alarm pheromone imaging experiments, respectively. Individuals with eyespots (indicative of intercastes; Ravary and Jaisson, 2004 and Teseo et al., 2014a) were excluded from our imaging study. Ants for live imaging were anesthetized on ice for ~3 minutes and then fastened to a custom two-photon imaging mount using blue-light curable glue. The antennae were restrained with a thin strip of Parafilm to decrease motion artifacts. A sheet of Parafilm with a hole for the ant's head was applied on top of the preparation, and a watertight seal was created around the border of the head using additional glue. The preparation was then bathed with fresh ant saline (127 mM NaCl, 7 mM KCl, 1.5 mM $CaCl_2$, 0.8 mM Na_2HPO_4, 0.4 mM KH_2PO_4, 4.8 mM TES, 3.2 mM Trehalose, pH 7.0; Zube et al., 2008) and suffused for the duration of the imaging session with additional ant saline to prevent desiccation, before excising a small imaging window in the cuticle using a sterile hypodermic needle and sharp forceps. The window was positioned above the brain, and connective and glandular tissue were removed to reveal the ALs. Care was taken to keep the antennae and antennal nerves intact. In some cases, a muscle between the ALs and near the esophagus was severed, which reduced the amount of brain

motion. This was advantageous for imaging, but not always feasible due to the small distance between the ALs and slight differences in the accessibility of the muscle from ant to ant.

Two-photon recording. AL volumes were recorded at 2X optical zoom and a resolution of 512x512x33 voxels (XYZ) with 5µm Z steps, resulting in a volume with dimensions of 148x148x165µm, large enough to capture calcium transients from the entire AL. As glomeruli are typically spheroid with a diameter of 10-20µm, each glomerulus was captured in many voxels in all three dimensions. Recordings were obtained at 0.83 volumes per second. We always imaged the right AL. At the beginning of each imaging experiment, we located the dorsal surface of the AL and set that as the top of the imaging volume. Laser power and gain were adjusted for each ant so that all glomeruli were visible but signal was unsaturated. Because we imaged at different depths, we compensated for loss of signal through tissue by increasing the laser power at greater depth using an exponential function. We regularly re-calibrated the position of the imaging volume, laser power, and gain in case there were any changes in baseline fluorescence or brain position during the experiment.

Stimulus presentation. Odors were presented using a custom-built olfactometer on 600mL/min of filtered, medical-grade air regulated with a pair of digital mass flow controllers (AliCat# MC-1SLPM-D-IPC/5M). A constant 'carrier' air stream (200mL/min) was presented to the ant for the duration of the imaging session to reduce mechanical stimulation of the antennae resulting from air turbulence, while a 'stimulus' portion of the air stream (400mL/min) was diverted and perfumed before rejoining the carrier stream at a manifold immediately upstream of the imaging preparation. By default, stimulus air bypassed control and odor vials and entered the manifold directly. During stimulus presentation, the air was perfumed by triggering high-speed three-way valves (Grainger# 6JJ52) controlled by an Arduino Uno and custom MatLab scripts, which

directed the air to control or odor vials. Imaging and stimulus trials were synchronized in time using Bruker PrairieView software (i.e., the same TTL signal initiated both imaging and odor stimulation). Odors were dissolved in paraffin oil vehicle to a total volume of 300µL (concentrations represent v/v in the vial), were stored in 4mL amber glass vials with PTFE/silicone septa and connected to valves and the odor manifold via sterile hypodermic needles and nylon Luer tapers. Odor vials were prepared at the beginning of each day of imaging experiments. The air stream was directed onto the ant's antennae using flexible PVC/vinyl tubing with an internal diameter of 1.588mm (United States Plastic Corp. Item #: 54411) from a distance of approximately 1mm.

All odor presentations had a 3s lead time and lasted for 5s. Before odor presentation, we presented the ant with the paraffin oil vehicle as a negative control and confirmed the absence of fluorescence changes before continuing the experiment. For the general odorant imaging experiment, each ant was then presented with a randomized sequence of 7-9 general odorants (48.0% concentration) which was repeated for three trials. The panel included the following eleven odorants: 3-hexanone, butyric acid, dodecyl acetate, ethanol, ethylpyrazine, geranyl acetate, isopropanol, linalool, propionic acid, terpineol, and (+)-valencene. Only responses to the 5 odorants that generated robust calcium responses that were consistent across ants are shown in Fig. 3.5A. We sometimes observed calcium activity from the other odorants, but responses were weak and not reproducible across trials in different ants (Fig. 3.5B). For the alarm pheromone imaging experiment, we first presented each ant with the paraffin oil vehicle and then with a positive control isopropanol stimulus. We only continued experiments with animals that showed calcium responses to the positive control but not the negative control. Each ant was presented with all five alarm pheromones in a random sequence which was first repeated for three trials at

the lower concentration, followed by three additional trials at the higher concentration (for a total of 30 pheromone presentations per animal). In rare cases, we observed large motion artifacts during a recording, in which case the trial was repeated. Vials and caps were reused after cleaning as follows: removal of remaining liquid, 2x wash with 100% ethanol alternating with 2x rinse in distilled water, 2x wash with 3% Alconox alternating with 2x rinse in distilled water, 2x rinse in distilled water, air dry.

Image processing and analysis. Image processing was done in Fiji/ImageJ (Schindelin et al., 2012). To initially characterize response to odorants, we loaded recordings, used the "Deinterleave" function to separate them into 33 slices corresponding to videos of each recording depth, ran the Image Stabilizer plugin (Li, 2008), applied the "Gaussian Blur" filter with 1-sigma, calculated F_0 from the mean of frames 1-5 (before any calcium changes were detected) and calculated $\Delta F/F_0$ by subtracting and then dividing the image stack from F_0. The peak fold change was calculated using the "Z Project" function set to average the $\Delta F/F_0$ from frames 9-14, when the calcium responses typically peaked. After applying a pseudocolor LUT, we examined the peak fold change at all 33 depth positions to get a sense of the organization of glomerular responses across the ALs. We determined that all responses were positive and responding glomeruli were generally well-separated in the x/y axes. We performed additional analyses using max z-projections. Z-projections were generated by running image stabilization on each imaging plane (Li, 2008), computing $\Delta F/F_0$, running the "Minimum" filter with 2-pixel radius to reduce noise, applying the "Z Project" function through all slices with maximum setting, and changing all values >4 to 4 or <-1 to -1 using the "changeValues" function, to equalize the LUT range. For analyzing glomerular response patterns across the whole AL, we examined all max z-projection images at the highest odor concentration for each ant and drew ROIs around every glomerular

region that responded to any odor in at least two trials (a small number of trials were excluded due to large motion artifacts that were only apparent after generating max projections). We then quantified the peak fold change across all trials for a particular odor and concentration and designated a region as responding if the value was ≥0.2. In cases where two odors activated glomeruli that appeared to overlap in the max z-projection, we examined the z-stacks to determine if the responses occurred at the same z-depth and excluded overlaps if the responses occurred at different depths. For visualizing the imaging volume (Fig. 3.4E), we used the first frame of a recording, and generated max z-projections using the z-project function. For the x-projection, we used the "Re-slice" function starting from the left to re-order the pixels, and then used the max z-project function. To visualize calcium responses throughout the imaging volume (Fig. 3E), the max z-projections of calcium responses were generated as before, but because imaging noise was more apparent in the x-projections due to higher resolution in that axis compared to the z-axis, the minimum filter was set to a 3-pixel radius.

For analyses of single glomeruli, we visually identified the z-plane containing the center of the glomerulus of interest for each trial, generated a max z-projection across 3 adjacent imaging planes (to reduce the impact of brain motion in the z-axis), and then calculated $\Delta F/F_0$. Peak fold change was quantified by averaging the $\Delta F/F_0$ over frames 9-14, the time range during which most odor-evoked calcium responses peaked.

Spatial relationships between PG_b, PG_a, and 6G were quantified by examining the first frame of a video plane in which all three glomeruli were visible, placing a marker at the center of each glomerulus, and calculating the vector connecting the centers, with PG_b at (0,0). The three glomeruli were visible in the same z-plane. In two individuals, the spatial relationship between PG_b and PG_a was not quantified because PG_a could not be identified.

Statistical analyses of odor responses. We analyzed the responses of the three glomeruli PG_b, PG_a, and 6G to different odors and concentrations. For every glomerulus/odor combination, peak fold change values from all trials were loaded into R, and a linear regression model was fit for the peak calcium response as a function of odor concentration, with a random effect for individual, using the glm function (R Core Team, 2021). Model predictions were generated and plotted with ggplot2 (Wickam, 2016) with 95% confidence intervals.

To examine temporal dynamics in the three focal glomeruli, normalized calcium response traces from each glomerulus were loaded into R (R Core Team, 2021). The first five recorded frames were used as the baseline, and calcium response onset was defined as the latency between the start of the stimulus presentation and the time point where ΔF/F0 exceeded the mean of the baseline + 3SD of the baseline. The time to response maximum was defined as the latency between the start of the stimulus presentation and the timepoint with the maximum value of ΔF/F0. Traces where ΔF/F0 never exceeded the mean of the baseline + 3SD of the baseline were excluded. Only glomerulus/pheromone combinations with typically robust responses were included (4-methyl-3-heptanone in PG_b; 4-methyl-3-heptanol and 4-methyl-3-hexanol in PG_b and PG_a; 6-methyl-5-hepten-2-one in 6G). Data were plotted with ggplot2 (Wickam, 2016). To test for effects of pheromone and glomerulus identity on calcium response temporal dynamics, we performed statistical analyses on the subset of data for which the same pheromone caused responses in more than one focal glomerulus, i.e., responses in PG_b and PG_a from trials with 4-methyl-3-heptanol and 4-methyl-3-hexanol. For each temporal parameter, we built a linear mixed effects model using the lme function in R (R Core Team, 2021), modeling the effects of pheromone, glomerulus, and an interaction of pheromone/glomerulus, with a random effect for trial ID nested within ant ID.

CHAPTER 6: APPENDIX

Odorant	Category	Generated robust AL responses?	Vapor pressure (mmHg) at RT
ethanol	General odorant	Yes	40
isopropanol	General odorant	Yes	33
3-hexanone	General odorant	Yes	13.9
4-methyl-3-heptanone	Ant alarm pheromone	Yes	5.03 (predicted)
propionic acid	General odorant	Yes	2.9
6-methyl-5-hepten-2-one	Ant alarm pheromone	Yes	1.78 (predicted)
ethylpyrazine	General odorant	Yes	1.67
4-methyl-3-hexanol	Ant alarm pheromone	Yes	1.55 (predicted)
4-methyl-3-heptanol	Ant alarm pheromone	Yes	0.43 (predicted)
butyric acid	General odorant	No	0.43
undecane	Ant alarm pheromone	No	0.41
linalool	General odorant	No	0.16
terpineol	General odorant	No	0.04
(+)-valencene	General odorant	No	0.033 (predicted)
geranyl acetate	General odorant	No	0.02
dodecyl acetate	General odorant	No	0.00047

Table 6.1. Vapor pressures of odorant stimuli. Odors are listed according to vapor pressure in descending order. Vapor pressure values were obtained from the PubChem database (National Institute for Biotechnology Information: https://pubchem.ncbi.nlm.nih.gov). For records with missing values from PubChem, predicted values are given instead, generated from EPISuite (US

EPA, 2022) and obtained from the ChemSpider database (Royal Society for Chemistry: https://www.chemspider.com).

REFERENCES

Abuin, L., Bargeton, B., Ulbrich, M.H., Isacoff, E.Y., Kellenberger, S., and Benton, R. (2011). Functional architecture of olfactory ionotropic glutamate receptors. Neuron 69, 44-60. https://doi.org/10.1016/j.neuron.2010.11.042.

Allan, R.A., Elgar, M.A., and Capon, R.J. (1996). Exploitation of an ant chemical alarm signal by the zodariid spider *Habronestes bradleyi Walckenaer*. Proc. R. Soc. B Biol. Sci. 263, 69–73. https://doi.org/10.1098/rspb.1996.0012.

Anderson, M.A.E., Gross, T.L., Myles, K.M., and Adelman, Z.N. (2010). Validation of novel promoter sequences derived from two endogenous ubiquitin genes in transgenic *Aedes aegypti*. Insect Mol. Biol. 19, 441–449. https://doi.org/10.1111/j.1365-2583.2010.01005.x.

Anton, S. and Homberg, U. (1999). Antennal lobe structure. In Insect Olfaction. Hansson, B.S., ed. (Berlin, Heidelberg: Springer Berlin Heidelberg), pp. 97-124.

Arzt, M., Deschamps, J., Schmied, C., Pietzsch, T., Schmidt, D., Tomancak, P., Haase, R., and Jug, F. (2022). LABKIT: labeling and segmentation toolkit for big image data. Front. Comput. Sci. 4, 777728. https://doi.org/10.3389/fcomp.2022.777728.

Ayre, G.L. and Blum, M.S. (1971). Attraction and alarm of ants (*Camponotus* spp.: Hymenoptera: Formicidae) by pheromones. Physiol. Zool. 44, 77–83. https://doi.org/10.1086/physzool.44.2.30155558.

Batra, S.W.T. (1966). Nests and social behavior of Halictine bees of India (Hymenoptera: Halictidae). Indian J. Entomol. 28, 375-393. https://digitalcommons.usu.edu/bee_lab_ba/105.

Batra, S.W.T. (1968). Behavior of some social and solitary Halictine bees within their nests: A comparative study (Hymenoptera: Halictidae). J. Kans. Entomol. Soc. 41, 120-133. http://www.jstor.org/stable/25083687.

Bellen, H.J, Levis, R.W., He, Y., Carlson, J.W., Evans-Holm, M., Bae, E., Kim, J., Metaxakis, A., Savakis, C., Schulze, K.L. et al. (2011). The Drosophila gene disruption project: progress using transposons with distinctive site specificities. Genetics 188, 731-743. https://doi.org/10.1534/genetics.111.126995.

Bento, J.M.S., Della Lucia, T.M.C., Do Nascimento, R.R., Bergmann, J., and Morgan, E.D. (2007). Response of workers of *Atta sexdens rubropilosa* (Hymenoptera: Formicidae) to mandibular gland compounds of virgin males and females. Physiol. Entomol. 32, 283–286. https://doi.org/10.1111/j.1365-3032.2007.00570.x.

Bergström, G. and Löfqvist, J. (1970). Chemical basis for odour communication in four species of *Lasius* ants. J. Insect Physiol. 16, 2353–2375. https://doi.org/10.1016/0022-1910(70)90157-5.

Benabentos, R., Hirose, S., Sucgang, R., Curk, T., Katoh, M., Ostrowski, E., Strassmann, J., Queller, D., Zupan, B., Shaulsky, G., et al. (2009). Polymorphic members of the *lag* gene family mediate kin discrimination in *Dictyostelium*. Curr. Biol. 19, 567–572. https://doi.org/10.1016/j.cub.2009.02.037.

Ben-Shaul, Y. (2015). Extracting social information from chemosensory cues: consideration of several scenarios and their functional implications. Front. Neurosci. 9, 439. https://doi.org/10.3389/fnins.2015.00439.

Benton, R., Dessimoz, C., and Moi, D. (2020). A putative origin of the insect chemosensory receptor superfamily in the last common eukaryotic ancestor. Elife 9, e62507. https://doi.org/10.7554/eLife.62507.

Bernardi, R., Cardani, C., Ghiringelli, D., Selva, A., Baggini, A., and Pavan, M. (1967). On the components of secretion of mandibular glands of the ant *Lasius (Dendrolasius) fuliginosus*. Tetrahedron Lett. 40, 3893–3896. https://doi.org/10.1016/S0040-4039(01)89747-1.

Blum, M.S. (1969). Alarm pheromones. Annu. Rev. Entomol. *14*, 57–81. https://doi.org/10.1146/annurev.en.14.010169.000421.

Blum, M.S. and Brand, J.M. (1972). Social insect pheromones: Their chemistry and function. Integr. Comp. Biol. 12, 553–576. https://doi.org/10.1093/icb/12.3.553.

Blum, S. and Hermann, H.R. (1978). Venoms and venom apparatuses of the Formicidae: Dolichoderinae and Aneuretinae. In Arthropod Venoms: Handbook of Experimental Pharmacology, S. Bettini, ed. (Berlin, Heidelberg: Springer Berlin Heidelberg), pp. 871–894.

Billen, J. (1986). Morphology and ultrastructure of the dufour's and venom gland in the ant, *Myrmica rubra* (L.) (Hymenoptera: Formicidae). Int. J. Insect Morphol. Embryol. 15, 13-25. https://doi.org/10.1016/0020-7322(86)90003-6.

Bodenhofer, U., Bonatesta, E., Horejš-Kainrath, C., and Hochreiter, S. (2015). msa: An R package for multiple sequence alignment. Bioinformatics 31, 3997–3999. https://doi.org/10.1093/bioinformatics/btv494.

Bolger, A.M., Lohse, M., and Usadel, B. (2014). Trimmomatic: A flexible trimmer for Illumina sequence data. Bioinformatics 30, 2114–2120. https://doi.org/10.1093/bioinformatics/btu170.

Bonavita-Cougourdan, A., Clément, J.L., and Lange, C. (1987). Nestmate recognition: the role of cuticular hydrocarbons in the ant Camponotus vagus scop. J. Entomol. Sci. 22, 1-10. https://doi.org/10.18474/0749-8004-22.1.1.

Boomsma, J.J. (2013). Beyond promiscuity: Mate-choice in commitments in social breeding. Philos. Trans. R. Soc. B Biol. Sci. 368, 20120050-20120050. https://doi.org/10.1098/rstb.2012.0050.

Boyle, K.E., Monaco, H.T., Deforet, M., Yan, J., Wang, Z., Rhee, K., and Xavier, J.B. (2017). Metabolism and the evolution of social behavior. Mol. Biol. Evol. 34, 2367–2379. https://doi.org/10.1093/molbev/msx174.

Boyle, K.E., Monaco, H., van Ditmarsch, D., Deforet, M., and Xavier, J.B. (2015). Integration of metabolic and quorum sensing signals governing the decision to cooperate in a bacterial social trait. PLoS Comput. Biol. 11, e1004279. https://doi.org/10.1371/journal.pcbi.1004279.

Brandstaetter, A.S., Rössler, W., and Kleineidam, C.J. (2010). Dummies versus air puffs: Efficient delivery for low-volatile odors. Chem. Senses 3, 323-333. https://doi.org/10.1093/chemse/bjq022.

Brandstaetter, A.S., Rössler, W., and Kleineidam, C.J. (2011). Friends and foes from an ant brain's point of view -- neuronal correlates of colony odors in a social insect. PLoS One 6, e21383. https://doi.org/10.1371/journal.pone.0021383.

Brandstaetter, A.S. and Kleineidam, C.J. (2011). Distributed representation of social odors indicates parallel processing in the antennal lobe of ants. J. Neurophysiol. 106, 2437–2449. https://doi.org/10.1152/jn.01106.2010.

Butterwick, J.A., del Mármol, J., Kim, K.H., Kahlson, M.A., Rogow, J.A., Walz, T., and Ruta, V. (2018). Cryo-EM structure of the insect olfactory receptor Orco. Nature 560, 447-452. https://doi.org/10.1038/s41586-018-0420-8.

Carcaud, J., Giurfa, M., and Sandoz, J.-C. (2015). Differential combinatorial coding of pheromones in two olfactory subsystems of the honey bee brain. J. Neurosci. 35, 4157-4167. https://doi.org/10.1523/JNEUROSCI.0734-14.2015.

Carcaud, J., Otte, M., Grünewald, B., Haase, A., Sandoz, J.-C., Beye, M. (2022). Multisite imaging of neural activity using a genetically encoded calcium sensor in the honey bee *Apis mellifera*. Preprint at bioRxiv, https://doi.org/10.1101/2022.04.22.489138.

Carlsson, M.A. and Hansson, B.S. (2003). Dose–response characteristics of glomerular activity in the moth antennal lobe. Chem. Senses 28, 269-278. https://doi.org/10.1093/chemse/28.4.269.

Campanacci, V., Lartigue, A., Hällberg, B.M., Jones, T.A., Giudici-Orticoni, M.-T., Tegoni, M., and Cambillau, C. (2003). Proc. Natl. Acad. Sci. U. S. A. 100, 5069-5074. https://doi.org/10.1073/pnas.0836654100.

Cary, L.C., Goebel, M., Corsaro, B.G., Wang, H.G., Rosen, E., and Fraser, M.J. (1989). Transposon mutagenesis of baculoviruses: analysis of *Trichoplusia ni* transposon *IFP2* insertions within the FP-locus of nuclear polyhedrosis viruses. Virology 172, 156–169. https://doi.org/10.1016/0042-6822(89)90117-7.

Cattaneo, A.M., Gonzalez, F., Bengtsson, J.M., Corey, E.A., Jacquin-Joly, E., Montagné, N., Salvagnin, U., Walker, W.B., Witzgall, P., Anfora, G., et al. (2017). Candidate pheromone receptors of codling moth *Cydia pomonella* respond to pheromones and kairomones. Sci. Rep. 7, 41105. https://doi.org/10.1038/srep41105.

Chandra, V., Gal, A., and Kronauer, D.J.C. (2021). Colony expansions underlie the evolution of army ant mass raiding. Proc. Natl. Acad. Sci. U. S. A. 118, e2026534118. https://doi.org/10.1073/pnas.2026534118.

Chen, T.-W., Wardill, T.J., Sun, Y., Pulver, S.R., Renninger, S.L., Baohan, A., Schreiter, E.R., Kerr, R.A., Orger, M.B., Jayaraman, V., et al. (2013). Ultrasensitive fluorescent proteins for imaging neuronal activity. Nature 499, 295–300. https://doi.org/10.1038/nature12354.

Christensen, T.A. and Hildebrand, J.G. (1987). Male-specific, sex pheromone-selective projection neurons in the antennal lobes of the moth *Manduca sexta*. J. Comp. Physiol. A 160, 553-569. https://doi.org/10.1007/BF00611929.

Chuang, J.S., Rivoire, O., and Leibler, S. (2009). Simpson's paradox in a synthetic microbial system. Science 323, 272–275. https://doi.org/10.1126/science.1166739.

Crespi, B.J. and Yanega, D. (1995). The definition of eusociality. Behav. Ecol. 6, 109-115. https://doi.org/10.1093/beheco/6.1.109.

Dahanukar, A., Hallem, E.A., and Carlson, J.R. (2005). Insect chemoreception. Curr. Opin. Neurobiol. 14, 423-430. https://doi.org/10.1016/j.conb.2005.06.001.

Dana, H., Sun, Y., Mohar, B., Hulse, B.K., Kerlin, A.M., Hasseman, J.P., Tsegaye, G., Tsang, A., Wong, A., Patel, R., et al. (2019). High-performance calcium sensors for imaging activity in neuronal populations and microcompartments. Nat. Methods 16, 649–657. https://doi.org/10.1038/s41592-019-0435-6.

Dani, F.R., Michelucci, E., Francese, S., Mastrobuoni, G., Cappellozza, S., La Marca, G., Niccolini, A., Felicioli, A., Moneti, G., and Pelosi, P. (2011). Chem. Senses 36, 335-344. https://doi.org/10.1093/chemse/bjq137.

Deisseroth, K. (2015). Optogenetics: 10 years of microbial opsins in neuroscience. Nat. Neurosci. 18, 1213-1225. https://doi.org/10.1038/nn.4091.

Deisseroth, K., Feng, G., Majewska, A.K., Miesenböck, G., Ting, A., and Schnitzer, M.J. (2006). Next-generation optical technologies for illuminating genetically targeted brain circuits. J. Neurosci. 26, 10380–10386. https://doi.org/10.1523/JNEUROSCI.3863-06.2006.

Dietemann, V., Peeters, C., Liebig, J., Thivet, V., and Hölldobler, B. (2003). Cuticular hydrocarbons mediate discrimination of reproductives and nonreproductives in the ant *Myrmica gulosa*. Proc. Natl. Acad. Sci. U. S. A. 100, 10341-10346. https://doi.org/10.1073/pnas.1834281100.

Dingermann, T., Reindl, N., Werner, H., Hildebrandt, M., Nellen, W., Harwood, A., Williams, J., Nerke, K. (1989). Optimization and in situ detection of *Escherichia coli* β-galactosidase gene expression in *Dictyostelium discoideum*. Gene 85, 353–362. https://doi.org/10.1016/0378-1119(89)90428-9.

Duan, Q. and Volkan, P.C. (2020). Ant olfaction: Smells like an insect, develops like a mammal. Curr. Biol. 30, R950–R952. https://doi.org/10.1016/j.cub.2020.06.074.

Duffield, R.M. and Blum, M.S. (1973). 4-Methyl-3-Heptanone: identification and function in *Neoponera villosa* (Hymenoptera: Formicidae). Ann. Entomol. Soc. Am. 66, 1357. https://doi.org/10.1093/aesa/66.6.1357.

Duffield, R.M., Blum, M.S., and Wheeler, J.M. (1976). Aklylpyrazine alarm pheromones in primitive ants with small colonial units. Comp. Biochem. Physiol. 54, 439-440. https://doi.org/10.1016/0305-0491(76)90116-4.

Duffield, R.M., Brand, J.M., and Blum, M.S. (1977). 6-methyl-5-hepten-2-one in *Formica* species: Identification and function as an alarm pheromone (Hymenoptera: Formicidae). Ann. Entomol. Soc. Am. 70, 309–310. https://doi.org/10.1093/aesa/70.3.309.

Dweck, H.K.M., Ebrahim, S.A.M., Thoma, M., Mohamed, A.A.M., Keesey, I.W., Trona, F., Lavista-Llanos, S., Svatoš, A., Sachse, S., Knaden, M., et al. (2007). Pheromones mediating copulation and attraction in *Drosophila*. Proc. Natl. Acad. Sci. U. S. A. 112, E2829-E2835. https://doi.org/10.1073/pnas.1504527112.

Enjin, A. and Suh, G.S.-S. (2013). Neural mechanisms of alarm pheromone signaling. Mol. Cells 35, 177-181. https://doi.org/10.1007/s10059-013-0056-3.

d'Ettorre, P., Heinze, J., Schulz, C., Francke, W., and Ayasse, M. (2004). Does she smell like a queen? Chemoreception of a cuticular hydrocarbon in the ant *Pachycondyla inversa*. J. Exp. Biol. 207, 1085-1091. https://doi.org/10.1242/jeb.00865.

d'Ettorre, P. and Lenoir, A. (2009). Nestmate recognition. In Ant Ecology. L. Lach, C. Parr, and K. Abbott, eds. Oxford, UK: Oxford University Press, pp. 194-209.

Ferkey, D.M., Hyde, R., Haspel, G., Dionne, H.M., Hess, H.A., Suzuki, H., Schafer, W.R., Koelle, M.R., and Hart, A.C. (2007). *C. elegans* G protein regulator RGS-3 controls sensitivity to sensory stimuli. Neuron 5, 39-52. https://doi.org/10.1016/j.neuron.2006.11.015.

Ferguson, S.T., Bakis, I., and Zwiebel, L.J. (2021). Advances in the study of olfaction in eusocial ants. Insects 12, 252. https://doi.org/10.3390/insects12030252.

Ferguson, S.T., Park, K.Y., Ruff, A.A., Bakis, I., and Zwiebel, L.J. (2020). Odor coding of nestmate recognition in the eusocial ant *Camponotus floridanus*. J. Exp. Biol. 223, jeb215400. https://doi.org/10.1242/jeb.215400.

Fishilevich, E. and Vosshall, L.B. (2005). Genetic and functional subdivision of the *Drosophila* antennal lobe. Curr. Biol. 15, 1548-1553. https://doi.org/10.1016/j.cub.2005.07.066.

Foster, K.R. (2004). Diminishing returns in social evolution: The not-so-tragic commons. J. Evol. Biol. 17, 1058–1072. https://10.1111/j.1420-9101.2004.00747.x.

Fraser, M.J., Ciszczon, T., Elick, T., and Bauser, C. (1996). Precise excision of TTAA-specific lepidopteran transposons *piggyBac* (IFP2) and *tagalong* (TFP3) from the baculovirus genome in cell lines from two species of Lepidoptera. Insect Mol. Biol. 5, 141–151. https://doi.org/10.1111/j.1365-2583.1996.tb00048.x.

Fuscà, D. and Kloppenburg, P. (2021). Cell Tissue Res. 383, 59-73. https://doi.org/10.1007/s00441-020-03387-3.

Galizia, C.G., Joerges, J., Küttner, A., Faber, T., and Menzel, R. (1997). A semi-in-vivo preparation for optical recording of the insect brain. J. Neurosci. Methods 76, 61-69. https://doi.org/10.1016/S0165-0270(97)00080-0.

Galizia, C.G., Nägler, K., Hölldobler, B., and Menzel, R. (1998). Odour coding is bilaterally symmetrical in the antennal lobes of honeybees (*Apis mellifera*). Eur. J. Neurosci. 10, 2964–2974. https://doi.org/10.1111/j.1460-9568.1998.00303.x.

Galizia, C.G., Sachse, S., Rappert, A., and Menzel, R. (1999a). The glomerular code for odor representation is species specific in the honeybee *Apis mellifera*. Nat. Neurosci. 2, 473–478. https://doi.org/10.1038/8144.

Galizia, C.G., Menzel, R., and Hölldobler, B. (1999b). Optical imaging of odor-evoked glomerular activity patterns in the antennal lobes of the ant *Camponotus rufipes*. Naturwissenschaften 86, 533–537. https://doi.org/10.1007/s001140050669.

Gao, Q., Yuan, B., and Chess, A. (2000). Convergent projections of *Drosophila* olfactory neurons to specific glomeruli in the antennal lobe. Nat. Neurosci. 3, 780–785. https://doi.org/10.1038/77680.

Ghaninia, M., Berger, S.L., Reinberg, D., Zwiebel., L.J., Ray, A., and Liebig, J. (2018). Antennal olfactory physiology and behavior of males of the ponerine ant *Harpegnathos saltator*. J. Chem. Ecol. 44, 999-1007. https://doi.org/10.1007/s10886-018-1013-6.

Gibson, D.G., Young, L., Chuang, R.Y., Venter, J.C., Hutchison, C.A., and Smith, H.O. (2009). Enzymatic assembly of DNA molecules up to several hundred kilobases. Nat. Methods 6, 343–345. https://doi.org/10.1038/nmeth.1318.

Gibson, D.G., Glass, J.I., Lartigue, C., Noskov, V.N., Chuang, R.Y., Algire, M.A., Benders, G.A., Montague, M.G., Ma, L., Moodie, M.M., et al. (2010). Creation of a bacterial cell controlled by a chemically synthesized genome. Science 329, 52–56. https://doi.org/10.1126/science.1190719.

Gilbert, O.M., Foster, K.R., Mehdiabadi, N.J., Strassmann, J.E., and Queller, D.C. (2007). High relatedness maintains multicellular cooperation in a social amoeba by controlling cheater mutants. Proc. Natl. Acad. Sci. U. S. A. 104, 8913–8917. https://doi.org/10.1073/pnas.0702723104.

Gregory, M., Alphey, L., Morrison, N.I., and Shimeld, S.M. (2016). Insect transformation with *piggyBac*: getting the number of injections just right. Insect Mol. Biol. 25, 259-271. https://doi.org/10.1111/imb.12220.

Griffin, A.S., West, S.A., and Buckling, A. (2004). Cooperation and competition in pathogenic bacteria. Nature 430, 1024–1027. https://doi.org/10.1038/nature02744.

Groth, A.C., Fish, M., Nusse, R., and Calos, M.P. (2004). Construction of transgenic *Drosophila* by using site-specific integrase from phase phiC31. Genetics 166, 1775-1782. https://doi.org/10.1534/genetics.166.4.1775.

Guerrieri, F., Schubert, M., Sandoz, J.C., and Giurfa, M. (2005). Perceptual and neural olfactory similarity in honeybees. PLoS Biol. 3, 0718–0732. https://doi.org/10.1371/journal.pbio.0030060.

Guttikonda, S.K., Marri, P., Mammadov, J., Ye, L., Soe, K., Richey, K., Cruse, J., Zhuang, M., Gao, Z., Evans, et al. (2016). Molecular characterization of transgenic events using next generation sequencing approach. PLoS One 11, e0149515. https://doi.org/10.1371/journal.pone.0149515.

Haase, A., Rigosi, E., Trona, F., Anfora, G., Vallortigara, G., Antolini, R., and Vinegoni, C. (2011). In-vivo two-photon imaging of the honey bee antennal lobe. Biomed. Opt. Express 2, 131-138. https://doi.org/10.1364/boe.2.000131.

Habenstein, J., Amini, E., Grübel, K., el Jundi, B., and Rössler, W. (2020). The brain of *Cataglyphis* ants: Neuronal organization and visual projections. J. Comp. Neurol. 528, 3479–3506. https://doi.org/10.1002/cne.24934.

Hallem, E.A. and Carlson, J.R. (2006). Coding of odors by a receptor repertoire. Cell 125, 143-160. https://doi.org/10.1016/j.cell.2006.01.050.

Hallem, E.A., Dahanukar, A., and Carlson, J.R. (2006). Insect odor and taste receptors. Annu. Rev. Entomol. 51, 113-135. https://doi.org/10.1146/annurev.ento.51.051705.113646.

Hallem, E.A., Ho, M.G., and Carlson, J.R. (2004). The molecular basis of odor coding in the *Drosophila* antenna. Cell 117, 956-979. https://doi.org/10.1016/j.cell.2004.05.012.

Hamilton, W.D. (1963). The evolution of altruistic behavior. Am. Nat. 97, 354–356. https://doi.org/10.1086/497114.

Hamilton, W.D. (1964a). The genetical evolution of social behavior I. J. Theor. Biol. 7, 1-16. https://doi.org/10.1016/0022-5193(64)90038-4.

Hamilton, W.D. (1964b). The genetical evolution of social behavior II. J. Theor. Biol. 7, 17-52. https://doi.org/10.1016/0022-5193(64)90039-6.

Han, S., Chen, W., and Elgar, M.A. (2022). An ambiguous function of an alarm pheromone in the collective displays of the Australian meat ant, *Iridomyrmex purpureus*. Ethology 128, 70–76. https://doi.org/10.1111/eth.13241.

Hansson, B.S., Knaden, M., Sachse, S., Stensmyr, M.C., and Wicher, D. (2009). Towards plant-odor-related olfactory neuroethology in *Drosophila*. Chemoecology 20, 51-61. https://doi.org/10.1007/s00049-009-0033-7.

Herre, M., Goldman, O.V., Lu, T.-C., Caballero-Vidal, G., Qi, Y., Gilbert, Z.N., Gong, Z., Morita, T., Rahiel, S., Ghaninia, M., et al. (2022). Non-canonical odor coding in the mosquito. Cell 185, 3104-3123.e28. https://doi.org/10.1016/j.cell.2022.07.024.

Hildebrand, J.G. and Shepherd, G.M. (1997). Mechanisms of olfactory discrimination: Converging evidence for common principles across phyla. Annu. Rev. Neurosci. 20, 595-631. https://doi.org/10.1146/annurev.neuro.20.1.595.

Hillery, A.E., and Fell, R.D. (2000). Chemistry and behavioral significance of rectal and accessory gland contents in *Camponotus pennsylvanicus* (Hymenoptera: Formicidae). Ann. Entomol. Soc. Am. 93, 1294–1299. https://doi.org/10.1603/0013-8746(2000)093[1294:CABSOR]2.0.CO;2.

Hölldobler, B. and Wilson, E.O. (1990). The Ants (Harvard University Press).

Hughes, W.O.H., Howse, P.E., Vilela, E.F., and Goulson, D. (2001). The response of grass-cutting ants to natural and synthetic versions of their alarm pheromone. Physiol. Entomol. 26, 165–172. https://doi.org/10.1046/j.1365-3032.2001.00230.x.

Hughes, W.O.H., Oldroyd, B.P., Beekman, M., and Ratnieks, F.L.W. (2008). Ancestral monogamy shows kin selection is key to the evolution of eusociality. Science 320, 1213-1217. https://doi.org/10.1126/science.1156108.

Insam, H. and Seewald, M.S.A. (2010). Volatile organic compounds (VOCs) in soils. Biol. Fertil. Soils 46, 199-213. https://doi.org/10.1007/s00374-010-0442-3.

Isogai, Y., Si, S., Pont-Lezica, L., Tan, T., Kapoor, V., Murthy, V.N., and Dulac, C. (2011). Molecular organization of vomeronasal chemoreception. Nature 478, 241–245. https://doi.org/10.1038/nature10437.Molecular.

Jasin, M. and Haber, J.E. (2016). The democratization of gene editing: insights from site-specific cleavage and double-strand break repair. DNA Repair 44, 6-16. https://doi.org/10.1016/j.dnarep.2016.05.001.

Joerges, J., Küttner, A., Galizia, C.G., and Menzel, R. (1997). Representations of odours and odour mixtures visualized in the honeybee brain. Nature 387, 285–288. https://doi.org/10.1038/387285a0.

Johansson, B. and Jones, T.M. (2007). The role of chemical communication in mate choice. Biol. Rev. 82, 265-289. https://doi.org/10.1111/j.1469-185X.2007.00009.x

Johns, D.C., Marx, R., Mains, R.E., O'Rourke, B., and Marbán, E. (1999). Inducible genetic suppression of neuronal excitability. J. Neurosci. 19, 1691–1697. https://doi.org/10.1523/jneurosci.19-05-01691.1999.

Jones, W.D., Cayirlioglu, P., Kadow, I.G., and Vosshall, L.B. (2007). Two chemosensory receptors together mediate carbon dioxide detection in *Drosophila*. Nature 445, 86-90. https://doi.org/10.1038/nature05466.

Kay, T., Keller, L., and Lehmann, L. (2020). The evolution of altruism and the serial rediscovery of the role of relatedness. Proc. Natl. Acad. Sci. U. S. A. 117, 28894–28898. https://doi.org/10.1073/pnas.2013596117.

Keegans, S.J., Billen, J., Morgan, D.E., and Gökcen, O.A. (1993). Volatile glandular secretions of three species of new world army ants, *Eciton burchelli, Labidus coecus*, and *Labidus praedator*. J. Chem. Ecol. 19, 2705–2719. https://doi.org/10.1007/BF00980702.

Kelber, C., Rössler, W., and Kleineidam, C.J. (2010). Phenotypic plasticity in number of glomeruli and sensory innervation of the antennal lobe in leaf-cutting ant workers (*A. vollenweideri*). Dev. Neurobiol. 70, 222–234. https://doi.org/10.1002/dneu.20782.

Kidokoro-Kobayashi, M., Iwakura, M., Fujiwara-Tsuji, N., Fujiwara, S., Sakura, M., Sakamoto, H., Higashi, S., Hefetz, A., and Ozaki, M. (2012). Chemical discrimination and aggressiveness via cuticular hydrocarbons in a supercolony-forming ant, *Formica yessensis*. PLoS One 7, e46840. https://doi.org/10.1371/journal.pone.0046840.

Kreft, J.-U. (2004). Biofilms promote altruism. Microbiology 150, 2751–2760. https://doi.org/10.1099/mic.0.26829-0.

Kronauer, D.J.C., Pierce, N.E., and Keller, L. (2012). Asexual reproduction in introduced and native populations of the ant *Cerapachys biroi.* Mol. Ecol. 21, 5221–5235. https://doi.org/10.1111/mec.12041.

Kuebler, L.S., Kelber, C., and Kleineidam, C.J. (2010). Distinct antennal lobe phenotypes in the leaf-cutting ant (*Atta vollenweideri*). J. Comp. Neurol. 518, 352–365. https://doi.org/10.1002/cne.22217.

Kurtovic, A., Widmer, A., and Dickson, B.J. (2007). A single class of olfactory neurons mediates behavioral responses to a *Drosophila* sex pheromone. Nature 446, 542-546. https://doi.org/10.1038/nature05672.

Laissue, P.P., Reiter, C., Hiesinger, P.R., Halter, S., Fischbach, K.F., and Stocker, R.F. (1999). Three-dimensional reconstruction of the antennal lobe in *Drosophila melanogaster*. J. Comp. Neurol. 405, 543-552. https://doi.org/10.1002/(SICI)1096-9861(19990322)405:4<543::AID-CNE7>3.0.CO;2-A.

Lalor, P.F. and Hughes, W.O.H. (2011). Alarm behaviour in *Eciton* army ants. Physiol. Entomol. 36, 1–7. https://doi.org/10.1111/j.1365-3032.2010.00749.x.

Largaespada, D.A. (2003). Generating and manipulating transgenic animals using transposable elements. Reprod. Biol. Endocrinol. 1. https://doi.org/10.1186/1477-7827-1-80.

Larkin, M.A., Blackshields, G., Brown, N.P., Chenna, R., Mcgettigan, P.A., McWilliam, H., Valentin, F., Wallace, I.M., Wilm, A., Lopez, R., et al. (2007). Clustal W and Clustal X version 2.0. Bioinformatics 23, 2947–2948. https://doi.org/10.1093/bioinformatics/btm404.

Larsson, M.C., Domingos, A.I., Jones, W.D., Chiappe, M.E., Amrein, H., and Vosshall, L.B. (2004). Or83b encodes a broadly expressed odorant receptor essential for *Drosophila* olfaction. Neuron 43, 703-714. https://doi.org/10.1016/j.neuron.2004.08.019.

Laurent, G. (1999). A systems perspective on early olfactory coding. Science 286, 723-728. https://doi.org/10.1126/science.286.5440.723.

Laurent, G. (2002). Olfactory network dynamics and the coding of multidimensional signals. Nat. Rev. Neurosci. 3, 884-895. https://doi.org/10.1038/nrn964.

Lenz, E.L., Krasnec, M.O., and Breed, M.D. (2013). Identification of undecane as an alarm pheromone of the ant *Formica argentea*. J. Insect Behav. 26, 101–108. https://doi.org/10.1007/s10905-012-9337-5.

Leonhardt, S.D., Brandstaetter, A.S., and Kleineidam, C.J. (2007). Reformation process of the neuronal template for nestmate-recognition cues in the carpenter ant *Camponotus floridanus*. J. Comp. Physiol. A. 193, 993-1000. https://doi.org/10.1007/s00359-007-0252-8.

Leonhardt, S.D., Menzel, F., Nehring, V., and Schmitt, T. (2016). Ecology and evolution of communication in social insects. Cell 164, 1277-1287. https://doi.org/10.1016/j.cell.2016.01.035.

Li, K. (2008). The image stabilizer plugin for imageJ. http://www.cs.cmu.edu/~kangli/code/Image_Stabilizer.html

Li, H. (2013). Aligning sequence reads, clone sequences and assembly contigs with BWA-MEM. ArXiv 00, 1–3. https://doi.org/10.48550/arXiv.1303.3997.

Li, H., Handsaker, B., Wysoker, A., Fennell, T., Ruan, J., Homer, N., Marth, G., Abecasis, G., and Durbin, R. (2009). The sequence alignment/map format and SAMtools. Bioinformatics 25, 2078–2079. https://doi.org/10.1093/bioinformatics/btp352.

Liebig, J., Peeters, C., Oldham, N.J., Markstädter, C., and Hölldobler, B. (2000). Are variations in the cuticular hydrocarbons of queens and workers a reliable signal of fertility in the ant *Harpegnathos saltator*? Proc. Natl. Acad. Sci. U. S. A. 97, 4124-4131. https://doi.org/10.1073/pnas.97.8.4124.

Lockey, K.H. (1988). Lipids of the insect cuticle: origin, composition and function. Comp. Biochem. Physiol. 89B, 595-645. https://doi.org/10.1016/0305-0491(88)90305-7.

Lodovichi, C. and Belluscio, L. (2012). Odorant receptors in the formation of the olfactory bulb circuitry. Physiology 27, 200–212. https://doi.org/10.1152/physiol.00015.2012.

Löfqvist, J. (1976). Formic acid and saturated hydrocarbons as alarm pheromones for the ant *Formica rufa*. J. Insect Physiol. 22, 1331–1346. https://doi.org/10.1016/0022-1910(76)90155-4.

Lopes, L.E., Frank, E.T., Kárpáti, Z., Schmitt, T., and Kronauer, D.J.C. (2022). The alarm pheromone and alarm response of the clonal raider ant. Preprint at bioRxiv, https://doi.org/10.1101/2022.12.04.518909.

de Mármol, J., Yedlin, M.A., and Ruta, V. (2021). The structural basis of odorant recognition in insect olfactory receptors. Nature 597, 126-131. https://doi.org/10.1038/s41586-021-03794-8.

Martin, S. and Drijfhout, F. (2009). A review of ant cuticular hydrocarbons. J. Chem. Ecol. 35, 1151-1161. https://doi.org/10.1007/s10886-009-9695-4.

Maschwitz, U.W. (1964). Alarm substances and alarm behavior in social Hymenoptera. Nature 204, 324–327. https://doi.org/10.1038/204324a0.

Masumoto, M., Ohde, T., Shiomi, K., Yaginuma, T., and Niimi, T. (2012). A baculovirus immediate-early gene, *ie1*, promoter drives efficient expression of a transgene in both *Drosophila melanogaster* and *Bombyx mori*. PLoS One 7, e49323. https://doi.org/10.1371/journal.pone.0049323.

McGurk, D.J. (1968). I. Studies of volatile compounds from ants II. Degradation studies and structure proof of cis, cis-nepetalactone. Oklahoma State University.

McGurk, D.J., Frost, J., Eisenbraun, E.J., Vick, K., Drew, W.A., and Young, J. (1966). Volatile compounds in ants: Identification of 4-methyl-3-heptanone from *Pogonomyrmex* ants. J. Insect Physiol. 12, 1435–1441. https://doi.org/10.1016/0022-1910(66)90157-0.

McKenzie, S.K., Fetter-Pruneda, I., Ruta, V., and Kronauer, D.J.C. (2016). Transcriptomics and neuroanatomy of the clonal raider ant implicate an expanded clade of odorant receptors in chemical communication. Proc. Natl. Acad. Sci. U. S. A. 113, 14091–14096. https://doi.org/10.1073/pnas.1610800113.

McKenzie, S.K. and Kronauer, D.J.C. (2018). The genomic architecture and molecular evolution of ant odorant receptors. Genome Res. 28, 1757–1765. https://doi.org/10.1101/gr.237123.118.

Michener, C.D. (1969). Comparative social behavior of bees. Annu. Rev. Entomol. 14, 299-342. https://doi.org/10.1146/annurev.en.14.010169.001503.

Mitaka, Y. and Akino, T. (2021). A review of termite pheromones: multifaceted, context-dependent, and rational chemical communications. Front. Ecol. Evol. 8, 595614. https://doi.org/10.3389/fevo.2020.595614.

Mizunami, M., Yamagata, N., and Nishino, H. (2010). Alarm pheromone processing in the ant brain: An evolutionary perspective. Front. Behav. Neurosci. 4, 1–9. https://doi.org/10.3389/fnbeh.2010.00028.

Morgulis, A., Coulouris, G., Raytselis, Y., Madden, T.L., Agarwala, R., and Schäffer, A.A. (2008). Database indexing for production MegaBLAST searches. Bioinformatics 24, 1757–1764. https://doi.org/10.1093/bioinformatics/btn322.

Moser, J.C., Brownlee, R.C., and Silverstein, R. (1968). Alarm pheromones of the ant *Atta texana*. J. Insect Physiol. 14, 529–535. https://doi.org/10.1016/0022-1910(68)90068-1.

Mukherjee, S. and Bassler, B.L. (2019). Bacterial quorum sensing in complex and dynamically changing environments. Nat. Rev. Microbiol. 17, 371-382. https://doi.org/10.1038/s41579-019-0186-5.

Münch, D. and Galizia, C.G. (2016). DoOR 2.0 - Comprehensive mapping of Drosophila melanogaster odorant responses. Sci. Rep. 6, 21841. https://doi.org/10.1038/srep21841.

Mysore, K., Subramanian, K.A., Sarasij, R.C., Suresh, A., Shyamala, B. V., VijayRaghavan, K., and Rodrigues, V. (2009). Caste and sex specific olfactory glomerular organization and brain architecture in two sympatric ant species *Camponotus sericeus* and *Camponotus compressus* (Fabricius, 1798). Arthropod Struct. Dev. 38, 458–497. https://doi.org/10.1016/j.asd.2009.06.001.

Nadell, C.D., Drescher, K. and Foster, K.R. (2016). Spatial structure, cooperation and competition in biofilms. Nat. Rev. Microbiol. 14, 589–600. https://doi.org/10.1038/nrmicro.2016.84.

Nadell, C.D., Xavier, J.B. & Foster, K.R. (2009). The sociobiology of biofilms. FEMS Microbiol. Rev. 33, 206–224. https://10.1111/j.1574-6976.2008.00150.x.

Nadell, C.D., Xavier, J.B., Levin, S.A., and Foster, K.R. (2008). The evolution of quorum sensing in bacterial biofilms. PLoS Biol. 6, 0171–0179. https://doi.org/10.1371/journal.pbio.0060014.

Najar-Rodriguez, A.J., Galizia, C.G., Stierle, J., and Dorn, S. (2010). Behavioral and neurophysiological responses of an insect to changing ratios of constituents in host plant-derived volatile mixtures. J. Exp. Biol. 213, 3388-3397. https://doi.org/10.1242/jeb.046284.

do Nascimento, R.R., Billen, J., and Morgan, E.D. (1993). The exocrine secretions of the jumping ant *Harpegnathos saltator*. Comp. Biochem. Physiol. 104B, 505–508. https://doi.org/10.1016/0305-0491(93)90274-9.

NCBI (2022). Genome Data Viewer entry for *Ooceraea biroi*. Washington, D.C.: National Institute for Biotechnology Information. https://www.ncbi.nlm.nih.gov/genome/gdv/browser/genome/?id=GCF_003672135.1

Nei, M., Niimura, Y., and Nozawa, M. (2008). The evolution of animal chemosensory receptor gene repertoires: roles of chance and necessity. Nat. Rev. Genet. 9, 951-963. https://doi.org/10.1038/nrg2480.

O'Brochta, D.A. and Reid, W. (2003). Gene vector and transposable element behavior in mosquitoes. J. Exp. Biol. 206, 3823–3834. https://doi.org/10.1242/jeb.00638.

Oldham, N.J., Morgan, E.D., Gobin, B., Schoeters, E., and Billen, J. (1994). Volatile secretions of old world army ant *Aenictus rotundatus* and chemotaxonomic implications of army ant dufour gland chemistry. J. Chem. Ecol. 20, 3297–3305. https://doi.org/10.1007/BF02033727.

Olsen, S.R., Bhandawat, V., and Wilson, R.I. (2007). Excitatory interactions between olfactory processing channels in the *Drosophila* antennal lobe. Neuron 54, 89-103. https://doi.org/10.1016/j.neuron.2007.03.010.

Otte, M., Netschitailo, O., Kaftonoglu, O., Wang, Y., Page Jr., R.E., and Beye, M. (2018). Improving genetic transformation rates in honeybees. Sci. Rep. 8, 16534. https://doi.org/10.1038/s41598-018-34724-w.

Oxley, P.R., Ji, L., Fetter-Pruneda, I., McKenzie, S.K., Li, C., Hu, H., Zhang, G., and Kronauer, D.J.C. (2014). The genome of the clonal raider ant *Cerapachys biroi*. Curr. Biol. 24, 451–458. https://doi.org/10.1016/j.cub.2014.01.018.

Ozaki, M., Wada-Katsumata, A., Fujikawa, K., Iwasaki, M., Yokohari, F., Satoji, Y., Nisimura, T., and Yamaoka, R. (2005). Ant nestmate and non-nestmate discrimination by a chemosensory sensillum. Science 309, 311-314. https://doi.org/10.1126/science.1105244.

Paoli, M., Anesi, A., Antolini, R., Guella, G., Vallortigara, G., and Haase, A. (2016). Differential odour coding of isotopomers in the honeybee brain. Sci. Rep. 6, 21893. https://doi.org/10.1038/srep21893.

Paoli, M. and Galizia, G.C. (2021). Olfactory coding in honeybees. Cell Tissue Res. 383, 35-58. https://doi.org/10.1007/s00441-020-03385-5.

Park, D., Park, S.-H., Ban, Y.W., Kim, Y.S., Park, K.-C.,Kim, N.-S., Kim, J.-K., and Choi, I.-Y. (2017). A bioinformatics approach for identifying transgene insertion sites using whole genome sequencing data. BMC Biotechnol. 17, 67. https://doi.org/10.1186/s12896-017-0386-x.

Pask, G.M., Slone, J.D., Millar, J.G., Das, P., Moreira, J.A., Zhou, X., Bello, J., Berger, S.L., Bonasio, R., Desplan, C., et al. (2017). Specialized odorant receptors in social insects that detect cuticular hydrocarbon cues and candidate pheromones. Nat. Commun. 8, 297. https://doi.org/10.1038/s41467-017-00099-1.

Pasteels, J.M., Verhaeghe, J.C., Braekman, J.C., Daloze, D., and Tursch, B. (1980). Caste-dependent pheromones in the head of the ant *Tetramorium caespitum*. J. Chem. Ecol. 6, 467–472. https://doi.org/10.1007/BF01402923.

Pasteels, J.M., Verhaeghe, J.C., Ottinger, R., Braekman, J.C., and Daloze, D. (1981). Absolute configuration of (3R,4S)-4-methyl-3-hexanol- a pheromone from the head of the ant *Tetramorium impurum foerster*. Insect Biochem. 11, 675–678. https://doi.org/10.1016/0020-1790(81)90057-3.

Pelz, D., Roeske, T., Syed, Z., de Bruyne, M., and Galizia, C.G. (2006). The molecular receptive range of an olfactory receptor in vivo (*Drosophila melanogaster* Or22a). J. Neurobiol. 66, 1544-1563. https://doi.org/10.1002/neu.20333.

Prieto-Godino, L.L., Rytz, R., Cruchet, S., Bargeton, B., Abuin, L., Silbering, A.F., Ruta, V., Dal Peraro, M., and Benton, R. (2017). Evolution of acid-sensing olfactory circuits in drosophilids. Neuron 93, 661-676.e6. https://doi.org/10.1016/j.neuron.2016.12.024.

Queller, D.C., Ponte, E., Bozzaro, S. and Strassmann, J.E. (2003). Single-gene greenbeard effects in the social amoeba *Dictyostelium discoideum*. Science. 299, 105–106. https://doi.org/10.1126/science.1077742.

R Core Team (2021). R: A language and environment for statistical computing. http://www.R-project.org.

Ratnieks, F.L.W. (1988). Reproductive harmony by mutual policing by workers in eusocial Hymenoptera. Am. Nat. 132, 217-236. https://doi.org/10.1086/284846.

Ratnieks, F.L.W., Foster, K.R., and Wenseleers, T. (2006). Conflict resolution in insect societies. Annu. Rev. Entomol. 51, 581-608. https://doi.org/10.1146/annurev.ento.51.110104.151003.

Ratnieks, F.L.W. and Visscher, P.K. (1989). Worker policing in the honeybee. Nature 342, 796-797. https://doi.org/10.1038/342796a0.

Ravary, F. and Jaisson, P. (2004). Absence of individual sterility in thelytokous colonies of the ant *Cerapachys biroi* Forel (Formicidae, Cerapachyinae). Insectes Soc. 51, 67–73. https://doi.org/10.1007/s00040-003-0724-y.

Ravary, F. and Jaisson, P. (2002). The reproductive cycle of thelytokous colonies of *Cerapachys biroi* Forel (Formicidae, Cerapachyinae). Insectes Soc. 49, 114–119. https://doi.org/10.1007/s00040-002-8288-9.

Ravary, F., Jahyny, B., and Jaisson, P. (2006). Brood stimulation controls the phasic reproductive cycle of the parthenogenetic ant *Cerapachys biroi*. Insectes Soc. 53, 20–26. https://doi.org/10.1007/s00040-005-0828-7.

Regnier, F.E. and Wilson, E.O. (1968). The alarm-defence system of the ant *Acanthomyops claviger*. J. Insect Physiol. 14, 955–970. https://doi.org/10.1016/0022-1910(68)90006-1.

Regnier, F.E. and Wilson, E.O. (1969). The alarm-defence system of the ant *Lasius alienus*. J. Insect Physiol. 15, 893–898. https://doi.org/10.1016/0022-1910(69)90129-2.

Riabinina, O., Luginbuhl, D., Marr, E., Liu, S., Wu, M.N., Luo, L., and Potter, C.J. (2015). Improved and expanded Q-system reagents for genetic manipulations. Nat. Methods 12, 37–54. https://doi.org/10.1016/bs.mcb.2015.01.016.Observing.

Riabinina, O., Task, D., Marr, E., Lin, C.-C., Alford, R., O'Brochta, D.A., and Potter, C.J. (2016). Organization of olfactory centres in the malaria mosquito *Anopheles gambiae*. Nat. Commun. 7, 13010. https://doi.org/10.1038/ncomms13010.

Rihani, K., Ferveur, J.-F., and Briand, L. (2021). The 40-year mystery of insect odorant-binding proteins. Biomolecules 11, 509. https://doi.org/10.3390/biom11040509.

Robertson, H.M. and Wanner, K.W. (2006). The chemoreceptor superfamily in the honey bee, *Apis mellifera*: Expansion of the odorant, but not gustatory, receptor family. Genome Res. 16, 1395-1403. https://doi.org/10.1101/gr.5057506.

Robinson, J.T., Thorvaldsdóttir, H., Winckler, W., Guttman, M., Lander, E.S., Getz, G., and Mesirov, J.P. (2011). Integrative genomics viewer. Nat. Biotechnol. 29, 24–26. https://doi.org/10.1038/nbt.1754.

Ryba, A.R., McKenzie, S.K., Olivos-Cisneros, L., Clowney, E.J., Pires, P.M., and Kronauer, D.J.C. (2020). Comparative Development of the ant chemosensory system. Curr. Biol. 30, 3223-3230.e4. https://doi.org/10.1016/j.cub.2020.05.072.

Rytz, R., Croset, V., and Benton, R. (2013). Ionotropic Receptors (IRs): chemosensory ionotropic glutamate receptors in *Drosophila* and beyond. Insect Biochem. Mol. Biol. 43, 888-897. https://doi.org/10.1016/j.ibmb.2013.02.007.

Sachse, S. and Galizia, C.G. (2003). The coding of odour-intensity in the honeybee antennal lobe: local computation optimizes odour representation. Eur. J. Neurosci. 18, 2119-2132. https://doi.org/10.1046/j.1460-9568.2003.02931.x.

Sachse, S., Rappert, A., and Galizia, C.G. (1999). The spatial representation of chemical structures in the antennal lobe of honeybees: Steps towards the olfactory code. Eur. J. Neurosci. 11, 3970–3982. https://doi.org/10.1046/j.1460-9568.1999.00826.x.

Sakurai, T., Nakagawa, T., Mitsuno, H., Mori, H., Endo, Y., Tanoue, S., Yasukochi, Y., Touhara, K., and Nishioka, T. (2004). Identification and functional characterization of a sex pheromone receptor in the silkmoth *Bombyx mori*. Proc. Natl. Acad. Sci. U. S. A. 101, 16653-16658. https://doi.org/10.1073/pnas.040759610.

Santorelli, L.A., Thompson, C.R.L., Villegas, E., Svetz, J., Dinh, C., Parikh, A., Sucgang, R., Kuspa, A., Strassmann, J.E., Queller, D.C., et al. (2008). Facultative cheater mutants reveal the genetic complexity of cooperation in social amoebae. Nature 451, 1107–1110. https://doi.org/10.1038/nature06558.

Scarano, F., Suresh, M.D., Tiraboschi, E., Cabirol, A., Nouvian, M., Nowotny, T., and Haase, A. (2022). Geosmin suppresses defensive behaviour and elicits unusual neural responses in honey bees. Preprint at bioRxiv, https://doi.org/10.1101/2021.10.06.463314.

Schaefer, M.L., Finger, T.E., and Restrepo, D. (2001). Variability of position of the P2 glomerulus within a map of the mouse olfactory bulb. J. Comp. Neurol. 436, 351–362. https://doi.org/10.1002/cne.1072.

Schindelin, J., Arganda-Carreras, I., Frise, E., Kaynig, V., Longair, M., Pietzsch, T., Preibisch, S., Rueden, C., Saalfeld, S., Schmid, B., et al. (2012). Fiji: An open-source platform for biological-image analysis. Nat. Methods 9, 676–682. https://doi.org/10.1038/nmeth.2019.

Schlief, M.L. and Wilson, R.I. (2007). Olfactory processing and behavior downstream from highly selective receptor neurons. Nat. Neurosci. 10, 623-630. https://doi.org/10.1038/nn1881.

Schneider, D. (1964). Insect antennae. Annu. Rev. Entomol. 9, 103-122. https://doi.org/10.1146/annurev.en.09.010164.000535.

Schulte, C., Theilenberg, E., Müller-Borg, M., and Beye, M. (2014). Highly efficient integration and expression of piggyBac-derived cassettes in the honeybee (*Apis mellifera*). Proc. Natl. Acad. Sci. U. S. A. 111, 9003-9008. https://doi.org/10.1073/pnas.1402341111.

Slone, J.D., Pask, G.M., Ferguson, S.T., Millar, J.G., Berger, S.L., Reinberg, D., Liebig, J., Ray, A., and Zwiebel, L. (2017). Functional characterization of odorant receptors in the ponerine ant, *Harpagnethos saltator*. Proc. Natl. Acad. Sci. U. S. A. 114, 8586-8591. https://doi.org/10.1073/pnas.1704647114.

Shang, Y., Claridge-Chang, A., Sjulson, L., Pypaert, M., and Miesenböck, G. (2007). Excitatory local circuits and their implications for olfactory processing in the fly antennal lobe. Cell 128, 601-612. https://doi.org/10.1016/j.cell.2006.12.034.

Sharma, K.R., Enzmann, B.L., Schmidt, Y., Moore, D., Jones, G.R., Parker, J., Berger, S.L., Reinberg, D., Zwiebel, L.J., Breit, B., et al. (2015). Cuticular hydrocarbon pheromones for social behavior and their coding in the ant antenna. Cell Rep. 12, 1261-1271. https://doi.org/10.1016/j.celrep.2015.07.031.

Smith, A.A. and Haight, K.L. (2008). Army ants as research and collection tools. J. Insect. Sci. 8, 71. https://doi.org/10.1673/031.008.7101.

Smith, C.D., Zimin, A., Hold, C., Abouheif, E., Benton, R., Cash, E., Croset, V., Currie, C.R., Elhaik, E., Elsik, E., et al. (2011). Draft genome of the globally widespread and invasive

Argentine ant (*Linepithema humile*). Proc. Natl. Acad. Sci. U. S. A. 108, 5673-5678. https://doi.org/10.1073/pnas.1008617108.

Smukalla, S., Caldara, M., Pochet, N., Beauvais, A., Guadagnini, S., Yan, C., Vinces, M.D. Janse, A., Prevost, M.C. Latgé, J.-P., et al. (2008). *FLO1* Is a variable green beard gene that drives biofilm-like cooperation in budding yeast. Cell 135, 726–737. https://doi.org/10.1016/j.cell.2008.09.037.

Stensmyr, M.C., Dweck, H.K.M., Farhan, A., Ibba, I., Strutz, A., Mukunda, L., Linz, J., Grabe, V., Steck, K., Lavista-Llanos, S., et al. (2012). A conserved dedicated olfactory circuit for detecting harmful microbes in *Drosophila*. Cell 151, 1345–1357. https://doi.org/10.1016/j.cell.2012.09.046.

Steiger, S., Schmitt, T., and Schaefer, H.M. (2010). The origin and dynamic evolution of chemical information transfer. Proc. R. Soc. B. 278, 970-979. https://doi.org/10.1098/rspb.2010.2285.

Stocker, R.F. (1994). The organization of the chemosensory system in *Drosophila melanogaster*: a review. Cell Tissue Res. 275, 3–26. https://doi.org/10.1007/BF00305372.

Stocker, R.F., Lienhard, M.C., Borst, A., and Fischbach, K.-F. (1990). Neuronal architecture of the antennal lobe in *Drosophila melanogaster*. Cell Tissue Res. 262, 9–34. https://doi.org/10.1007/BF00327741.

Stökl, J. and Steiger, S. (2017). Evolutionary origin of insect pheromones. Curr. Opin. Insect Sci. 24, 36-42. https://doi.org/10.1016/j.cois.2017.09.004.

Stökl, J., Strutz, A., Dafni, A., Svatos, A., Doubsky, J., Knaden, M., Sachse, S., Hansson, B.S., and Stensmyr, M.C. (2010). A deceptive pollination system targeting drosophilids through olfactory mimicry of yeast. Curr. Biol. 20, 1846–1852. https://doi.org/10.1016/j.cub.2010.09.033.

Strassmann, J.E., Gilbert, O.M., and Queller, D.C. (2011). Kin discrimination and cooperation in microbes. Annu. Rev. Microbiol. 65, 349–367. https://doi.org/10.1146/annurev.micro.112408.134109.

Strassmann, J.E. and Queller, D.C. (2011). Evolution of cooperation and control of cheating in a social microbe. Proc. Natl. Acad. Sci. U. S. A. 108, 10855–10862. https://doi.org/10.1073/pnas.1102451108.

Strassmann, J.E., Zhu, Y., and Queller, D.C. (2000). Altruism and social cheating in the social amoeba *Dictyostelium discoideum*. Nature 408, 965–967. https://doi.org/10.1038/35050087.

Strausfeld, N.J. and Hildebrand, J.G. (1999). Olfactory systems: Common design, uncommon origins? Curr. Opin. Neurobiol. 9, 634–639. https://doi.org/10.1016/S0959-4388(99)00019-7.

Strotmann, J., Conzelmann, S., Beck, A., Feinstein, P., Breer, H., and Mombaerts, P. (2000). Local permutations in the glomerular array of the mouse olfactory bulb. J. Neurosci. 20, 6927–6938. https://doi.org/10.1523/jneurosci.20-18-06927.2000.

Su, C.-Y., Martelli, C., Emonet, T., and Carlson, J.R. (2011). Temporal coding of odor mixtures in an olfactory receptor neuron. Proc. Natl. Acad. Sci. U. S. A. 108, 5075-5080. https://doi.org/10.1073/pnas.1100369108.

Suzuki, M. G., Funaguma, S., Kanda, T., Tamura, T., and Shimada, T. (2003). Analysis of the biological functions of a doublesex homologue in *Bombyx mori*. Dev. Genes Evol. 213, 345–354. https://doi.org/10.1007/s00427-003-0334-8.

Takeichi, Y., Tsubi, T., Miyazaki, N., Murata, K., Yasuyama, K., Inoue, K., Suzaki, T., Kubo, H., Kajiwara, N., Takano, J., et al. (2018). Putative neural network within an olfactory sensory unit for nestmate and non-nestmate discrimination in the Japanese carpenter ant: the

ultra-structures and mathematical simulation. Front. Cell. Neurosci. 19, 310. https://doi.org/10.3389/fncel.2018.00310.

Tarnita, C. E. (2017). The ecology and evolution of social behavior in microbes. J. Exp. Biol. 220, 18–24. https://doi.org/10.1242/jeb.145631.

Task, D., Lin, C.-C., Vulpe, A., Afify, A., Ballou, S., Brbic, M., Schlegel, P., Raji, J., Jefferis, G., et al. (2022). Chemoreceptor co-expression in *Drosophila melanogaster* olfactory neurons. Elife 11, e72599. https://doi.org/10.7554/eLife.72599.

Terrapon, N., Li, C., Robertson, H.M., Ji, L., Meng, X., Booth, W., Chen, Z., Childers, C.P., Glastad, K.M., Gokhale, K., et al. (2014). Molecular traces of alternative social organization in a termite genome. Nat. Commun. 5, 3636. https://doi.org/10.1038/ncomms4636.

Teseo, S., Châline, N., Jaisson, P., and Kronauer, D.J.C. (2014a). Epistasis between adults and larvae underlies caste fate and fitness in a clonal ant. Nat. Commun. 5, 3363. https://doi.org/10.1038/ncomms4363.

Teseo, S., Lecoutey, E., Kronauer, D.J.C., Hefetz, A., Lenoir, A., Jaisson, P., and Châline, N. (2014b). Genetic distance and age affect the cuticular chemical profiles of the clonal ant *Cerapachys biroi.* J. Chem. Ecol. 40, 429-438. https://doi.org/10.1007/s10886-014-0428-y.

Tian, L., Hires, S.A., and Looger, L.L. (2012). Imaging neuronal activity with genetically encoded calcium indicators. Cold Spring Harb. Protoc. 6, 647-656. https://doi.org/10.1101/pdb.top069609.

Tinbergen, N. (1952). "Derived" activities, their causation, biological significance, origin, and emancipation during evolution. Q. Rev. Biol. 1, 1-32. https://doi.org/10.1086/398642.

Trible, W., Olivos-Cisneros, L., McKenzie, Saragosti, J., Chang, N.-C. S.K., Matthews, B.J., Oxley, P.R., and Kronauer, D.J.C. (2017). *orco* mutagenesis causes loss of antennal lobe glomeruli and impaired social behavior in ants. Cell 170, 727–735. https://doi.org/10.1016/j.cell.2017.07.001.

Trible, W., McKenzie, S.K., and Kronauer, D.J.C. (2020). Globally invasive populations of the clonal raider ant are derived from Bangladesh. Biol. Lett. 16, 20200105-20200105. https://doi.org/10.1098/rsbl.2020.0105.

Trivers, R. and Hare, H. (1976). Haplodiploidy and the evolution of the social insects. Science, 191, 249-263. https://doi.org/10.1126/science.1108197.

Tsuji, K. and Yamauchi, K. (1995). Production of females by parthenogenesis in the ant, *Cerapachys biroi*. Insectes Soc. 42, 333–336. https://doi.org/10.1007/BF01240430.

Uchida, N., Takahashi, Y.K., Tanifuji, M., and Mori, K. (2000). Odor maps in the mammalian olfactory bulb: domain organization and odorant structural features. Nat. Neurosci. 3, 1035-1043. https://doi.org/10.1038/79857.

Ulrich, Y., Saragosti, J., Tokita, C.K., Tarnita, C.E. & Kronauer, D.J.C. (2018). Fitness benefits and emergent division of labour at the onset of group living. Nature 560, 635–638. https://doi.org/10.1038/s41586-018-0422-6.

Ulrich, Y., Kawakatsu, M., Tokita, C.K., Saragosti, J., Chandra, V., Tarnita, C.E., and Kronauer, D.J.C. (2021). Response thresholds alone cannot explain empirical patterns of division of labor in social insects. PLoS Biol. 19, e3001269. https://doi.org/10.1371/journal.pbio.3001269.

US EPA (2022). Estimation Programs Interface Suite™ for Microsoft® Windows, v 4.11. Washington, D.C.: United States Environmental Protection Agency.

Vander Meer, R.K., and Alonso, L.E. (1998). Pheromone directed behavior in ants. In Pheromone Communication in Social Insects. R. K. Vander Meer, M. D. Breed, M. Winston, K. E. Espelie, eds. Boulder, CO, USA: Westview Press, pp. 159–192.

Verheggen, F.J. Haubruge, E. and Mescher, M.C. (2010). Alarm pheromones-chemical signaling in response to danger. Vitam. Horm. 83, 215-239. https://doi.org/10.1016/S0083-6729(10)83009-2.

Vosshall, L.B., Wong, A.M., and Axel, R. (2000). An olfactory sensory map in the fly brain. Cell 102, 147–159. https://doi.org/10.1016/S0092-8674(00)00021-0.

Wagner, D., Tissot, M., Cuevas, W., and Gordon, D.M. (2000). Harvester ants utilize cuticular hydrocarbons in nestmate recognition. J. Chem. Ecol. 26, 2245-2257. https://doi.org/10.1023/A:1005529224856

Wang, J.W., Wong, A.M., Flores, J., Vosshall, L.B., and Axel, R. (2003). Two-photon calcium imaging reveals an odor-evoked map of activity in the fly brain. Cell 112, 271–282. https://doi.org/10.1016/S0092-8674(03)00004-7.

West, S.A., Diggle, S.P., Buckling, A., Gardner, A. and Griffin, A.S. (2007). The social lives of microbes. Annu. Rev. Ecol. Evol. Syst. 38, 53–77. https://doi.org/10.1146/annurev.ecolsys.38.091206.095740.

Wickam, H. (2016). ggplot2: Elegant Graphics for Data Analysis (Springer-Verlag).

Wilson, E.O. and Regnier, F.E.J. (1971). The evolution of the alarm-defense system in the Formicine ants. Am. Nat. 105, 279–289. https://doi.org/10.1086/282724.

Xavier, J.B. and Foster, K.R. (2007). Cooperation and conflict in microbial biofilms. Proc. Natl. Acad. Sci. U. S. A. 104, 876–881. https://doi.org/10.1073/pnas.060765110.

Xavier, J.B., Kim, W. and Foster, K.R. (2011). A molecular mechanism that stabilizes cooperative secretions in *Pseudomonas aeruginosa*. Mol. Microbiol. 79, 166–179. https://doi.org/10.1111/j.1365-2958.2010.07436.x.

Yamagata, N., Nishino, H., and Mizunami, M. (2006). Pheromone-sensitive glomeruli in the primary olfactory centre of ants. Proc. R. Soc. B Biol. Sci. 273, 2219–2225. https://doi.org/10.1098/rspb.2006.3565.

Yan, H. and Liebig, J. (2021). Genetic basis of chemical communication in eusocial insects. Genes Dev. 35, 470-482. https://doi.org/10.1101/gad.346965.120

Yan, H., Opachaloemphan, C., Mancini, G., Yang, H., Gallitto, M., Mlejnek, J., Leibholz, A., Haight, K., Ghaninia, M., Huo, L., et al. (2017). An engineered *orco* mutation in ants produces aberrant social behavior and defective neural development. Cell 170, 736–747. https://doi.org/10.1016/j.cell.2017.06.051.

Yan, J., Monaco, H., and Xavier, J.B. (2019). The ultimate guide to bacterial swarming: An experimental model to study the evolution of cooperative behavior. Annu. Rev. Microbiol. 73, 293–312. https://doi.org/10.1146/annurev-micro-020518-120033.

Yohe, L.R. and Brand, P. (2018). Evolutionary ecology of chemosensation and its role in sensory drive. Curr. Zool. 64, 525-533. https://doi.org/10.1093/cz/zoy048.

Zapiec, B. and Mombaerts, P. (2015). Multiplex assessment of the positions of odorant receptor-specific glomeruli in the mouse olfactory bulb by serial two-photon tomography. Proc. Natl. Acad. Sci. U. S. A. 112, E5873–E5882. https://doi.org/10.1073/pnas.1512135112.

Zhao, Z. and McBride, C.S. (2020). Evolution of olfactory circuits in insects. J. Comp. Physiol. A Neuroethol. Sensory, Neural, Behav. Physiol. 206, 353–367. https://doi.org/10.1007/s00359-020-01399-6.

Zhao, Z., Zung, J.L., Hinze, A., Kriete, A.L., Iqbal, A., Younger, M.A., Matthews, B.J., Merhof, D., Thiberge, S., Ignell, R., et al. (2022). Mosquito brains encode unique features of human odour to drive host seeking. Nature 605, 706-712. https://doi.org/10.1038/s41586-022-04675-4.

Zhou, X., Slone, J.D., Rokas, A., Berger, S.L., Liebig, J., Ray, A., Reinberg, D., and Zwiebel, L.J. (2012). Phylogenetic and transcriptomic analyses of chemosensory receptors in a pair of divergent ant species reveals sex-specific signatures of odor coding. PLoS Genet. 8, e1002930. https://doi.org/10.1371/journal.pgen.1002930.

Zhou, X., Rokas, A., Berger, S.L., Liebig, J., Ray, A., and Zwiebel, L.J. (2015). Chemoreceptor evolution in Hymenoptera and its implications for the evolution of eusociality. Genome Biol. Evol. 10, 2490-2500. https://doi.org/10.1093/gbe/evv149.

Zube, C., Kleineidam, C.J., Kirschner, S., Neef, J., and Rössler, W. (2008). Organization of the olfactory pathway and odor processing in the antennal lobe of the ant *Camponotus floridanus*. J. Comp. Neurol. 506, 425–441. https://doi.org/10.1002/cne.21548.

van Zweden, J.S., Dreier, S., d'Ettorre, P. (2009). Disentangling environmental and heritable nestmate recognition cues in a carpenter ant. J. Insect. Physiol. 55, 159-164. https://doi.org/10.1016/j.jinsphys.2008.11.001.